Electronic Supplementary Material (ESI) for ChemComm.

Supporting Information

UV degradation of poly(lactic acid) materials through copolymerisation with a sugar-derived cyclic xanthate

Craig A. Hardy,[a] Gabriele Kociok-Köhn[b] and Antoine Buchard[a]*

[a]Department of Chemistry, Centre for Sustainable and Circular Technologies, University of Bath, Claverton Down, Bath BA2 7AY, UK

[b]Materials and Chemical Characterisation Facility (MC^2), University of Bath, Claverton Down, Bath, BA2 7AY, UK.

Email: a.buchard@bath.ac.uk

Table of Contents

Materials and Methods

Unless otherwise stated, all starting materials and reagents were obtained from Sigma-Aldrich, Acros Organics or Alfa Aesar and used without further purification. All solvents were obtained from either Fisher Scientific or VWR Chemicals, except for anhydrous solvents, which were purchased from Sigma-Aldrich or Acros Organics and used without further purification. Tri-*O*-acetyl-ᴅ-glucal was purchased from Carbosynth. 4-Methylbenzyl alcohol was recrystallised from dry diethyl ether and stored in a glovebox under Argon prior to use and TBD was purified and dried over CaH_2 prior to use by dissolution in dry THF. Where appropriate, the progress of reactions was monitored by thin layer chromatography using silica coated aluminium plates (Kieselgel 60G F254) purchased from VWR Chemicals and visualized using a potassium permanganate ($KMnO_4$) stain. The purification of intermediates and final products was accomplished by flash column chromatography, using silica gel (Fluka, pore size 60 Å, 70-230 mesh, 63-200 µm), and the purity of the final compounds was determined by NMR spectroscopy.

NMR spectra were recorded on a Brucker 400 and 500 spectrometers operating at a frequencies of 400 MHz (^1H) and 101 MHz (^{13}C) and 500 MHz (^1H) and 126 MHz (^{13}C) respectively. The NMR spectra were recorded in $CDCl_3$, relative to reference points of the deuterated solvent. Chemical shifts (δ) are quoted in ppm and coupling constants (*J*) are quoted in Hertz. Abbreviations used to describe the multiplicity of the peaks observed are defined as follows: s = singlet, d = doublet, t = triplet, m = multiplet, dd = doublet of doublets and so on.

Size-exclusion chromatography (SEC) was carried out using a THF eluent. Multi analysis software was used to process the data. Polymer samples were dissolved at a concentration of 1 mg mL^{-1}. Samples were recorded on an Agilent 1260 Infinity series instrument at 1 mL min^{-1} at 35 °C using two PLgel 5 µm MIXED-D 300 × 7.5 mm columns in series. Samples were detected with a differential refractive index (RI) detector. Number-average molecular weight ($M_{n,SEC}$), and dispersities, ($Đ_M$ (M_w/M_n)) were calculated against a polystyrene calibration (11 polystyrene standards of narrow molecular weight, ranging from M_w 615–568000 Da).

Differential scanning calorimetry (DSC) was carried out using a MicroSC multicell calorimeter from Setaram; the Calisto program was employed to collect and process the data. The measurement cell and the reference cell were both a 1 mL Hastelloy C cell; a mass of 2–5 mg of polymeric material was loaded into the measurement cell with the reference cell empty. The experiments were performed under N_2 and the sample heated and cooled at a rate of 10 K min^{-1} unless otherwise stated.

A second heating and cooling cycle was carried out immediately following completion of the first, unless otherwise stated. Data was plotted using Origin 2018.

Thermogravimetric analysis (TGA) was carried out using A Setsys Evolution TGA 16/18 from Setaram; the Calisto program was employed to collect and process the data. The sample was loaded into a 170 µL alumina crucible and the analytical chamber purged with argon (200 mL min^{-1}) for 20 minutes prior to starting the analysis. The sample was then heated under an argon flow (20 mL min^{-1}) from 30 to 600 °C at a rate of 10 °C min^{-1}, unless otherwise stated.

In-situ IR analysis was carried out using a ReactIR 702L system from Mettler Toledo and the iC IR 7.1 Office software was employed to collect and process the data. The experiments were performed under argon, and measurements were recorded using a DiComp (Diamond) IR probe and TE MCT detector over a sampling range of 3000–650 cm^{-1}.

UV-Vis analysis was carried out using a recorded in solution using an Avantes AvaLight-DH-S-BAL light source and an Avantes AvaSpec-2048L spectrometer. Data was plotted using Origin 2018.

UV degradation were carried out within a EvoluChem™ PhotoRedOx Box using a EvoluChem™ 30W LED light source with the following specifications: input voltage AC200-240V, beam angle 20 degrees and wavelength 365nm. Polymer and copolymer degradation solutions were made up to a concentration of 0.044 mol L^{-1}, within glass screw neck sample vials 18x30 mm.

Single Crystal X-ray Diffraction (SCXRD) analysis for **1** was carried out at 150(2) K on a Rigaku Xcalibur, EosS2 single crystal diffractometer using graphite monochromated Mo-Kα radiation (λ = 0.71073 Å). Unit cell determination, data collection and data reduction were performed using the CrysAlisPro software.6 The structure was solved with SHELXT and refined by a full-matrix least-squares procedure based on F2 (SHELXL-2018/3)7. All non-hydrogen atoms were refined anisotropically. Hydrogen atoms were placed onto calculated positions and refined using a riding model.

General Procedures

1. Synthesis and Characterisation of Cyclic Xanthate Monomer, 1

Synthesis of (2*R*,3*S*)-3-acetoxy-3,6-dihydro-2*H*-pyran-2-yl)methyl acetate

A solution of tri-*O*-acetyl-ᴅ-glucal (12.0 g, 44.1 mmol, 1.0 equiv.) in anhydrous DCM (50 mL) was cooled to 0 °C, under argon, and treated with triethylsilane (8.45 mL, 52.9 mmol, 1.2 equiv.), followed by $BF_3{\cdot}OEt_2$ (ca. 48%, BF_3) (5.6 mL, 44.1 mmol, 1.0 equiv.). The reaction was then stirred at 0 °C for 3 h. Once complete the reaction was quenched with $NaHCO_3$ (1 mol L^{-1}, 100 mL) and the organic phase was extracted using DCM (2 x 50 mL), washed with brine (100 mL) and water (2 x 100 mL), dried over $MgSO_4$, and the solvent was then evaporated in *vacuo* to yield a colourless oil, which was used directly in the next reaction without further purification (9.44 g, 100 %). Spectroscopic data was consistent with the literature.[1]

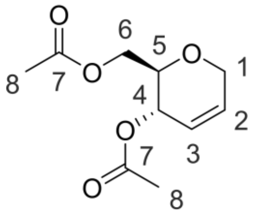

δ_H (400 MHz; chloroform-d): 5.93 (C^3H, 1H, dddd, J_{HH} = 10.3, 2.7, 2.7, 1.8 Hz), 5.74 (C^2H, 1H, dddd, J_{HH} = 10.3, 2.3, 2.3, 2.2 Hz), 5.28-5.19 (C^4H, 1H, m), 4.23-4.18 (C^1H, C^6H, 3H, m), 4.16 (C^6H, 1H, dd, J_{HH} = 12.1, 5.9 Hz), 3.71 (C^5H, 1H, ddd, J_{HH} = 8.6, 5.9, 2.9 Hz), 2.08 (C^7H, 3H, s), 2.06 (C^7H, 3H, s) ppm; δ_C (101 MHz; chloroform-d): 171.0 (C^7), 170.4 (C^7), 129.6 (C^3), 124.3 (C^2), 73.9 (C^5), 65.4 (C^4), 65.2 C^1), 63.4 (C^6), 21.2 (C^8), 20.9 (C^8) ppm.

NMR of (2*R,*3*S*)-3-acetoxy-3,6-dihydro-2*H*-pyran-2-yl)methyl acetate

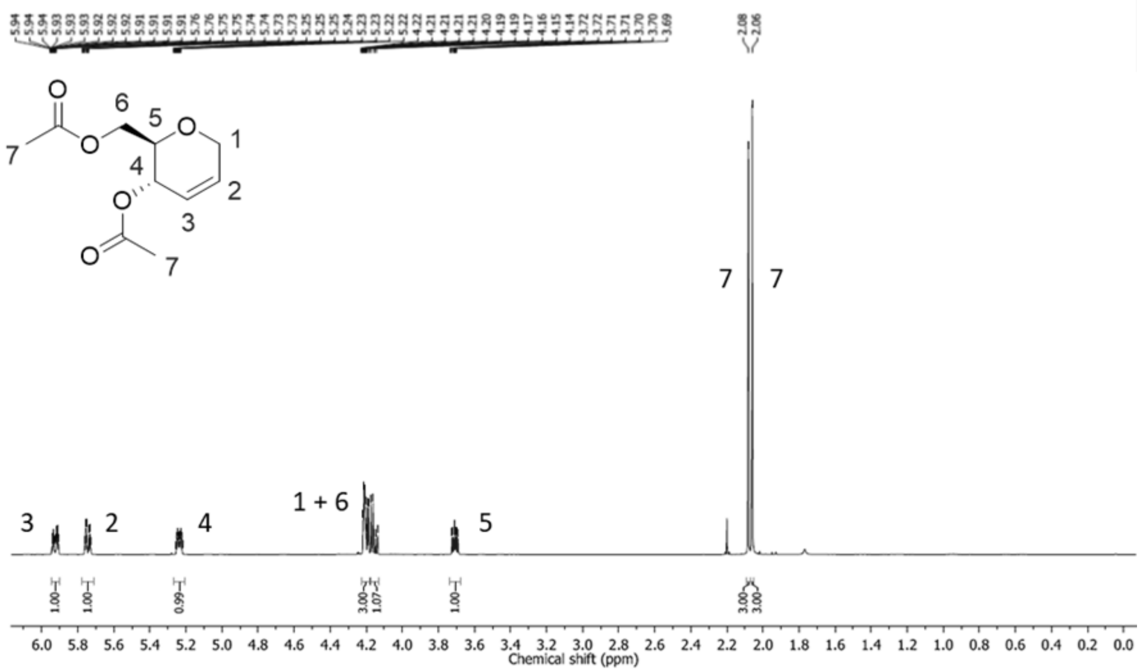

Fig. S1 Annotated ^{1}H NMR spectrum of (2R,3S)-3-acetoxy-3,6-dihydro-2H-pyran-2-yl)methyl acetate in chloroform-d.

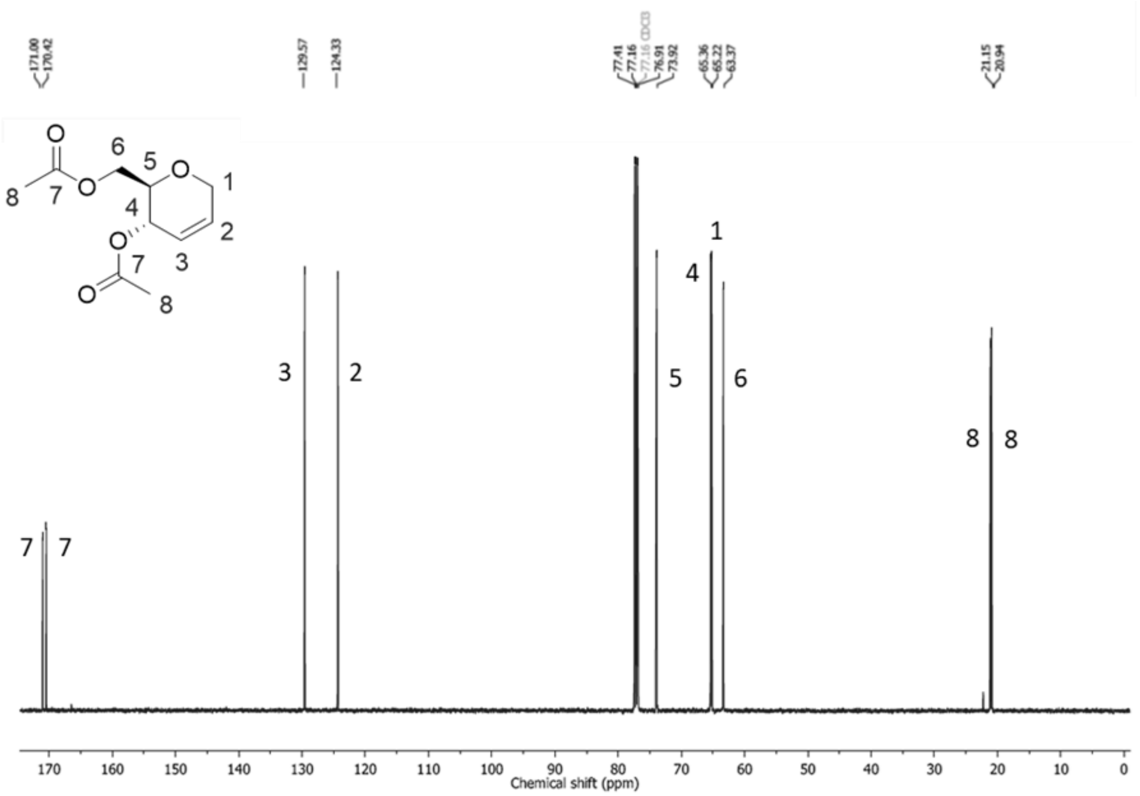

Fig. S2 Annotated ^{13}C{^{1}H} NMR spectrum of *(2*R,*3*S*)-3-acetoxy-3,6-dihydro-2*H*-pyran-2-yl)methyl acetate* in chloroform-d.

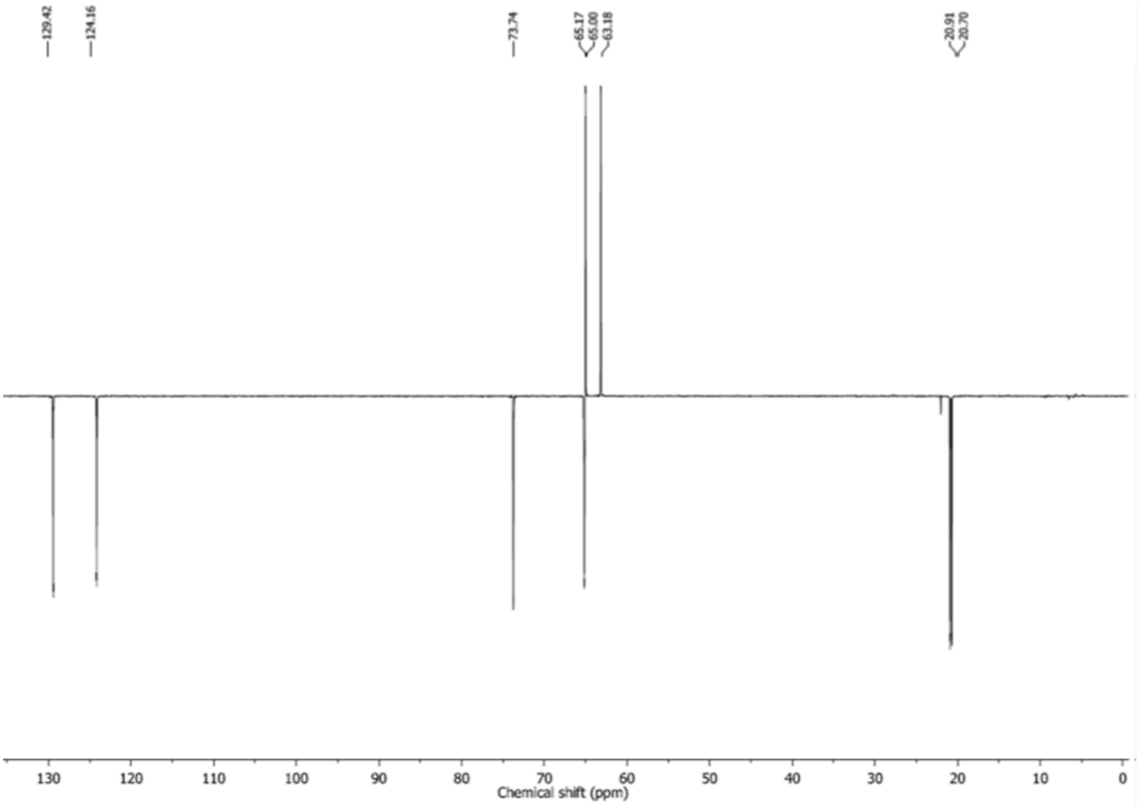

Fig. S3 $^{13}C\{^1H\}$ DEPT135 NMR spectrum of *(2*R*,3*S*)-3-acetoxy-3,6-dihydro-2*H*-pyran-2-yl)methyl acetate* in chloroform-d.

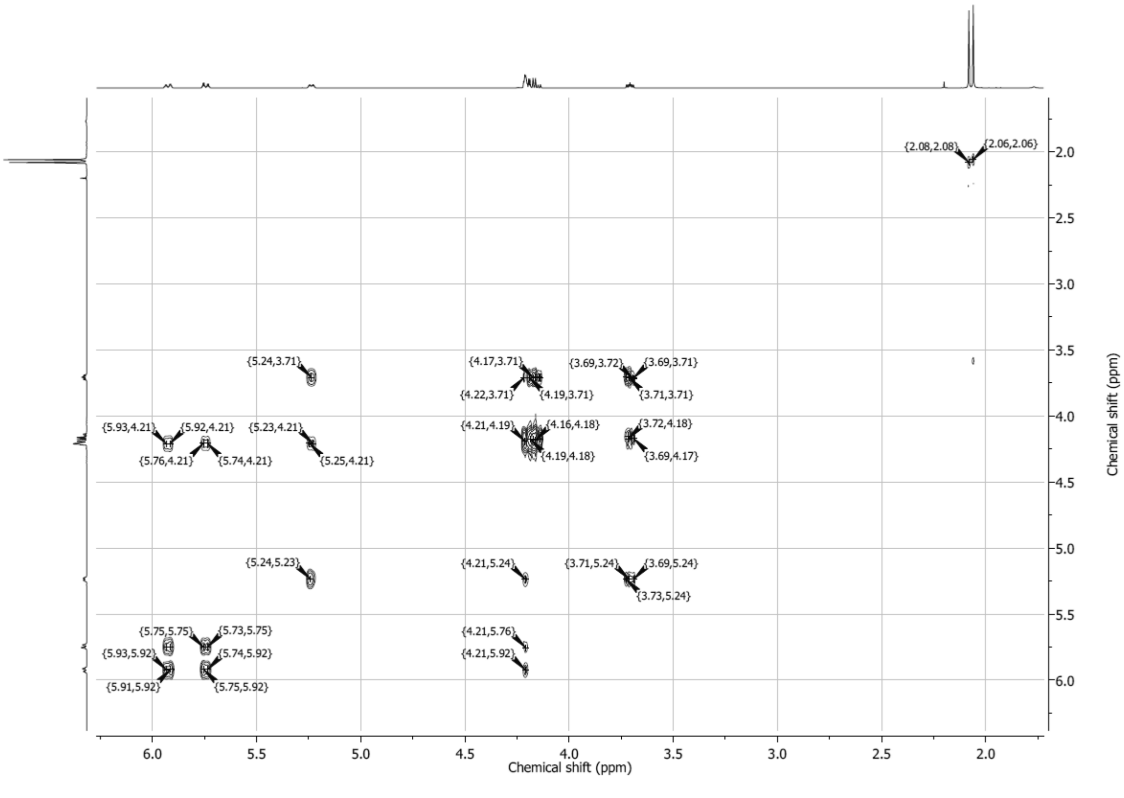

Fig. S4 COSY (^1H–^1H) NMR spectrum of *(2*R*,3*S*)-3-acetoxy-3,6-dihydro-2*H*-pyran-2-yl)methyl acetate* in chloroform-d.

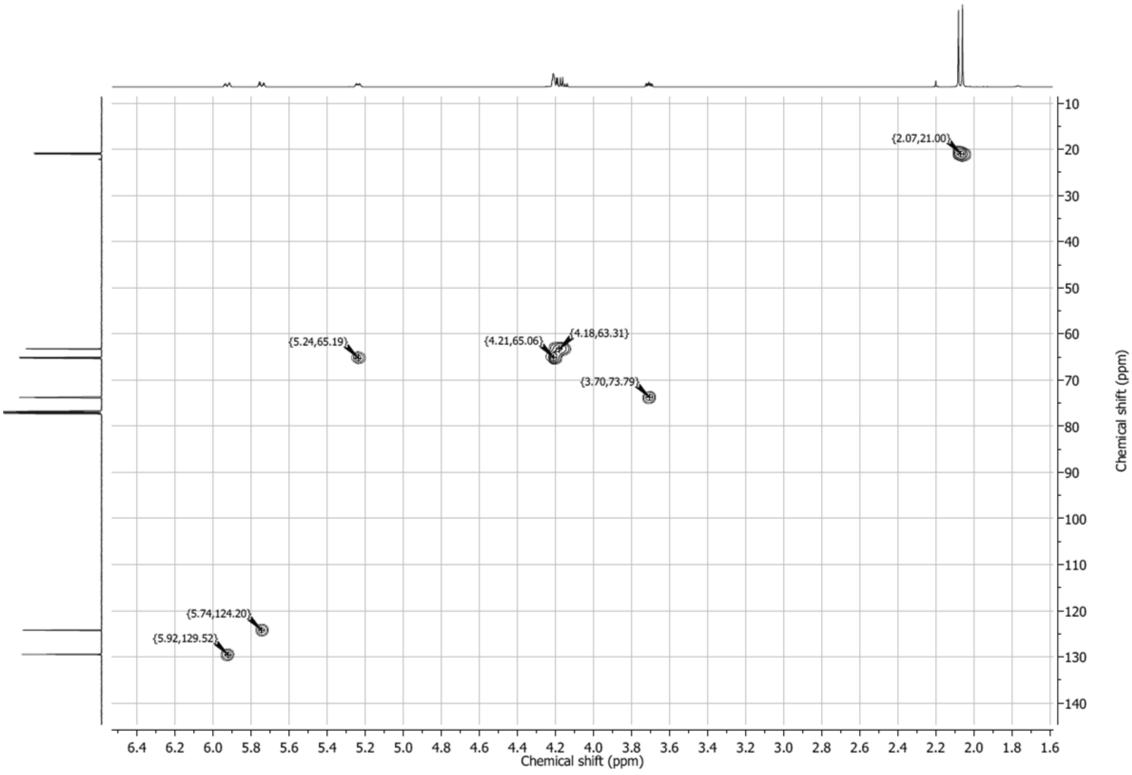

Fig. S5 HSQC (^1H–^{13}C) NMR spectrum of *(2*R*,3*S*)-3-acetoxy-3,6-dihydro-2*H*-pyran-2-yl)methyl acetate* in chloroform-d.

Synthesis of (2*R*,3*S*)-2-(hydroxymethyl)-3,6-dihydro-2*H*-pyran-3-ol

A solution of (2*R,*3*S*)-3-acetoxy-3,6-dihydro-2*H*-pyran-2-yl)methyl acetate (9.40 g, 43.9 mmol, 1.0 equiv.) in anhydrous methanol (50 mL) was treated with a solution of NaOMe (0.237 g, 4.39 mmol, 0.1 equiv.) in anhydrous methanol (2 mL) under argon and stirred at room temperature for 3 h. Once complete, ammonium chloride (0.47 g, 8.78 mmol, 0.2 equiv.) was added to the reaction and stirred for 15 mins. The reaction mixture was concentrated in *vacuo*, and then diluted with chloroform (100 mL), the resultant precipitate was removed by filtration, and the filtrate was concentrated in *vacuo* to yield a pale yellow oil (5.68 g, 99 %). Spectroscopic data was consistent with the literature.[2]

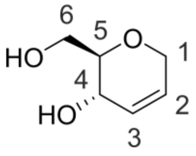

δ_H (400 MHz; chloroform-d): 5.91-5.74 (C^2H, C^3H, 2H, m), 4.24-4.12 (C^1H, C^4H, 3H, m), 3.89 (C^6H, 1H, dd, J_{HH} = 11.6, 3.8 Hz), 3.80 (C^6H, 1H, dd, J_{HH} = 11.6, 5.5 Hz), 3.34 (C^5H, 1H, ddd, J_{HH} = 8.1, 5.4, 3.9 Hz) ppm; δ_C (101 MHz; chloroform-d): 128.8 (C^3), 127.8 (C^2), 78.8 (C^5), 65.6 (C^4), 64.2 (C^1), 63.1 (C^6) ppm.

NMR of (2*R*,3*S*)-2-(hydroxymethyl)-3,6-dihydro-2*H*-pyran-3-ol

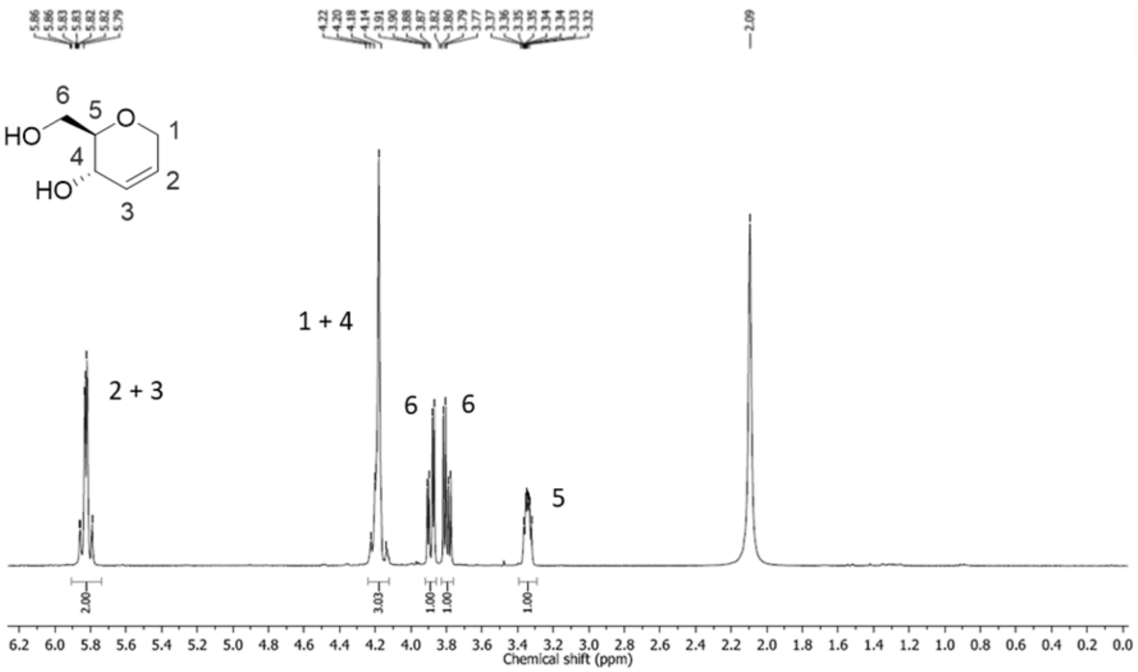

Fig. S6 Annotated ^{1}H NMR spectrum of *(2R,3S)-2-(hydroxymethyl)-3,6-dihydro-2H-pyran-3-ol* in chloroform-d.

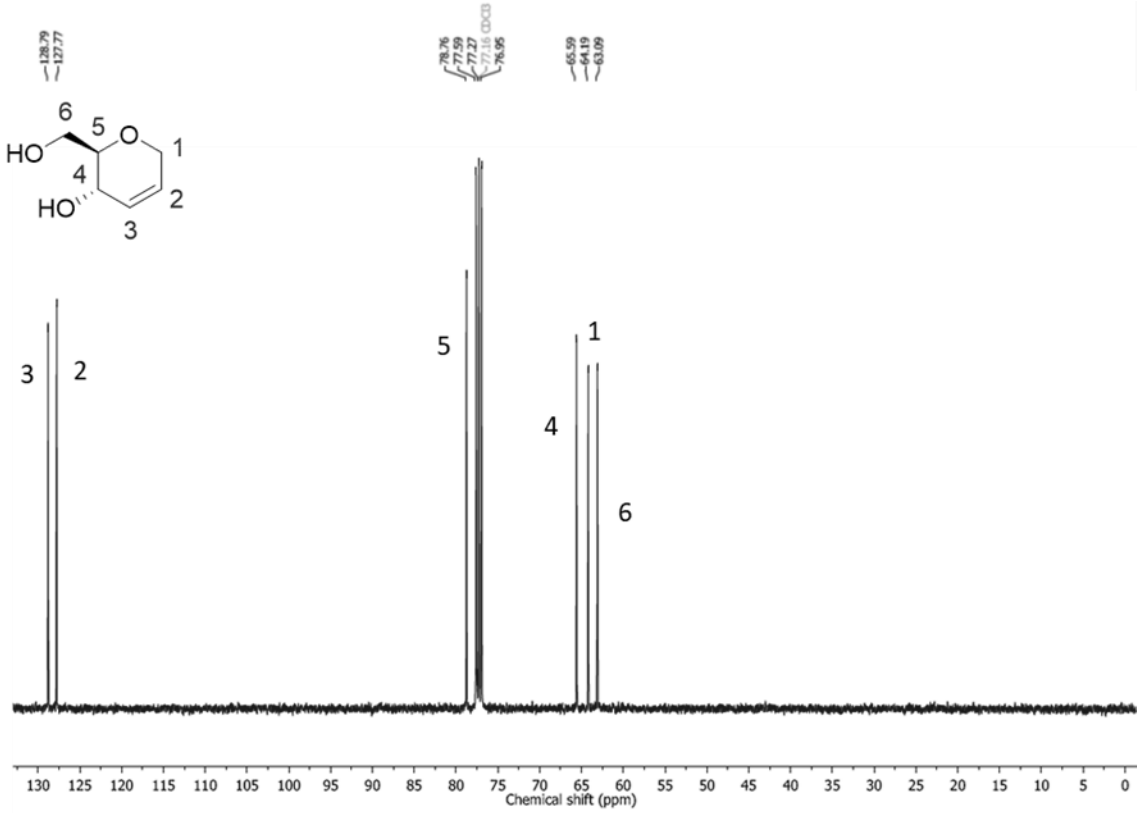

Fig. S7 Annotated ^{13}C{^{1}H} NMR spectrum of *(2R,3S)-2-(hydroxymethyl)-3,6-dihydro-2H-pyran-3-ol* in chloroform-d.

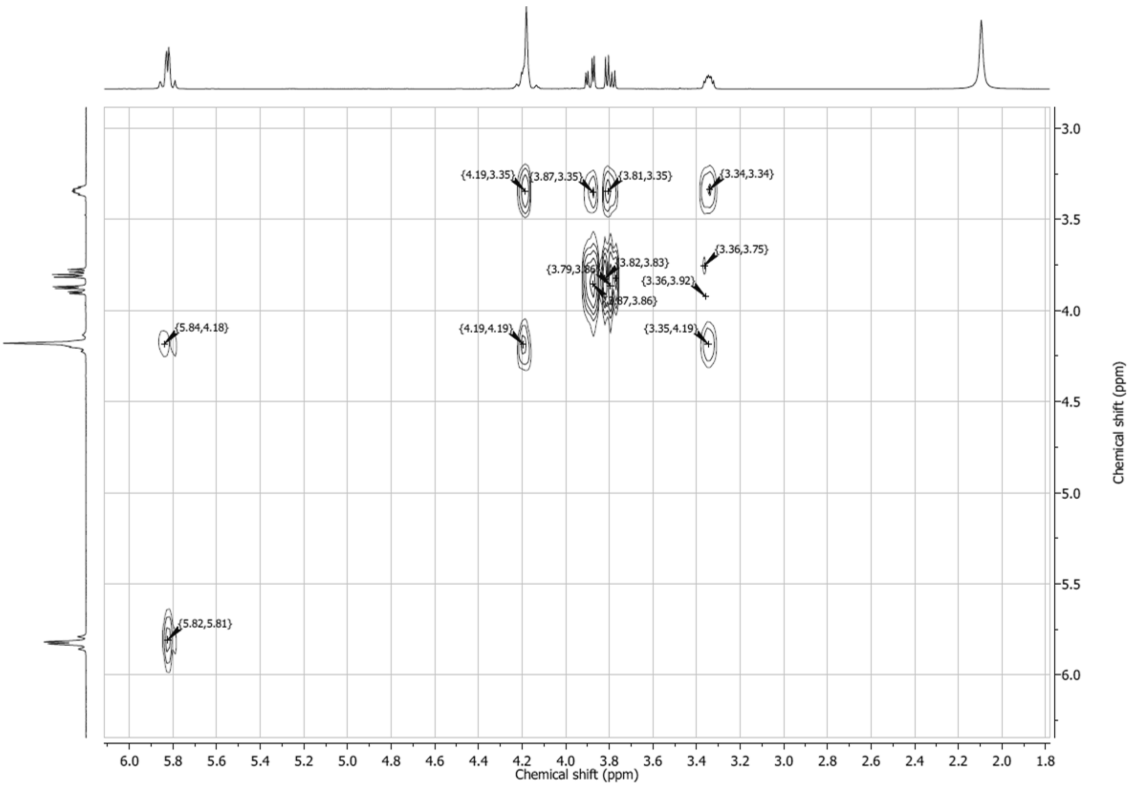

Fig. S8 COSY (^{1}H–^{1}H) NMR spectrum of *(2R,3S)-2-(hydroxymethyl)-3,6-dihydro-2H-pyran-3-ol* in chloroform-d.

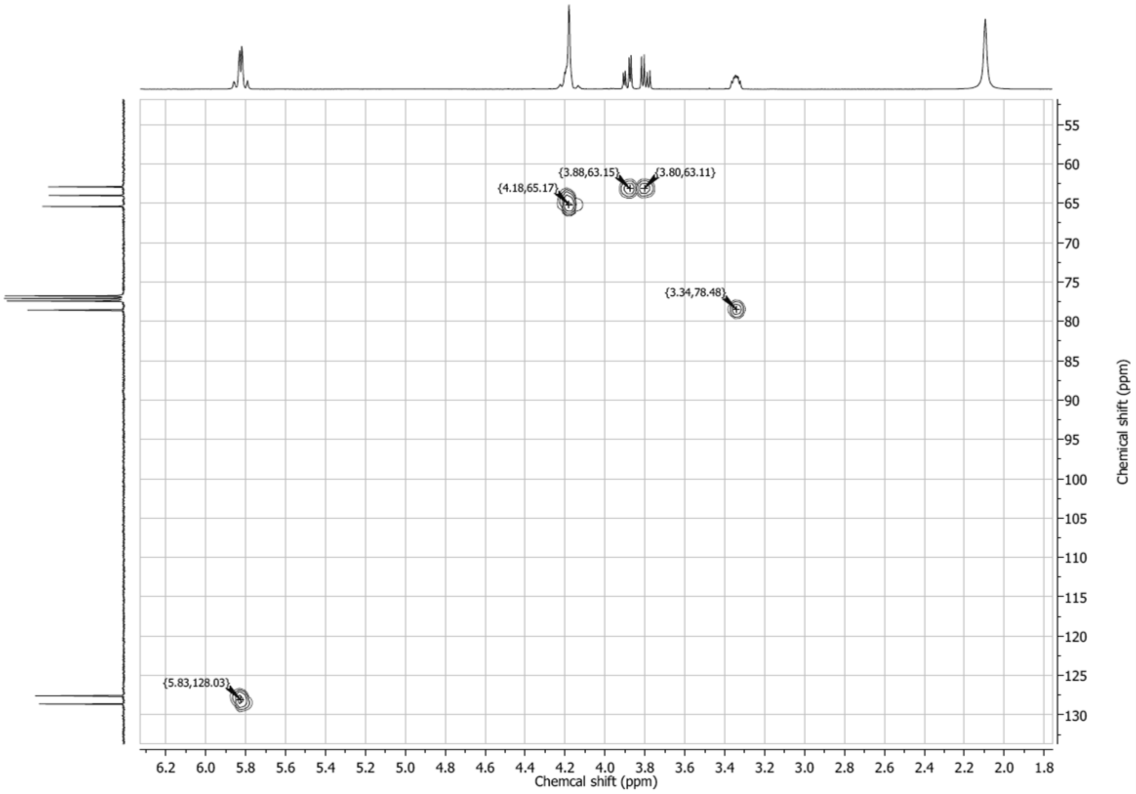

Fig. S9 HSQC (^{1}H–^{13}C) NMR spectrum of *(2R,3S)-2-(hydroxymethyl)-3,6-dihydro-2H-pyran-3-ol* in chloroform-d.

Synthesis of (2*R*,3*S*)-3-hydroxy-3,6-dihydro-2*H*-pyran-2-yl)methyl 4-methylbenzenesulfonate

(2*R*,3*S*)-2-(hydroxymethyl)-3,6-dihydro-2*H*-pyran-3-ol (4.80 g, 36.9 mmol, 1.0 equiv.) was dissolved in anhydrous pyridine (42.2 mL) and treated imminently with toluenesulfonyl chloride (7.71 g, 40.6 mmol, 1.1 equiv.) under argon. The reaction mixture was then stirred at room temperature for 20 h. Once complete, DCM (100 mL) and water (100 mL) were added to the reaction mixture. The organic phase was separated from the aqueous phase, dried with $MgSO_4$ and concentrated in *vacuo*. The crude was taken up in DCM (100 mL) and washed with $HCl_{(aq)}$ (ca. 3%, 2 x 25 mL), $NaHCO_3$ (1 mol L^{-1}, 50 mL) and water (50 mL), dried over $MgSO_4$ and concentrated in *vacuo* to yield an off-white solid, which was used directly in the next reaction without further purification (7.76 g, 74 %).

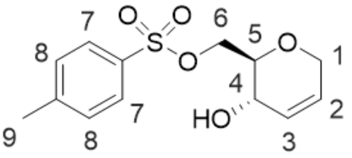

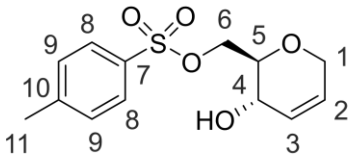

δ_H (400 MHz; chloroform-d): 7.81 (C^{7}H, 2H, d, J_{HH} = 8.4 Hz), 7.35 (C^{8}H, 2H, d, J_{HH} = 8.0 Hz), 5.84-5.75 (C^{2}H, C^{3}H, 2H, m), 4.27 (C^{1}H, 2H, d, J_{HH} = 4.0 Hz), 4.16-4.10 (C^{4}H, C^{6}H, 3H, m), 3.45 (C^{5}H, 1H, ddd, J_{HH} = 8.0, 4.0, 4.0 Hz), 2.44 (C^{9}H, 3H, s) ppm; δ_C (101 MHz; chloroform-d): 145.1 (C^{10}), 132.9 (C^7), 130.0 (C^9), 128.1 (C^8), 128.0 (C^2), 128.0 (C^3), 76.8 (C^5), 69.6 (C^6), 65.5 (C^1), 63.3 (C^4), 21.8 (C^{11}) ppm.

NMR of (2*R*,3*S*)-3-hydroxy-3,6-dihydro-2*H*-pyran-2-yl)methyl 4-methylbenzenesulfonate

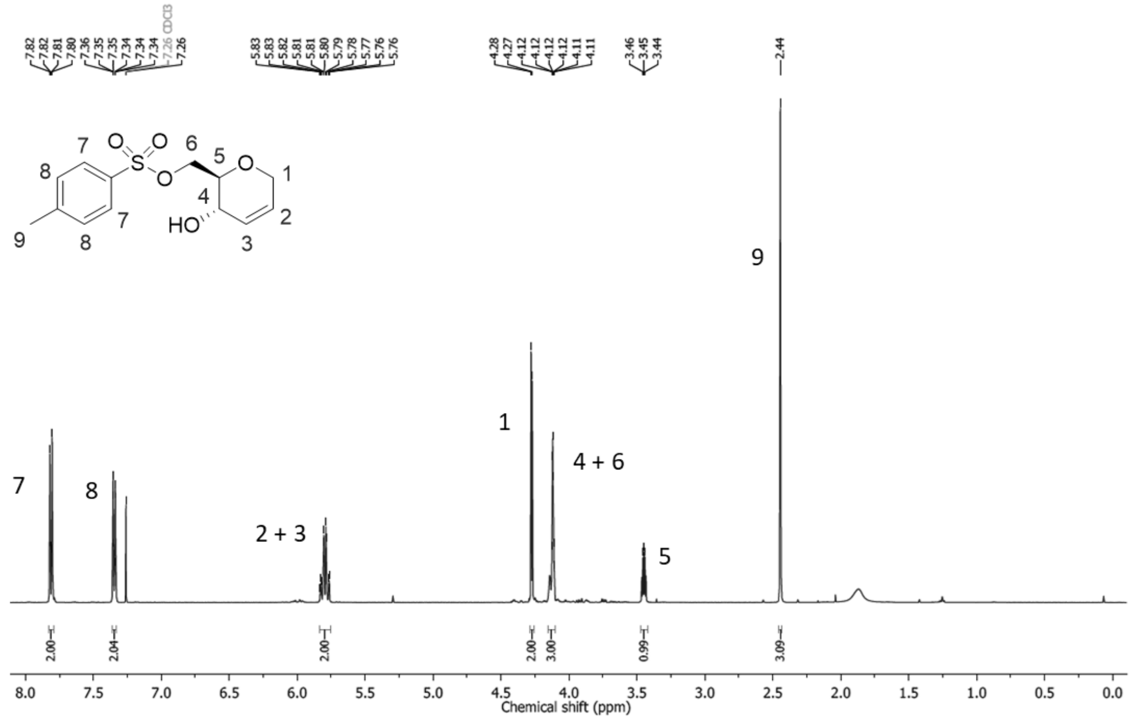

Fig. S10 Annotated ^{1}H NMR spectrum of *(2R,3S)-3-hydroxy-3,6-dihydro-2H-pyran-2-yl)methyl 4-methylbenzenesulfonate* in chloroform-d.

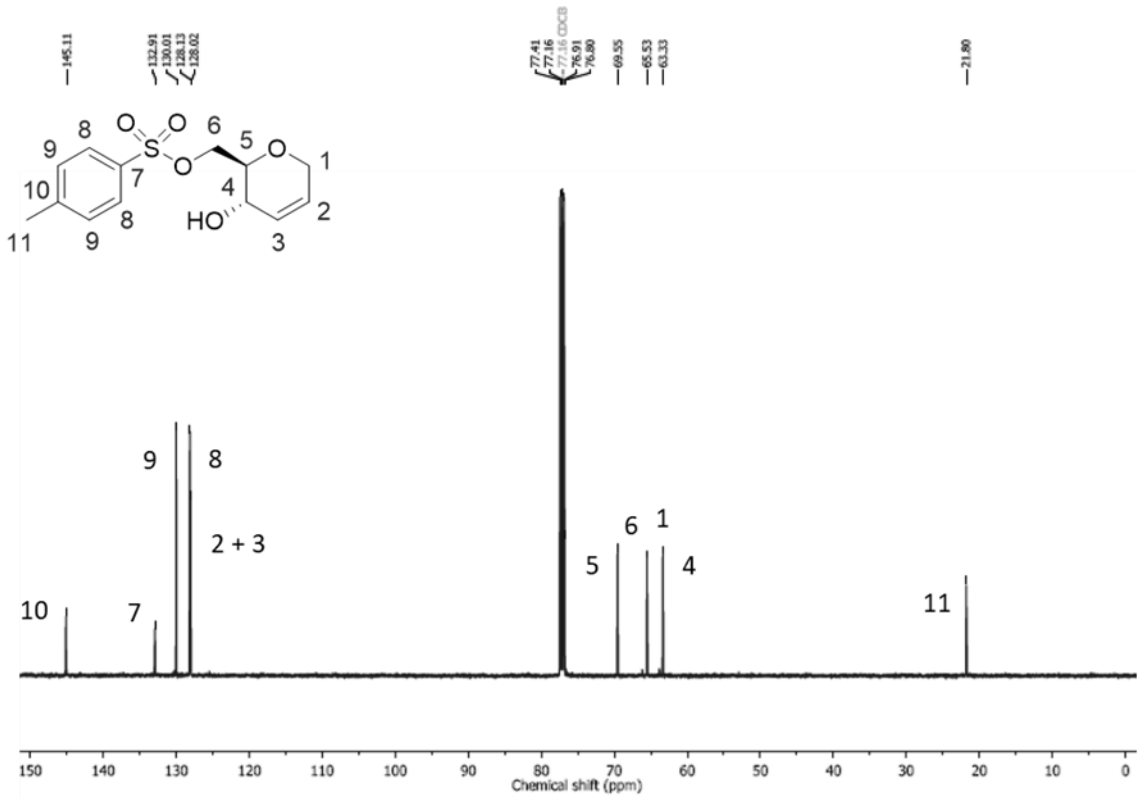

Fig. S11 Annotated $^{13}C\{^{1}H\}$ NMR spectrum of *(2R,3S)-3-hydroxy-3,6-dihydro-2H-pyran-2-yl)methyl 4-methylbenzenesulfonate* in chloroform-d.

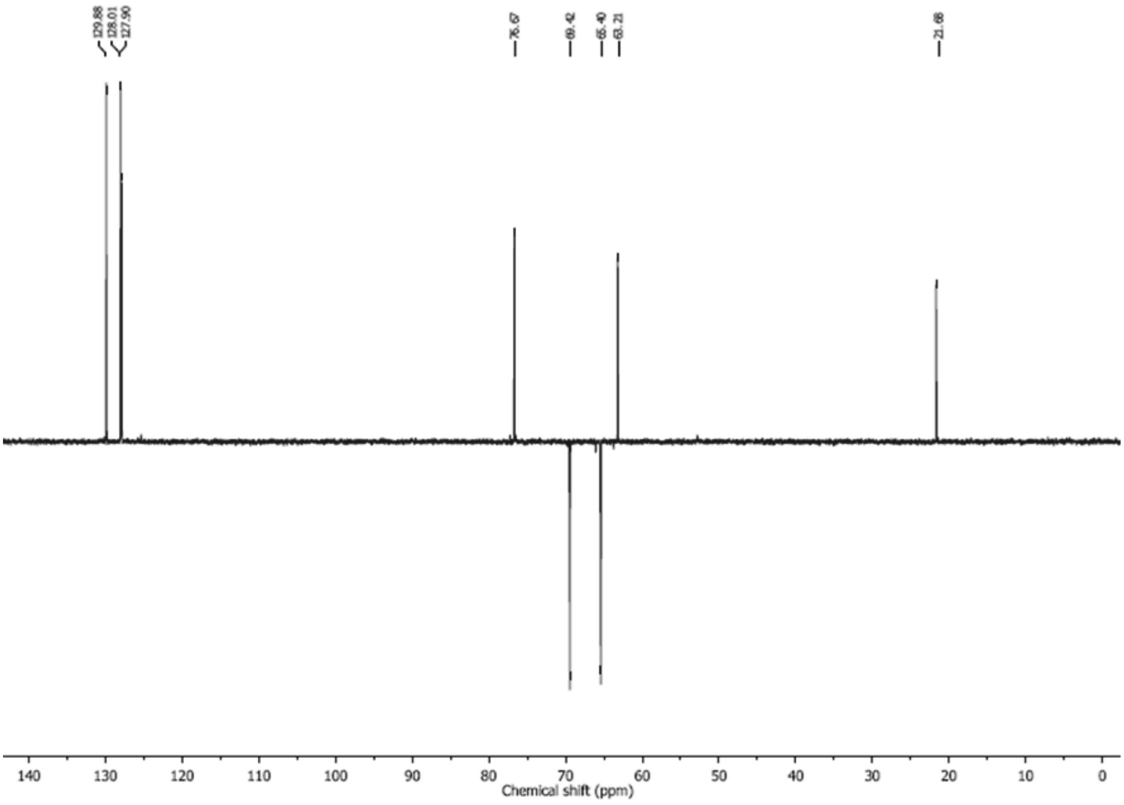

Fig. S12 $^{13}C\{^{1}H\}$ DEPT135 NMR spectrum of *(2R,3S)-3-hydroxy-3,6-dihydro-2H-pyran-2-yl)methyl 4-methylbenzenesulfonate* in chloroform-d.

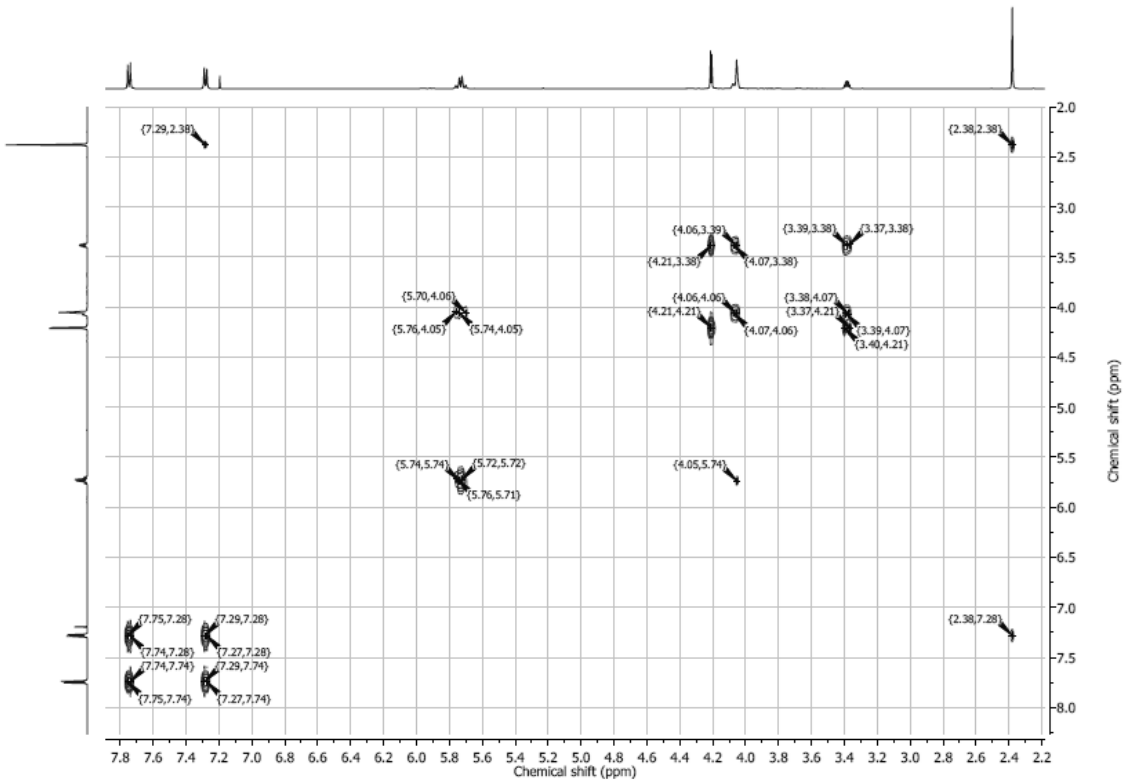

Fig. S13 COSY (^{1}H–^{1}H) NMR spectrum of *(2R,3S)-3-hydroxy-3,6-dihydro-2H-pyran-2-yl)methyl 4-methylbenzenesulfonate* in chloroform-d.

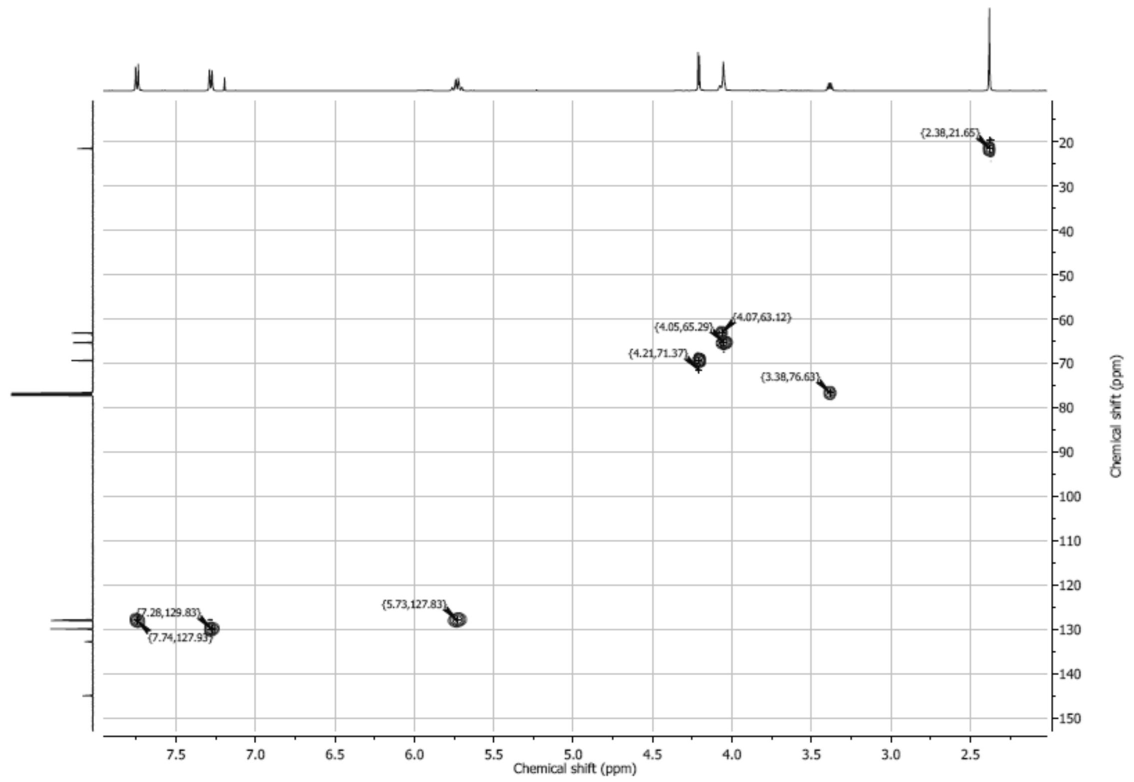

Fig. S14 HSQC (^{1}H–^{13}C) NMR spectrum of *(2R,3S)-3-hydroxy-3,6-dihydro-2H-pyran-2-yl)methyl 4-methylbenzenesulfonate* in chloroform-d.

Synthesis of (4aS,8aS)-4,4a,6,8a-tetrahydropyrano[2,3-e][1,3]oxathiine-2-thione (1)

A 0.5 mol L^{-1} solution of (2*R*,3*S*)-3-hydroxy-3,6-dihydro-2*H*-pyran-2-yl)methyl 4-methylbenzenesulfonate (7.46 g, 26.2 mmol, 1.0 equiv.) in dry THF (52.3 mL) was treated dropwise with a solution of 1 mol L^{-1} potassium tert-butoxide (26.2 mL, 26.2 mmol, 1.0 equiv.) in anhydrous THF at 0 °C under argon. Carbon disulphide (3.17 mL, 52.3 mmol, 2.0 equiv.) was then added dropwise to the reaction mixture and stirred at 0 °C for 3 h. Once complete, Et_2O (100 mL) was added and the reaction mixture was filtered through a celite pad and concentrated in *vacuo* to yield a murky yellow precipitate. The crude product was purified *via* flash column chromatography on SiO_2 using a DCM mobile phase, the filtrate was concentrated in *vacuo* to yield small yellow crystals (3.94 g, 80 %). The product was purified further by recrystallization using absolute ethanol, and isolated *via* filtration as pale-yellow crystals.

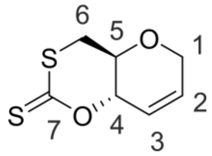

δ_H (400 MHz; chloroform-d): 6.07-5.9 (C^2H, C^3H, 2H, m), 4.82-4.75 (C^4H, 1H, m), 4.36-4.30 (C^1H, 1H, m), 4.30-4.24 (C^1H, 1H, m), 3.89 (C^5H, 1H, ddd, J_{HH} = 10.1, 8.4, 6.2 Hz), 3.18-3.10 (C^6H, 2H, m) ppm; δ_C (101 MHz; chloroform-d): 207.6 (C^7), 130.4 (C^2), 122.8 (C^3), 77.8 (C^4), 68.4 (C^5), 66.2 (C^1), 35.0 (C^6) ppm. ν_{max} (cm^{-1}): 2850 (CH), 1180 (C(S)SO), 1010 (CS).

NMR of (4aS,8aS)-4,4a,6,8a-tetrahydropyrano[2,3-e][1,3]oxathiine-2-thione (1)

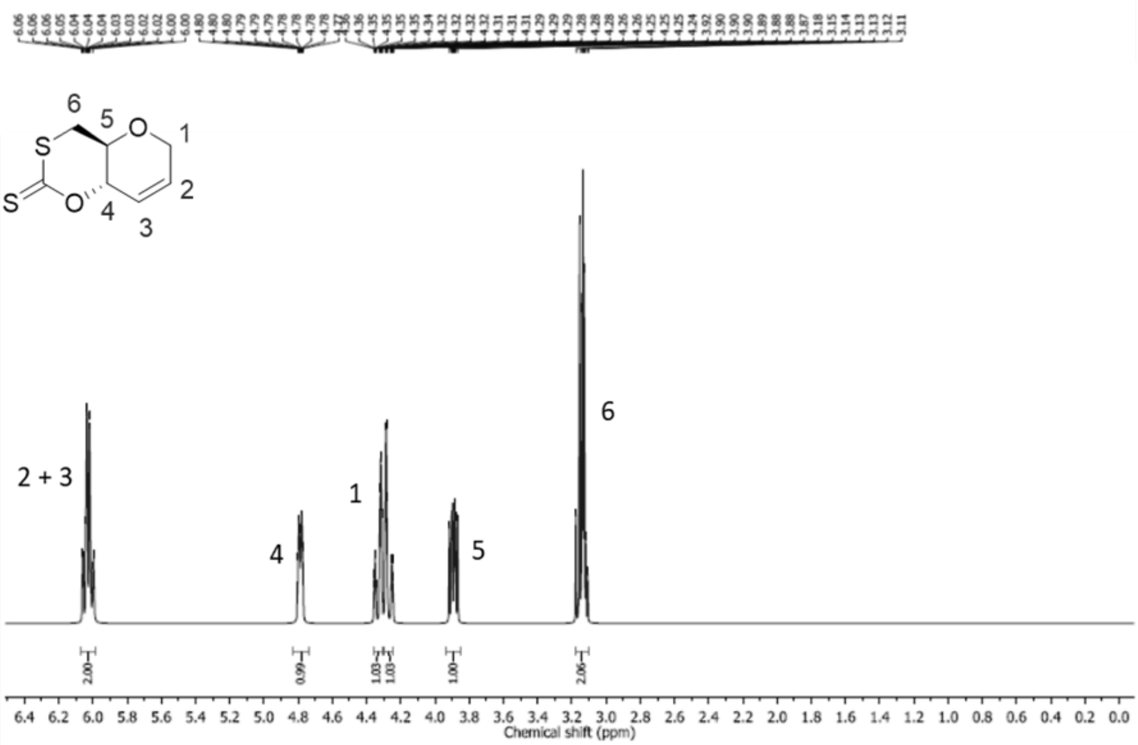

Fig. S15 Annotated ^1H NMR spectrum of **1** in chloroform-d.

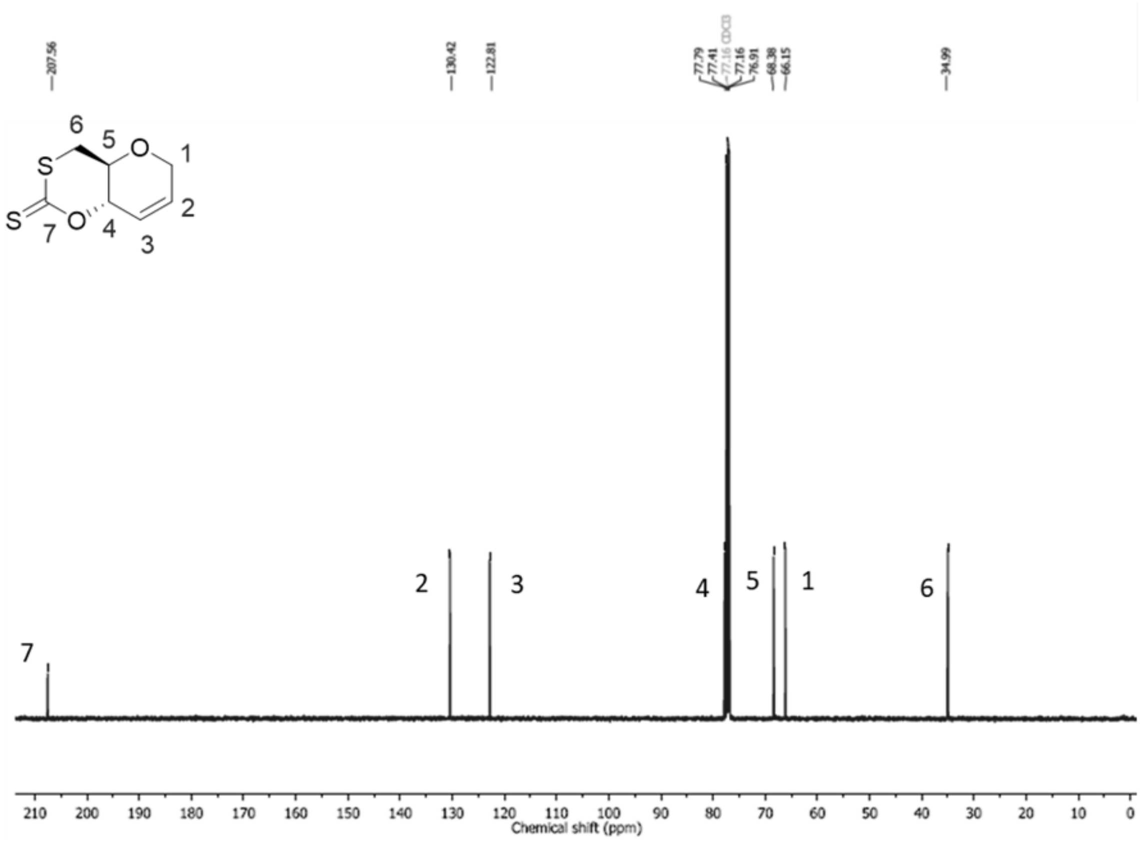

Fig. S16 Annotated $^{13}C\{^1H\}$ NMR spectrum of **1** in chloroform-d.

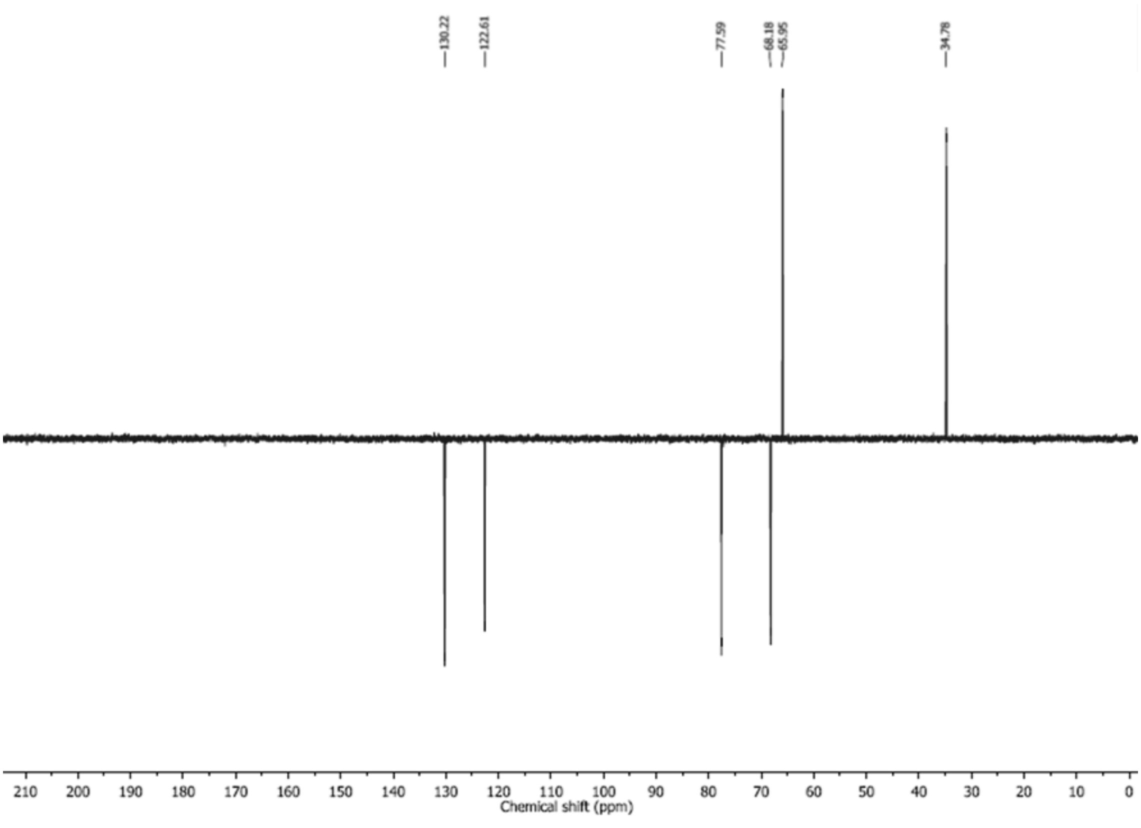

Fig. S17 $^{13}C\{^1H\}$ DEPT135 NMR spectrum of **1** in chloroform-d.

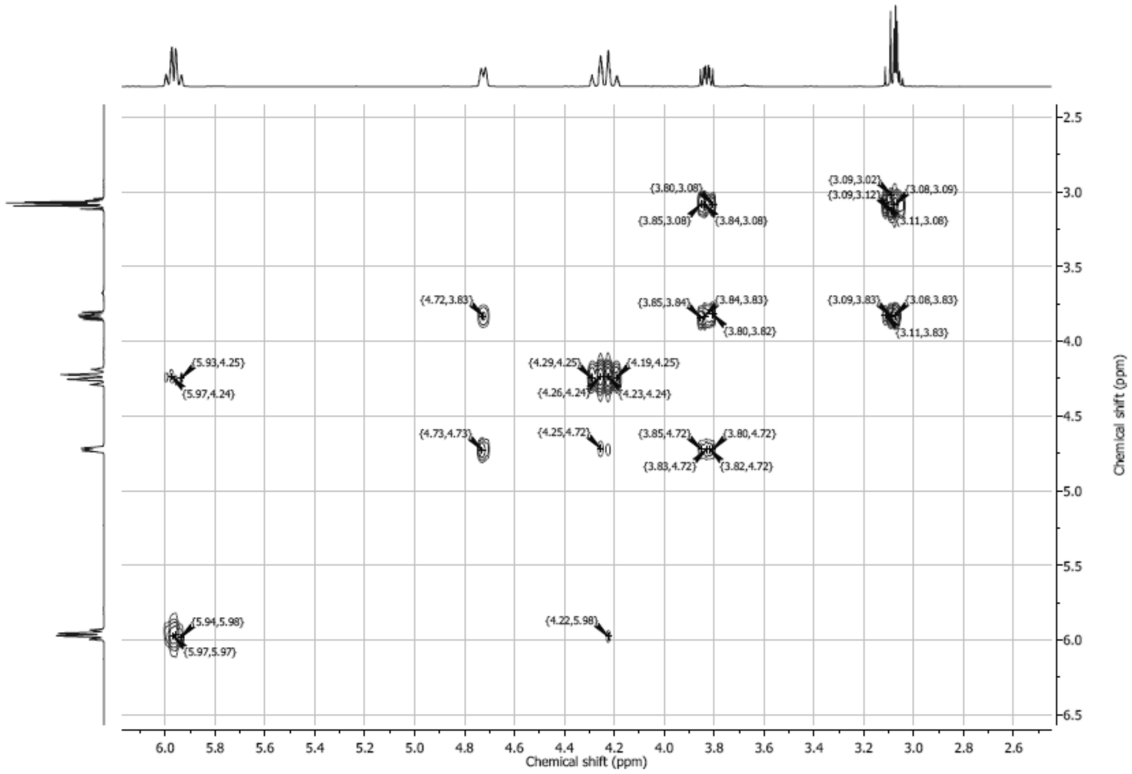

Fig. S18 COSY (^1H–^1H) NMR spectrum of **1** in chloroform-d.

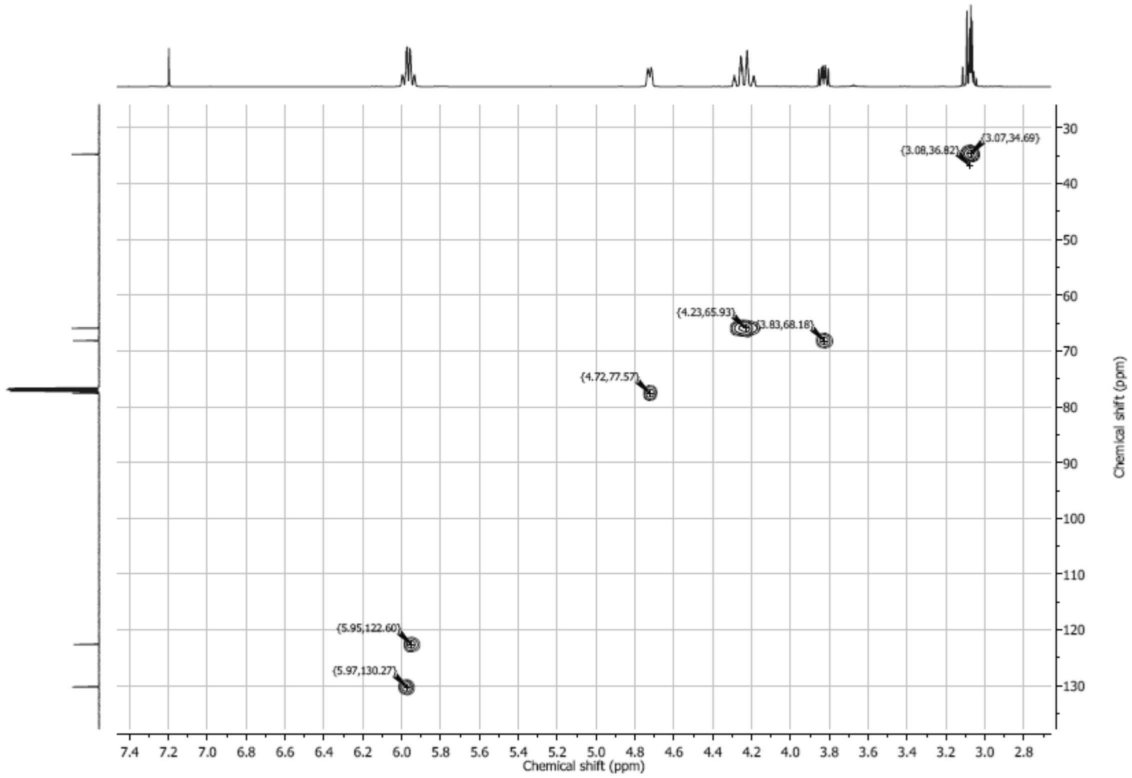

Fig. S19 HSQC (^1H–^{13}C) NMR spectrum of **1** in chloroform-d.

FT-IR of (4aS,8aS)-4,4a,6,8a-tetrahydropyrano[2,3-e][1,3]oxathiine-2-thione (1)

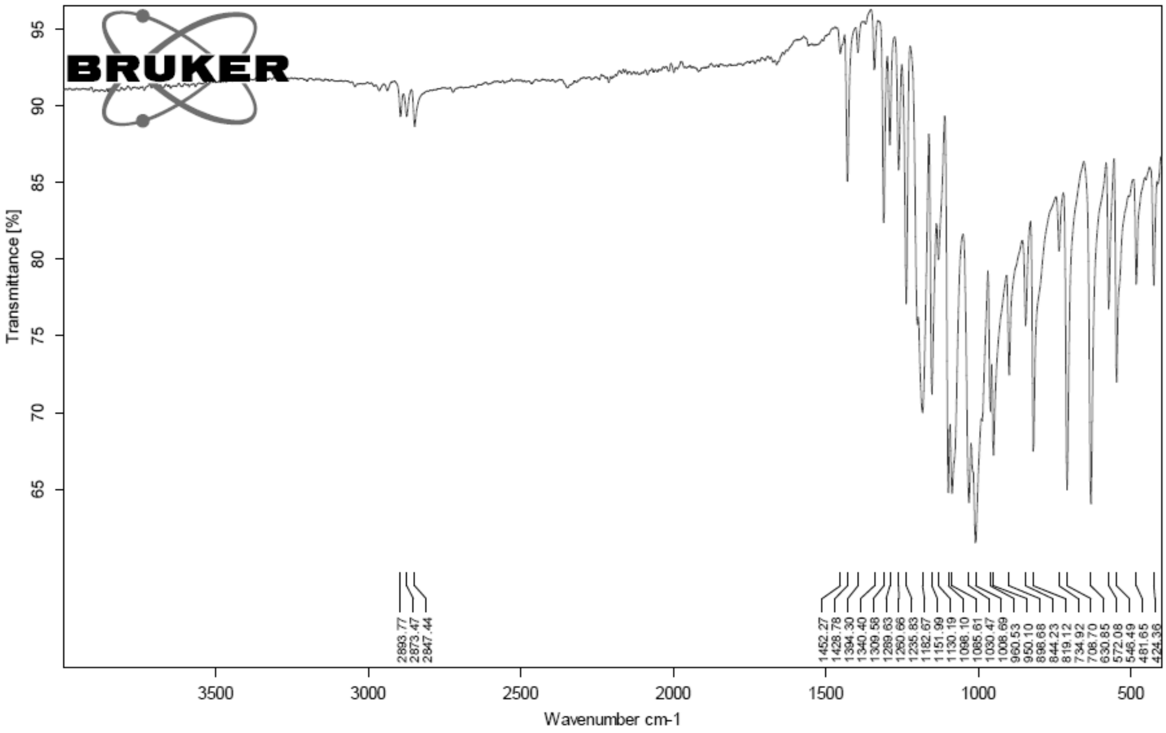

Fig. S20 Labelled FT-IR spectrum of **1**.

DSC of (4aS,8aS)-4,4a,6,8a-tetrahydropyrano[2,3-e][1,3]oxathiine-2-thione (1)

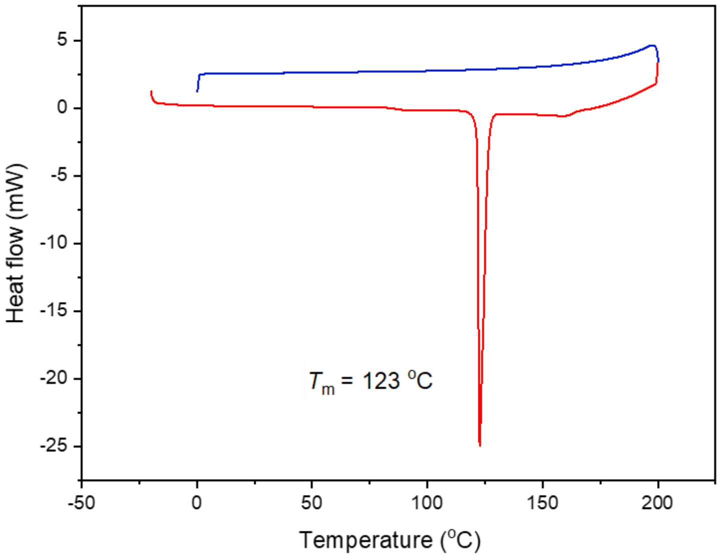

Fig. S21 DSC trace of **1**, first heating and cooling cycles between -20 and 200 °C. Single exothermic peak, corresponding to the melting temperature (T_m) = 123 °C of the monomer.

TGA of (4aS,8aS)-4,4a,6,8a-tetrahydropyrano[2,3-e][1,3]oxathiine-2-thione (1)

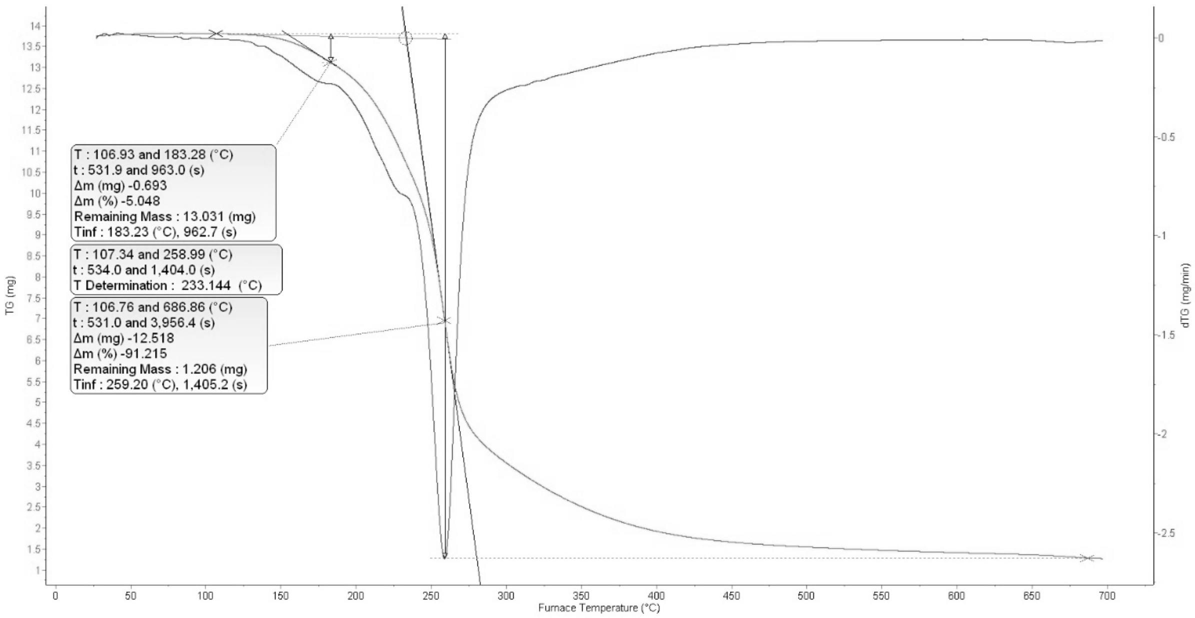

Fig. S22 TGA trace of monomer **1**. The monomer was heated from 30 to 700 °C under argon at 10 °C min^{-1}. Obtained values: $T_{d5\%}$ = 183 °C and $T_{d,max}$ = 259 °C with 9% char remaining at 700 °C.

Crystal Data and Structure Refinement for 1 (CCDC Number - 2089243)

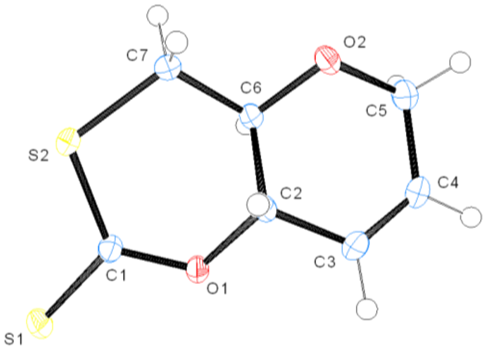

Fig. S23 ORTEP drawing of the crystal structure of **1** with thermal ellipsoids at the 50% probability level. Selected bond lengths and dihedral angles (°): S(1)–C(1) 1.646 (2), S(2)–C(1) 1.733 (2), S(2)–C(7) 1.819 (2), O(1)–C(1) 1.333 (2), O(1)–C(2) 1.458 (3), C(1) –S(2)–C(7) 106.63 (10), C(1)–O(1)–C(2) 120.23 (16), O(1)–C(1)–S(1) 119.06 (15), O(1)–C(1)–S(2) 122.85 (15), S(1)–C(1)–S(2) 118.08 (12).

Identification code	e20ab1	
Empirical formula	$C_7 H_8 O_2 S_2$	
Formula weight	188.25	
Temperature	150.00(10) K	
Wavelength	0.71073 Å	
Crystal system	Orthorhombic	
Space group	$P2_12_12_1$	
Unit cell dimensions	a = 6.2400(3) Å	α = 90°.
	b = 7.3164(4) Å	β = 90°.
	c = 17.7083(8) Å	γ = 90°.
Volume	808.46(7) $Å^3$	
Z	4	
Density (calculated)	1.547 Mg/m^3	
Absorption coefficient	0.601 mm^{-1}	
F(000)	392	
Crystal size	0.429 x 0.327 x 0.101 mm^3	
Theta range for data collection	3.462 to 30.268°.	
Index ranges	-8<=h<=8, -8<=k<=10, -25<=l<=24	
Reflections collected	7475	
Independent reflections	2183 [R(int) = 0.0277]	
Completeness to theta = 25.242°	99.8 %	
Absorption correction	Semi-empirical from equivalents	
Max. and min. transmission	1.00000 and 0.90790	
Refinement method	Full-matrix least-squares on F^2	
Data / restraints / parameters	2183 / 0 / 100	
Goodness-of-fit on F^2	1.094	
Final R indices [I>2sigma(I)]	R1 = 0.0328, wR2 = 0.0673	
R indices (all data)	R1 = 0.0382, wR2 = 0.0692	
Absolute structure parameter	-0.02(5)	
Extinction coefficient	n/a	
Largest diff. peak and hole	0.388 and -0.337 e.$Å^{-3}$	

Independent reflections	1504 [R(int) = 0.0243]
Completeness to theta = 67.684°	99.9 %
Absorption correction	Gaussian
Max. and min. transmission	1.000 and 0.136
Refinement method	Full-matrix least-squares on F^2
Data / restraints / parameters	1504 / 1 / 100
Goodness-of-fit on F^2	1.065
Final R indices [I>2sigma(I)]	R1 = 0.0281, wR2 = 0.0738
R indices (all data)	R1 = 0.0281, wR2 = 0.0738
Absolute structure parameter	0.014(17)
Extinction coefficient	n/a
Largest diff. peak and hole	0.353 and -0.330 e.Å^{-3}

2. General Polymerisation Procedures

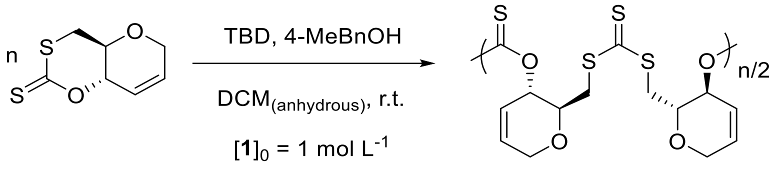

Under an argon atmosphere 4-MeBnOH (16 µL, 0.5 mol L^{-1} in anhydrous DCM, 0.008 mmol, 1.0 equiv.) and TBD (16 µL, 0.5 mol L^{-1} in anhydrous DCM, 0.008 mmol, 1.0 equiv.) were added to a solution of monomer **1** (0.150 g, 0.797 mmol, 100 equiv.) in anhydrous DCM (0.80 mL, 1.0 mol L^{-1}). The mixture was stirred at room temperature for 24 h and quenched by the addition of a benzoic acid solution (≈30 equiv.). The solvent removed under reduced pressure and the crude solid was dissolved in $CHCl_3$ and precipitated from Et_2O. The product was isolated by centrifugation (3500 rpm, 2 x 5 minutes), washed twice with Et_2O and dried under vacuum. The polymer was isolated as a pale-yellow solid.

δ_H (500 MHz; chloroform-d): 6.02-5.92 (C^2H, C^3H, 2H, m), 5.75-5.68 (C^4H, 1H, m), 4.30-4.12 (C^1H, 2H, m), 3.98-3.80 (C^5H, C^6H, 2H, m), 3.68-3.58 (C^6H, 1H, m) ppm; δ_C (126 MHz; chloroform-d): 223.2 (C^7), 194.1 (C^8), 130.7 (C^2), 122.8 (C^3), 76.3 (C^5), 73.7 (C^4), 65.0 (C^1), 38.6 (C^6) ppm. ν_{max} (cm^{-1}): 2830 (CH), 1270 ($C(S)S_2$), 1220 ($C(S)O_2$), 1070 (CS).

NMR Spectroscopic Characterisation of the Polymer Derived from 1

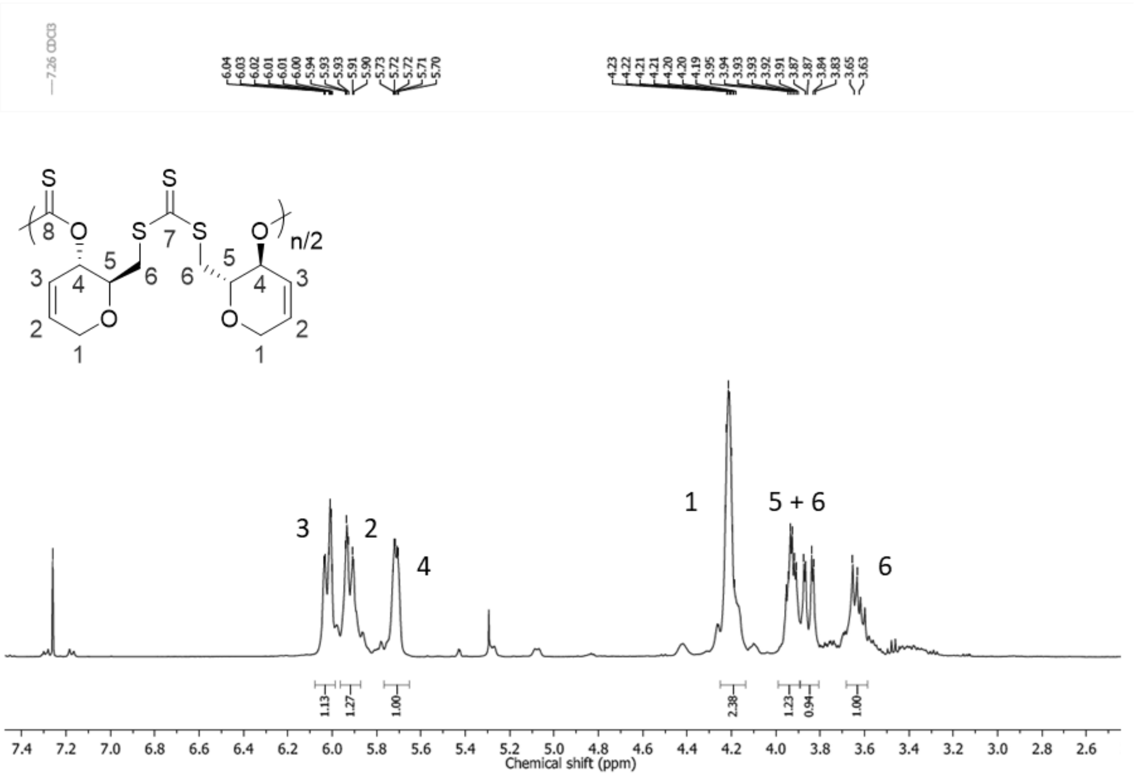

Fig. S24 Annotated ^{1}H NMR of poly(**1**) (M_n 8700 g mol^{-1} ($Đ$ 1.8)) in chloroform-d (Table 1, Run 4).

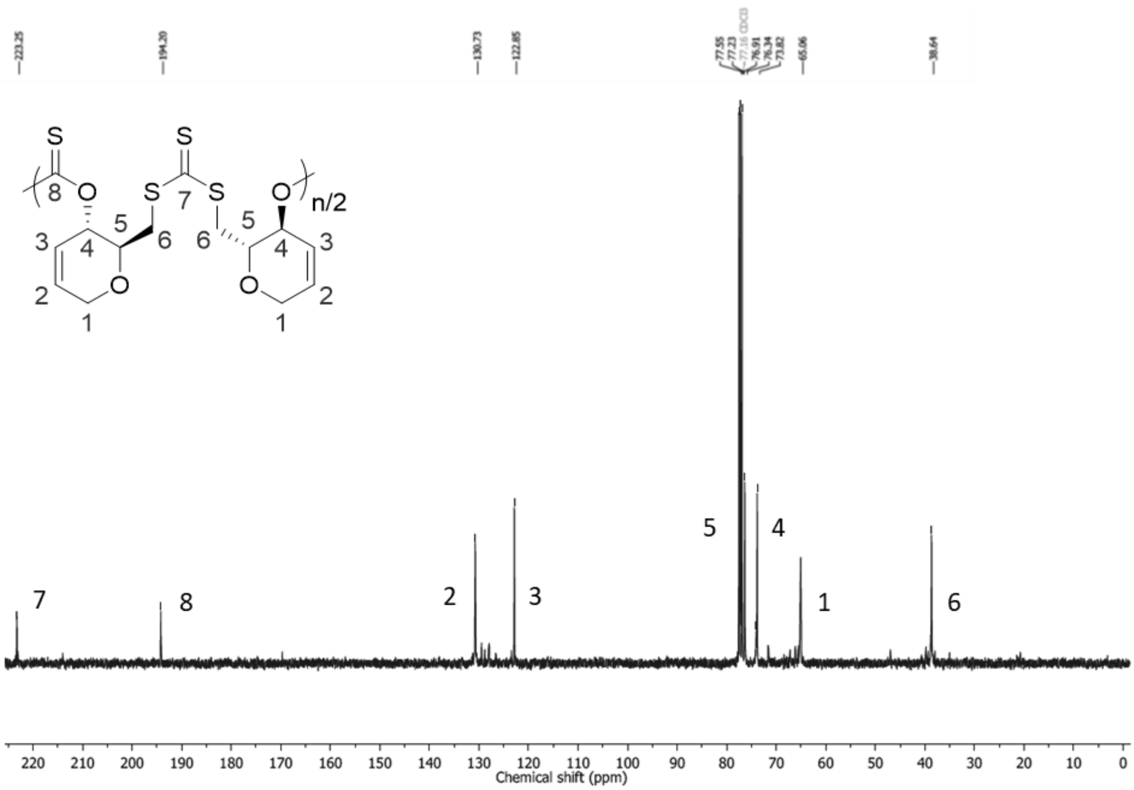

.

Fig. S25 Annotated $^{13}C\{^{1}H\}$ NMR of poly(**1**) (M_n 8700 g mol^{-1} (*Đ* 1.8)) in chloroform-d (Table 1, Run 4).

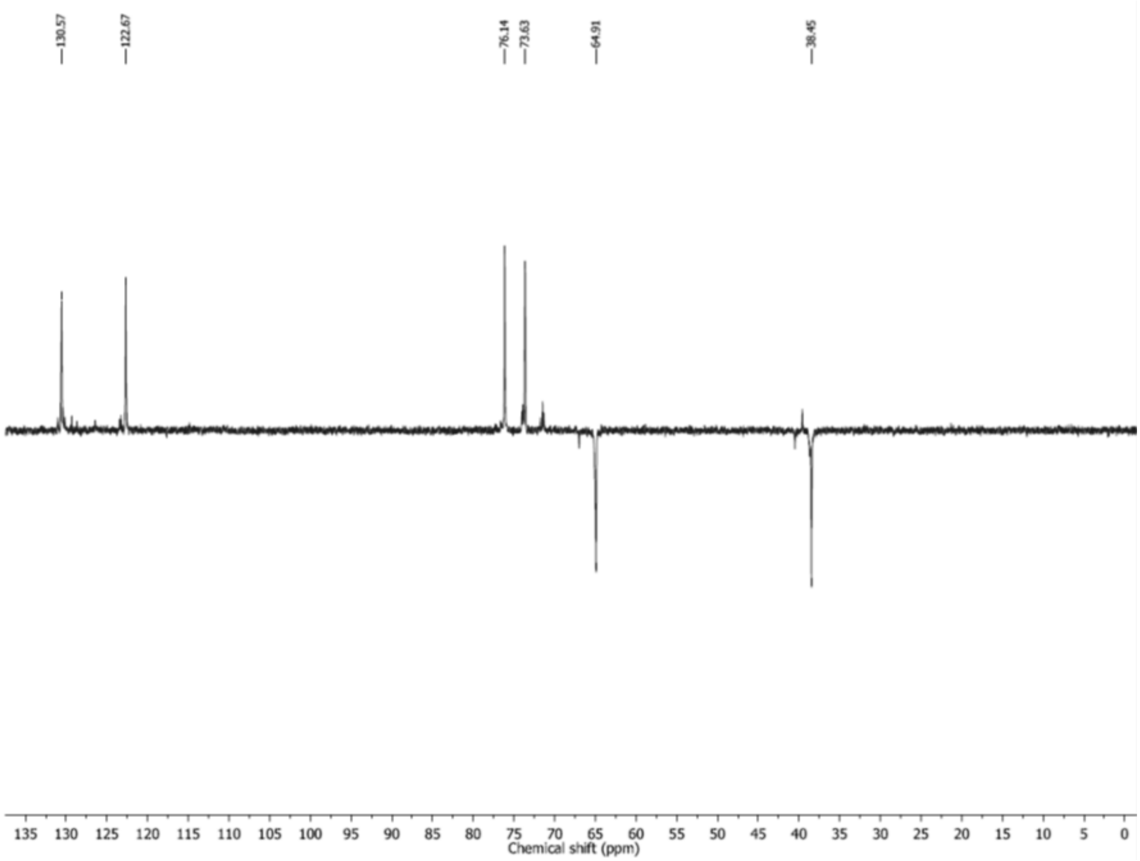

Fig. S26 $^{13}C\{^{1}H\}$ DEPT135 NMR spectrum of poly(**1**) (M_n 8700 g mol^{-1} (*Đ* 1.8)) in chloroform-d (Table 1, Run 4).

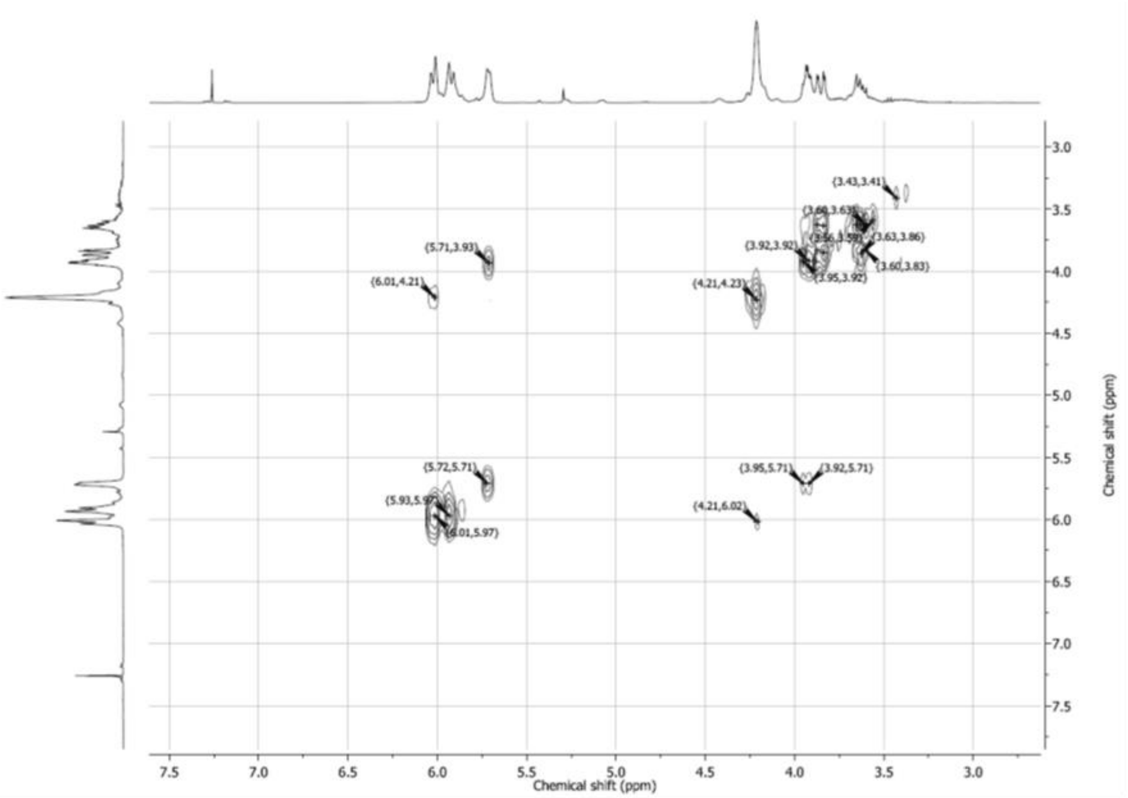

Fig. S27 COSY (^1H–^1H) NMR spectrum of poly(**1**) (*M*$_n$ 8700 g mol^{-1} (*Đ* 1.8)) in chloroform-d (Table 1, Run 4).

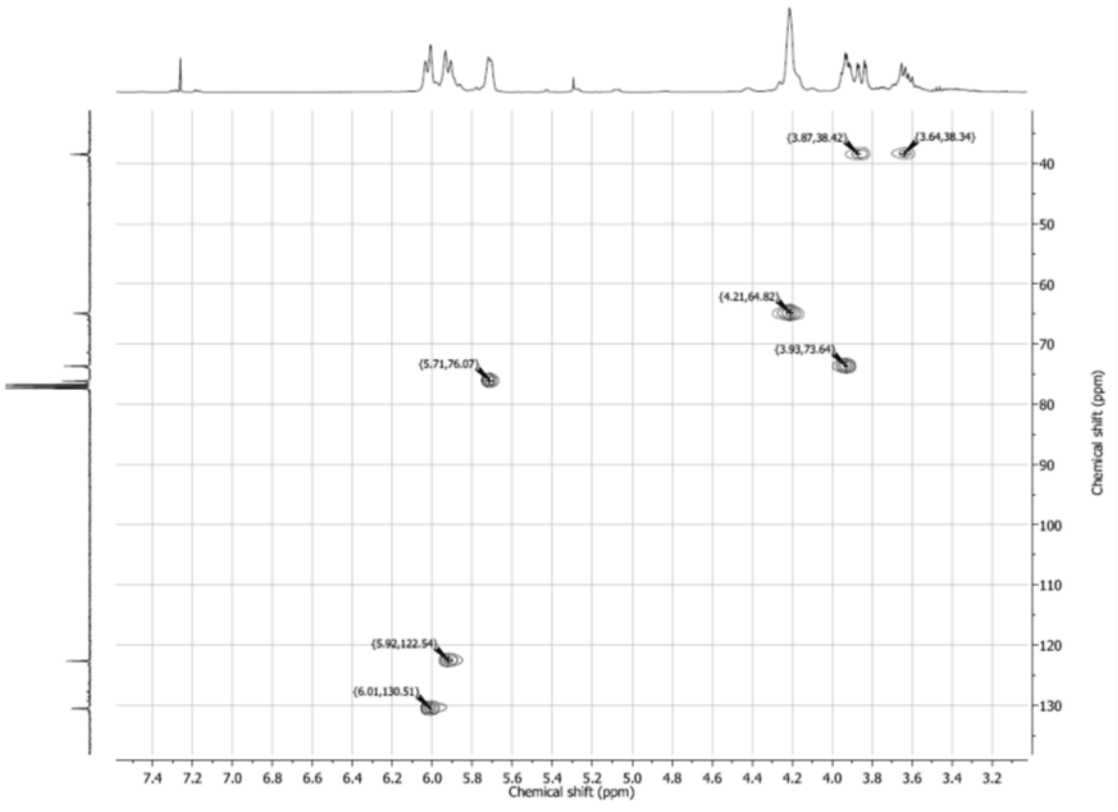

Fig. S28 HSQC (^1H–^{13}C) NMR spectrum of poly(**1**) (*M*$_n$ 8700 g mol^{-1} (*Đ* 1.8)) in chloroform-d (Table 1, Run 4).

FT-IR of the Polymer Derived from 1

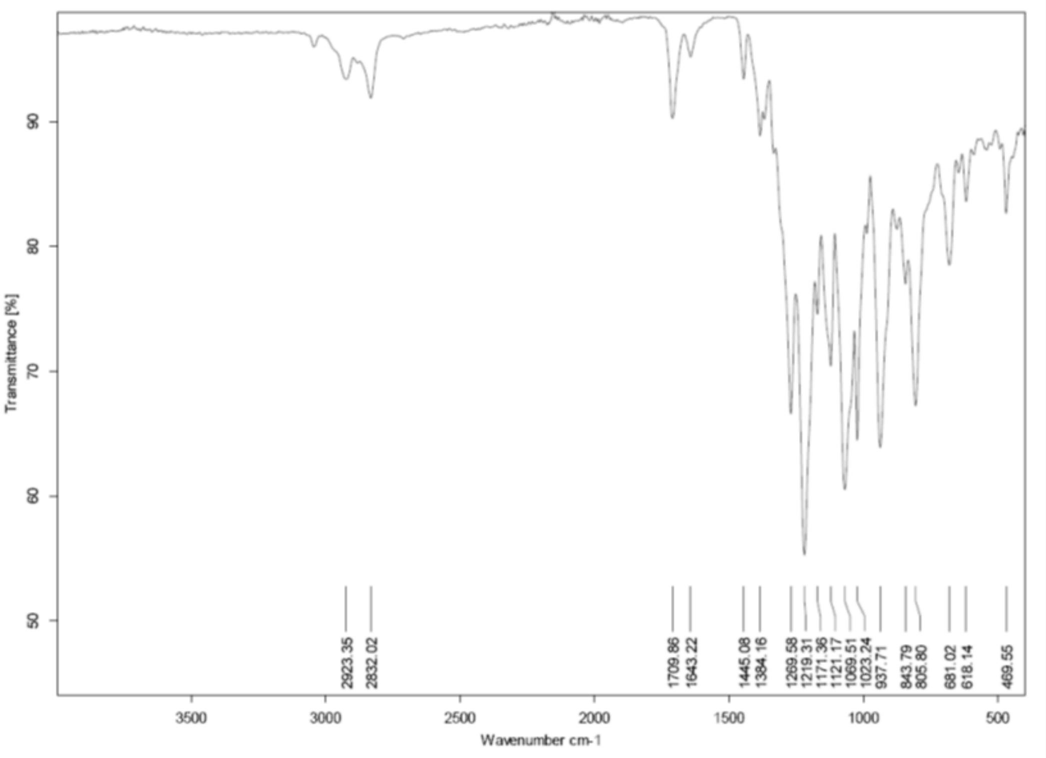

Fig. S29 Labelled FT-IR spectrum of poly(**1**) (M_n 8700 g mol^{-1} ($Đ$ 1.8)) (Table 1, Run 4).

Size-Exclusion Chromatography of the Polymer Derived from 1

Molecular Weight Averages

Peak	Mp (g/mol)	Mn (g/mol)	Mw (g/mol)	Mz (g/mol)	Mz+1 (g/mol)	Mv (g/mol)	PD
Peak 1	15189	8722	15256	23031	31072	21891	1.749

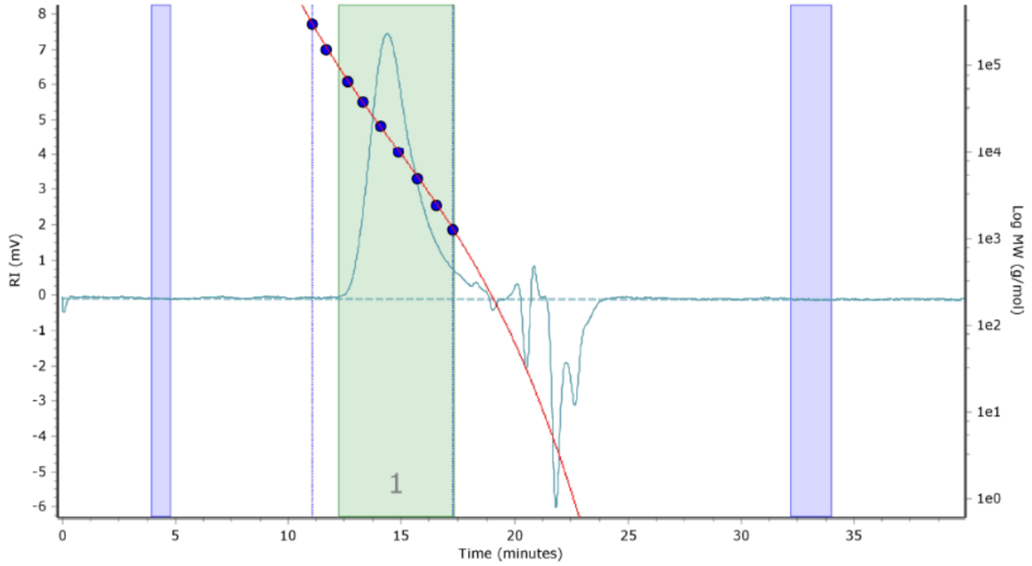

Fig. S30 SEC trace of poly(**1**) (M_n 8700 g mol^{-1} ($Đ$ 1.8)) (Table 1, Run 4).

Molecular Weight Averages

Peak	Mp (g/mol)	Mn (g/mol)	Mw (g/mol)	Mz (g/mol)	Mz+1 (g/mol)	Mv (g/mol)	PD
Peak 1	19343	10909	19993	31146	42699	29503	1.833

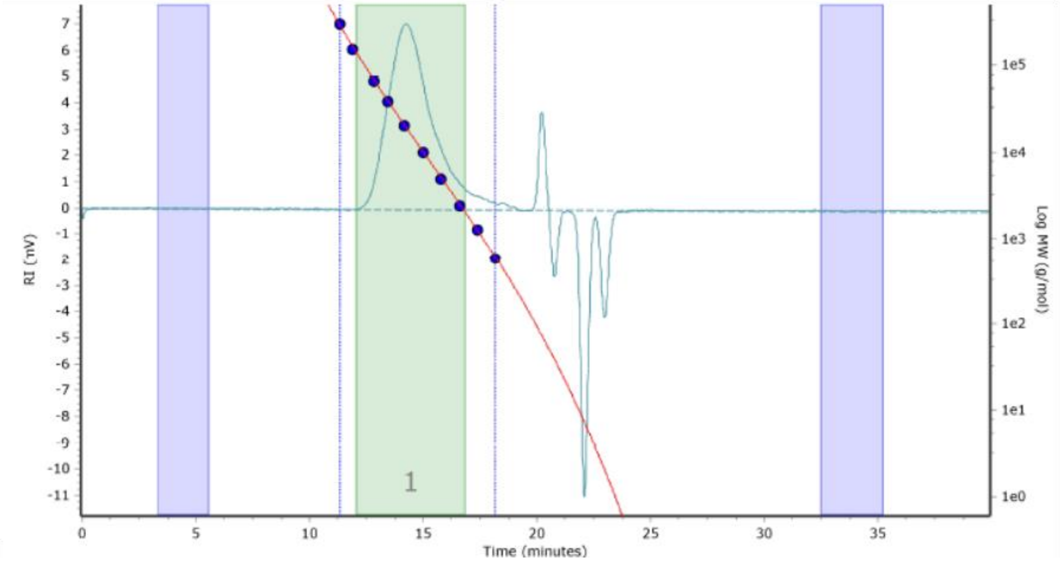

Fig. S31 SEC trace of poly(**1**) (M_n 10700 g mol^{-1} (*Đ* 1.8)) (Table 1, Run 10).

Molecular Weight Averages

Peak	Mp (g/mol)	Mn (g/mol)	Mw (g/mol)	Mz (g/mol)	Mz+1 (g/mol)	Mv (g/mol)	PD
Peak 1	44609	20357	43839	75082	106000	70602	2.154
Peak 2	3552	1529	1870	2221	2515	2173	1.223

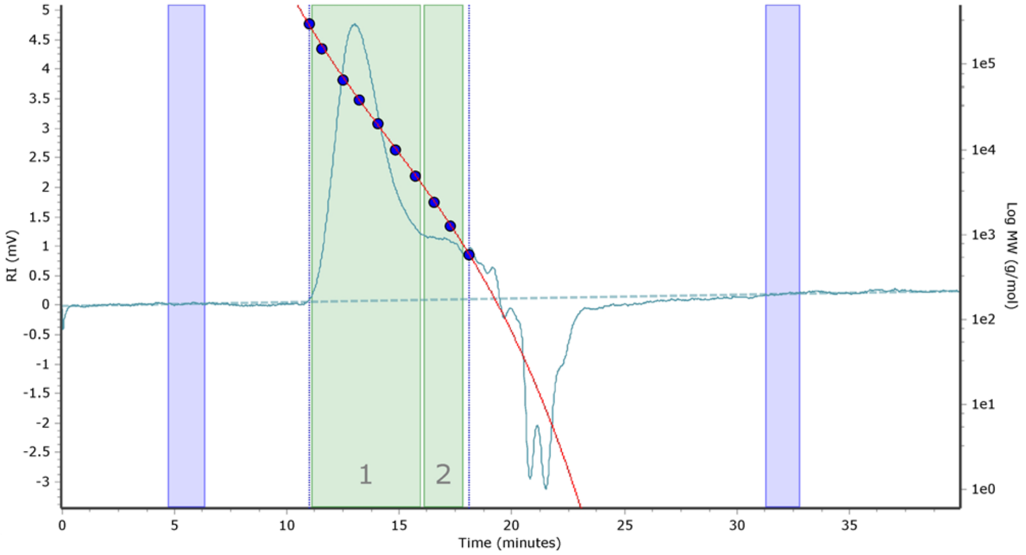

Fig. S32 SEC trace of the poly(**1**), TBD control reaction (after 6 h), showing M_n 20400 g mol^{-1} (Đ 2.15) and M_n 1500 g mol^{-1} (Đ 1.22).

Shoulder peak indicates the formation of cyclic polymer species.

DSC of the Polymer Derived from 1

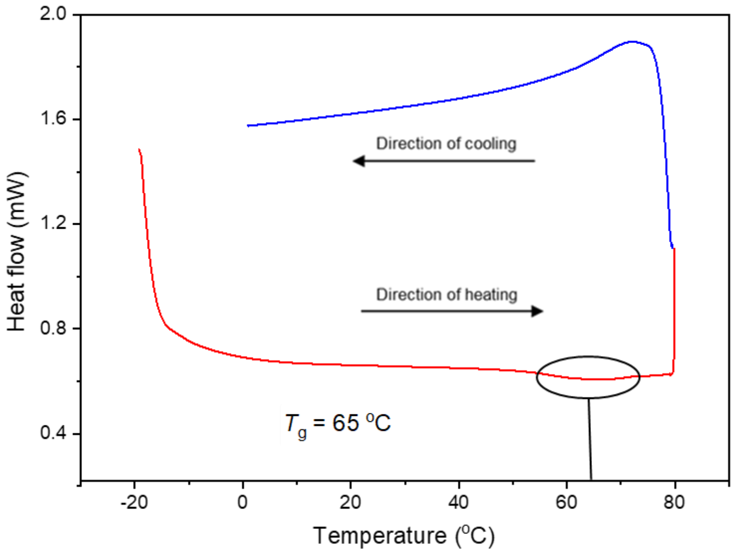

Fig. S33 DSC trace of poly(**1**) (M_n 10700 g mol^{-1} ($Đ$ 1.8)) (Table 1, Run 10), first heating and cooling cycle between -20 and 80 °C. Single exothermic peak, corresponding to the glass transition temperature (T_g) = 65 °C of the polymer.

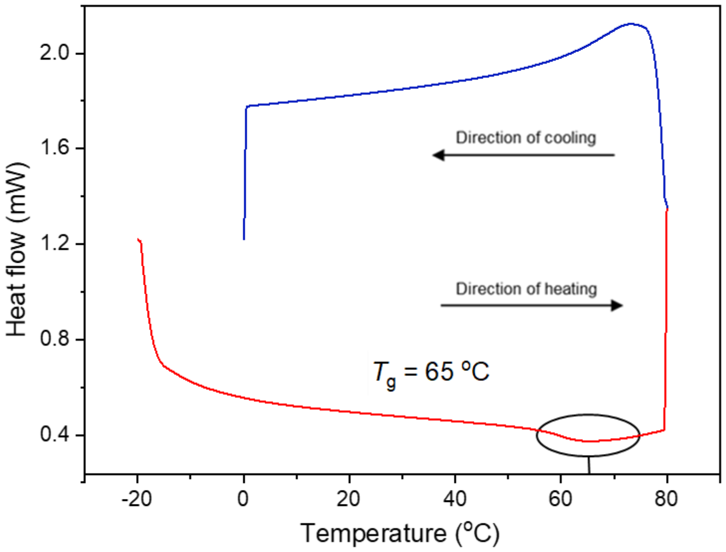

Fig. S34 DSC trace of poly(**1**) (M_n 6800 g mol^{-1} ($Đ$ 1.6)) (Table 1, Run 2), first heating and cooling cycle between -20 and 80 °C. Single exothermic peak, corresponding to the glass transition temperature (T_g) = 65 °C of the polymer.

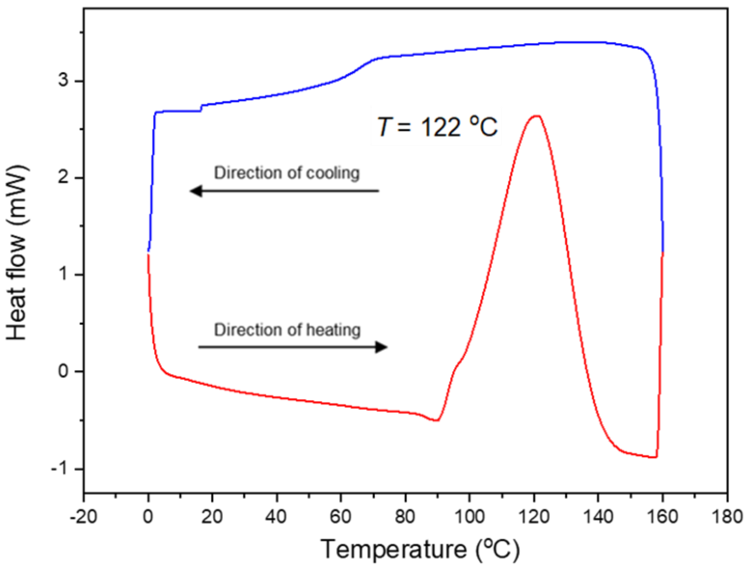

Fig. S35 DSC trace of poly(**1**) (M_n 6800 g mol^{-1} ($Đ$ 1.6)) (Table 1, Run 2), second heating and cooling cycle between 0 and 160 °C. Single endothermic peak, potentially corresponding to a proposed alteration in the polymer structure T = 122 °C.

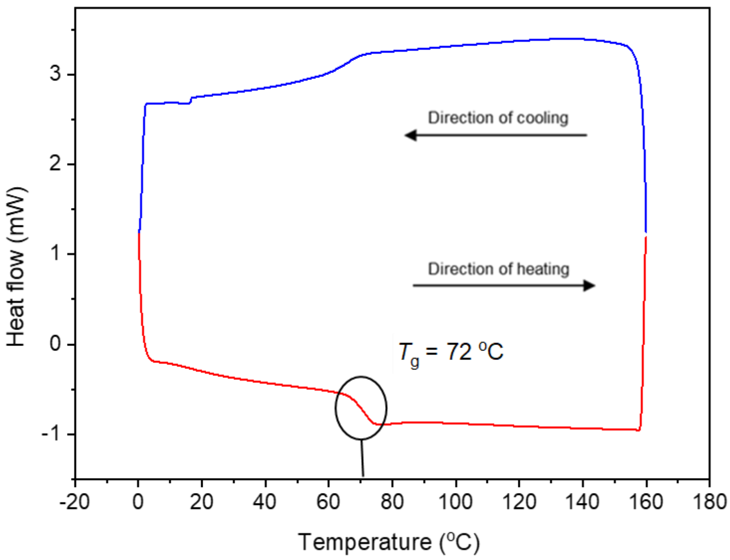

Fig. S36 DSC trace of poly(**1**) (M_n 6800 g mol^{-1} ($Đ$ 1.6)) (Table 1, Run 2), third heating and cooling cycle between 0 and 160 °C. Single exothermic peak, corresponding to the glass transition temperature (T_g) = 72 °C of the polymer.

TGA of the Polymer Derived from 1

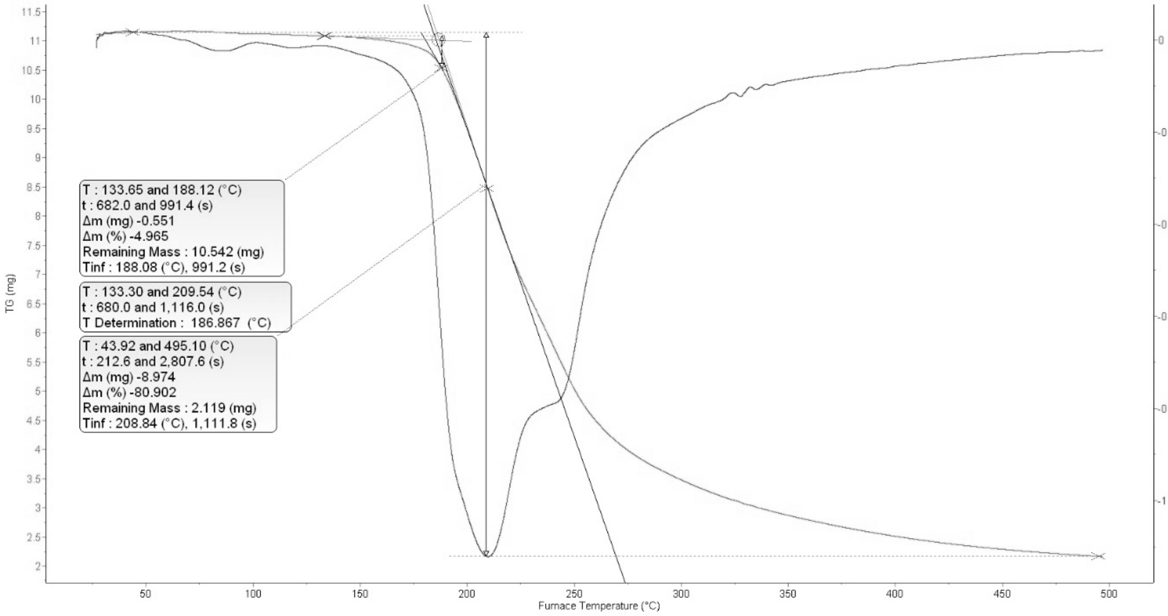

Fig. S37 TGA trace of poly(**1**) (M_n 10700 g mol^{-1} (Đ 1.8)) (Table 1, Run 10). The monomer was heated from 30 to 500 °C under argon at 10 °C min^{-1}. Obtained values: $T_{d5\%}$ = 188 °C and $T_{d,max}$ = 210 °C with 19% char remaining at 500 °C.

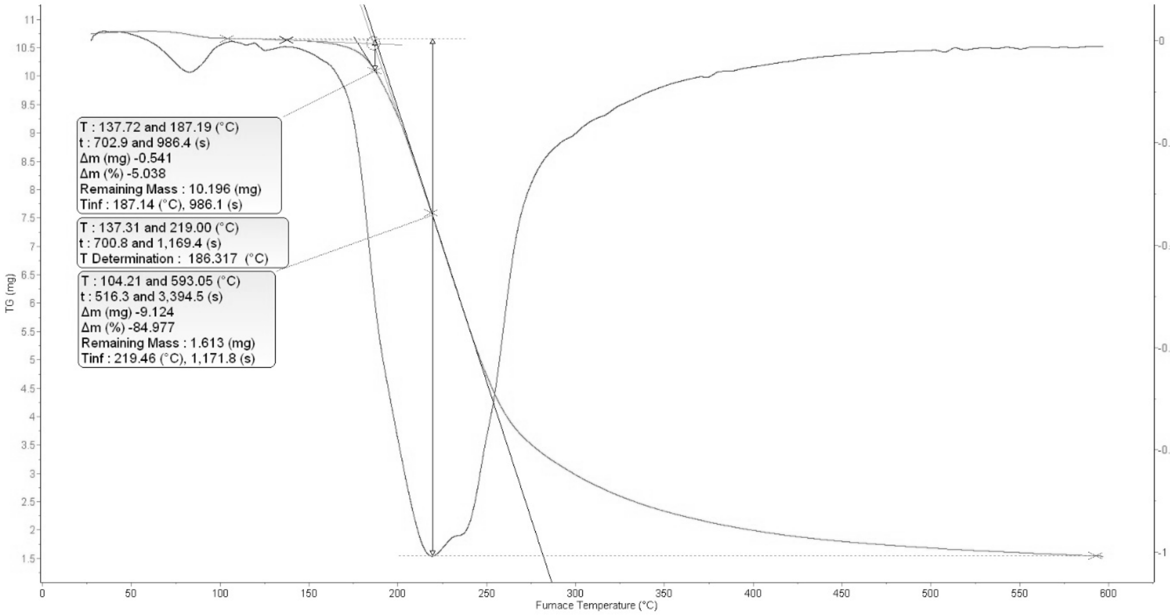

Fig. S38 TGA trace of poly(**1**) (M_n 6800 g mol^{-1} (Đ 1.6)) (Table 1, Run 2), The monomer was heated from 30 to 600 °C under argon at 10 °C min^{-1}. Obtained values: $T_{d5\%}$ = 187 °C and $T_{d,max}$ = 219 °C with 15% char remaining at 600 °C

UV-Vis analysis of the Polymer Derived from 1

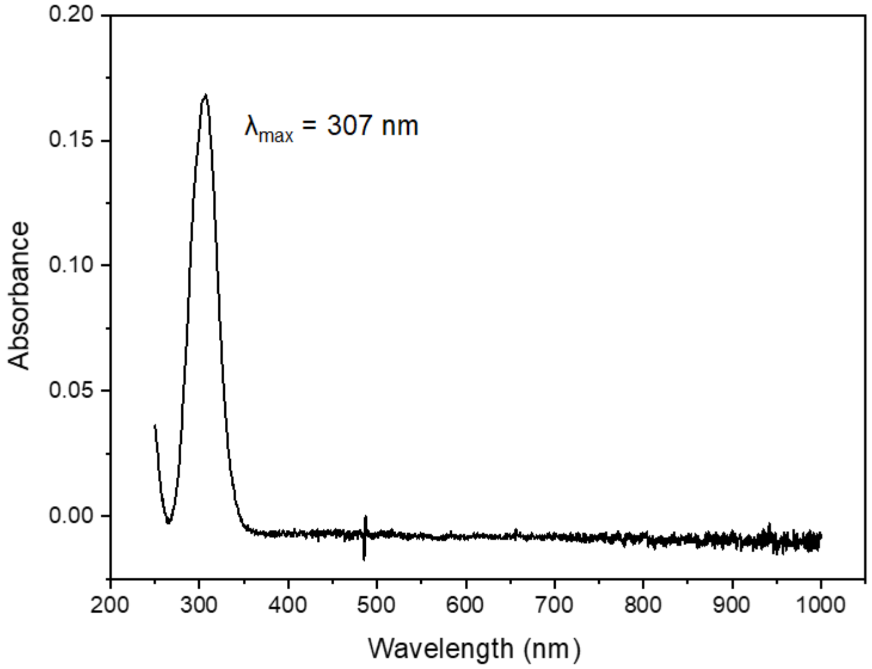

Fig. S39 UV-Vis absorption spectra of poly(**1**) upon irradiation of sample solution in THF in a 10-mm glass cell ($[\text{poly}(\mathbf{1})]_0 = 2.2 \times 10^{-5}$ mol L^{-1} based on polymer repeat unit, at room temperature). Single absorption peak detected, $\lambda_{max} = 307$ nm.

3. Polymerisation Studies

Ring-opening polymerisation of 1 with different organo-catalysts

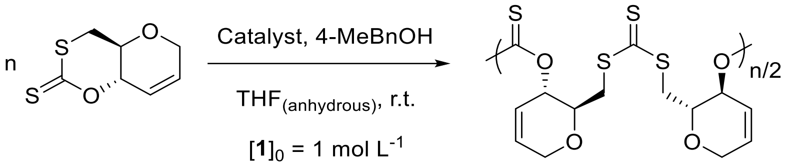

Table S1 Ring-opening polymerisation of **1** with differing organo-catalysts.[a]

Run	Catalyst	$[\mathbf{1}]_0$:$[\mathrm{C}]_0$:$[\mathrm{I}]_0$[(b)]	Time (h)	Conv.[(c)] (%)	$M_{n,\mathrm{CALC}}$[(d)]	$M_{n,\mathrm{SEC}}$[(e)]	$M_{w,\mathrm{SEC}}$[(e)]	$Đ$[(e)]
1	TBD	100:1:0	6	70	13200	20400	43800	2.15
2	TBD	100:1:1	24	82	15600	6000	9700	1.60
3	DBU	100:1:1	24	75	14200	6300	10600	1.67
4	MTBD	100:1:1	24	47	9000	6500	9700	1.49
5	KHMDS	100:1:1	24	25	4800	3200	4500	1.39
6	TMG	100:1:1	24	0	-	-	-	-
7	DMAP	100:1:1	24	0	-	-	-	-
8	$(\mathrm{PhNH})_2\mathrm{CO}$	100:1:1	24	0	-	-	-	-

[a]Polymerizations were carried out at room temperature, under an argon atmosphere, in anhydrous THF solvent with initial $[\mathbf{1}]_0$ = 1 mol L^{-1} (**1** = monomer); [b]I = 4-methylbenzyl alcohol, C = organo-catalyst; [c]Monomer conversion to polymer, calculated based on the relative integration of the H-4′ proton signal of **1** (δ_H = 4.79) and poly(**1**) (δ_H = 5.75-5.68), in the ^{1}H NMR spectrum; [d]Number-average molecular weight as calculated using $M_r(I)+(M_r(\mathrm{monomer}) \times [\mathrm{monomer}]_0/[I]_0 \times \mathrm{conv}/100\%)$, units given in g mol^{-1}; [e]Number-average molecular weight and Dispersity ($M_{n,\mathrm{SEC}}$, $M_{w,\mathrm{SEC}}$, $Đ$), calculated by SEC relative to polystyrene standards in THF eluent, units given in g mol^{-1}.

Kinetic Experiments

Kinetic experiments were carried out by taking aliquots of the polymerisation mixture at specific time intervals and quenching with excess benzoic acid in DCM. Solvent was removed in *vacuo* and each aliquots was analysed *via* NMR spectroscopy us to determine the monomer conversion at these intervals.

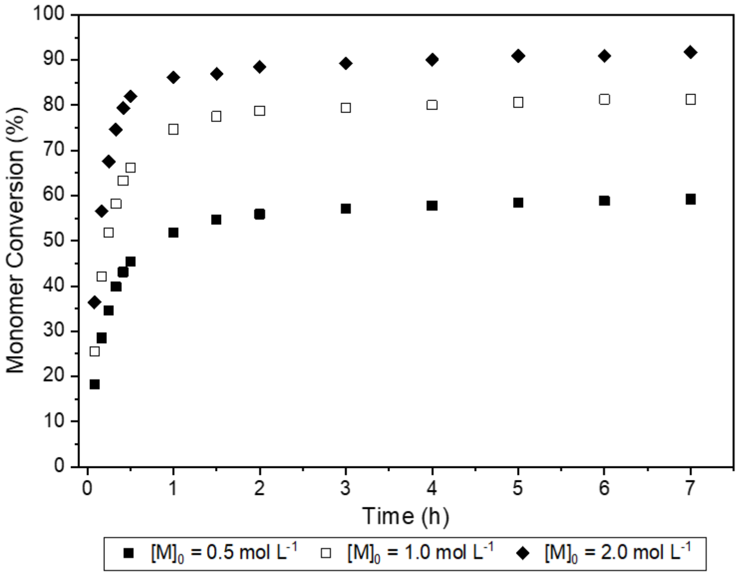

Fig. S40 ROP of **1** with 4-MeBnOH and TBD catalyst: conversion *versus* time for $[\mathbf{1}]_0$ = 0.5, 1.0 and 2.0 mol L^{-1}. Carried out at 20 °C in DCM for $[\mathbf{1}]_0$: $[TBD]_0$: $[4\text{-MeBnOH}]_0$ ratio of 100: 1: 1. Monomer conversion was determined by ^1H NMR spectroscopy by relative integration of the H-4′ proton signal of **1** (δ_H = 4.79) and poly(**1**) (δ_H = 5.75-5.68), in the NMR spectrum.

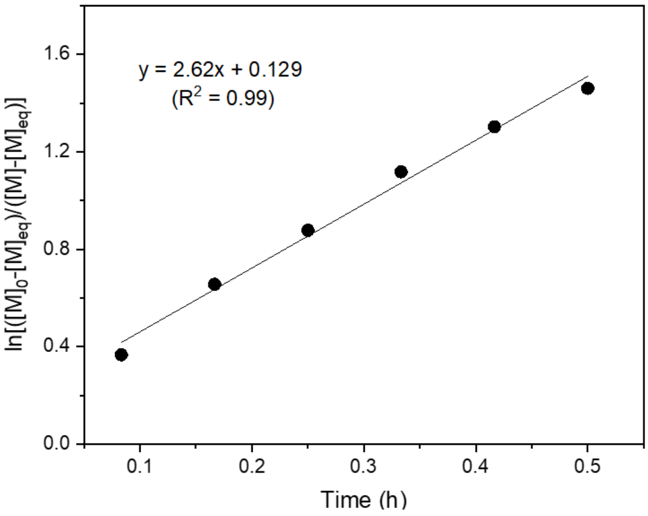

Fig. S41 Kinetic plot for equilibrium ROP of **1** with 4-MeBnOH and TBD catalyst. Carried out at 20 °C in DCM for $[\mathbf{1}]_0$: $[TBD]_0$: $[4\text{-MeBnOH}]_0$ ratio of 100: 1: 1 and $[\mathbf{1}]_0$ = 0.5 mol L^{-1}. An equilibrium monomer conversion $[\mathbf{1}]_{eq}$ = 0.408 mol L^{-1} was used giving an apparent pseudo-first order rate constant k_{app} = 2.62 ± 0.005 h^{-1} (linear fit, R^2 = 0.99).

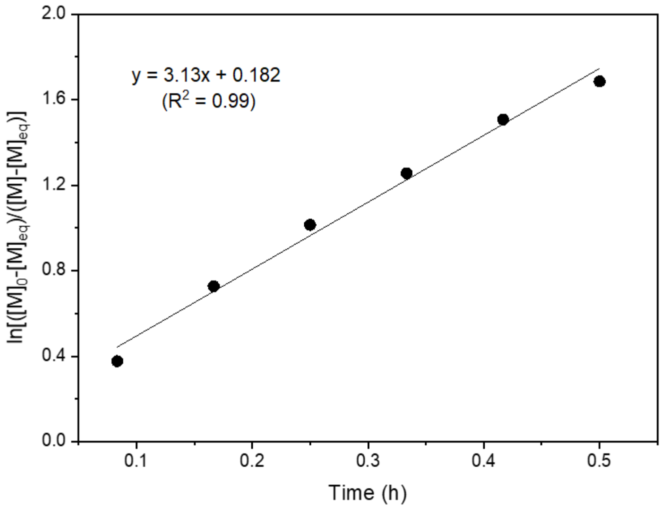

Fig. S42 Kinetic plot for equilibrium ROP of **1** with 4-MeBnOH and TBD catalyst. Carried out at 20 °C in DCM for $[\mathbf{1}]_0$: $[\mathrm{TBD}]_0$: $[\mathrm{4\text{-}MeBnOH}]_0$ ratio of 100: 1: 1 and $[\mathbf{1}]_0 = 1.0$ mol L^{-1}. An equilibrium monomer conversion $[\mathbf{1}]_{eq} = 0.187$ mol L^{-1} was used giving an apparent pseudo-first order rate constant $k_{app} = 3.13 \pm 0.005$ h^{-1} (linear fit, $R^2 = 0.99$).

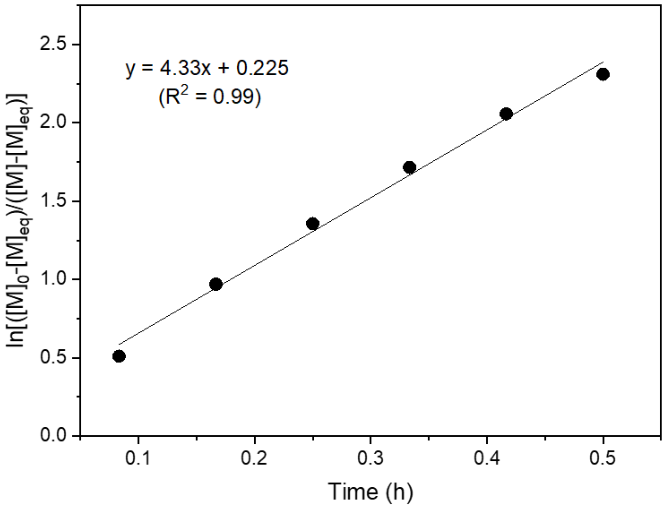

Fig. S43 Kinetic plot for equilibrium ROP of **1** with 4-MeBnOH and TBD catalyst. Carried out at 20 °C in DCM for $[\mathbf{1}]_0$: $[\mathrm{TBD}]_0$: $[\mathrm{4\text{-}MeBnOH}]_0$ ratio of 100: 1: 1 and $[\mathbf{1}]_0 = 2.0$ mol L^{-1}. An equilibrium monomer conversion $[\mathbf{1}]_{eq} = 0.090$ mol L^{-1} was used giving an apparent pseudo-first order rate constant $k_{app} = 4.33 \pm 0.005$ h^{-1} (linear fit, $R^2 = 0.99$).

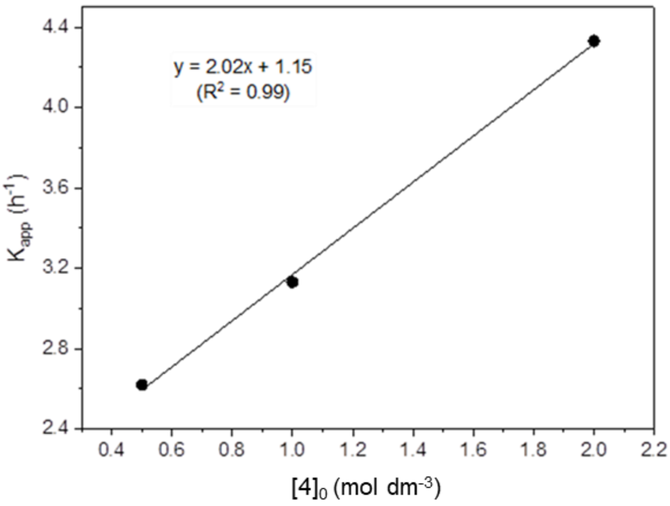

Fig. S44 Plot of K_{app} versus $[\mathbf{1}]_0$ for equilibrium ROP of **1** with 4-MeBnOH and TBD catalyst. Carried out at 20 °C in DCM for $[\mathbf{1}]_0$: $[\text{TBD}]_0$: $[\text{4-MeBnOH}]_0$ ratio of 100: 1: 1 and $[\mathbf{1}]_0 = 0.5$, 1.0 and 2.0 mol L^{-1} (linear fit, $R^2 = 0.99$).

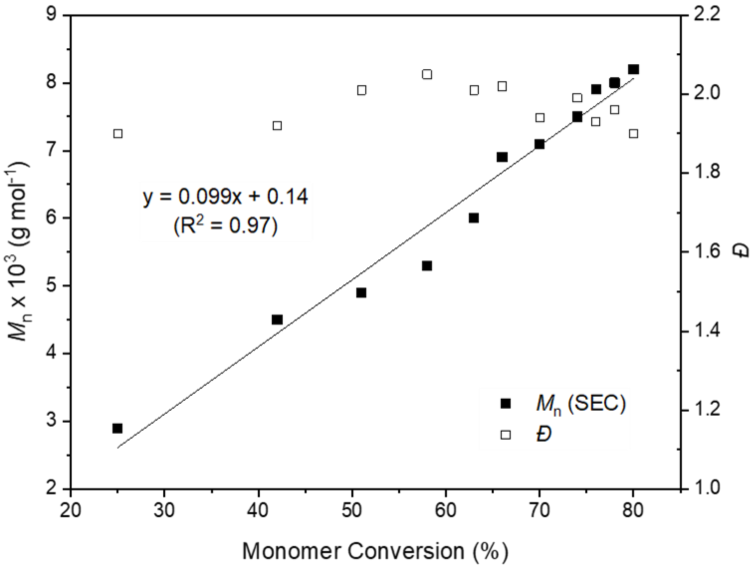

Fig. S45 Plot of M_n and $Đ$ *versus* monomer conversion for the polymerisation carried out at 20 °C with $[\mathbf{1}]_0 = 1.0$ mol L^{-1} and 100: 1: 1 $[\mathbf{1}]_0$: $[\text{TBD}]_0$: $[\text{I}]_0$. Conversion was determined by ^{1}H NMR spectroscopy of aliquots quenched with excess benzoic acid. M_n was estimated by SEC *versus* polystyrene standards using a refractive index (RI) detector and THF eluent.

Temperature Experiments - Determination of ROP thermodynamic parameters

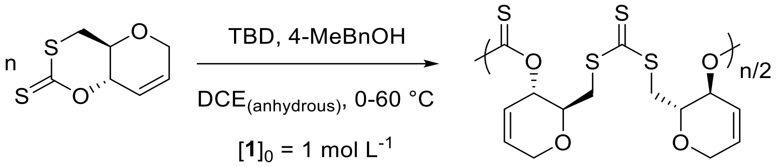

Table S2 Ring-opening polymerisation of **1** over a 0-60 °C temperature range.[a]

Run	Temp. (°C)	$[\mathbf{1}]_0$:$[\mathrm{TBD}]_0$:$[\mathrm{I}]_0$[(b)]	Time (h)	Conv.[(c)] (%)	$M_{n,\mathrm{CALC}}$[(d)]	$M_{n,\mathrm{SEC}}$[(e)]	$M_{w,\mathrm{SEC}}$[(e)]	$Đ$[(e)]
1	0	100:1:1	24	85	16100	5000	10100	2.00
2	10	100:1:1	24	81	15400	4800	9200	1.90
3	20	100:1:1	24	73	13900	4600	8400	1.81
4	30	100:1:1	24	63	12000	4500	8400	1.85
5	40	100:1:1	24	44	8400	4400	7400	1.69
6	50	100:1:1	24	19	3700	3600	5400	1.53
7	60	100:1:1	24	2	500	-	-	-

[a]Polymerisations were carried out at different temperatures, under an argon atmosphere, in anhydrous 1,2-dichloroethane solvent with initial $[\mathbf{1}]_0 = 1$ mol L^{-1} (**1** = monomer); [b]I = 4-methylbenzylalcohol; [c]Monomer conversion to polymer, calculated based on the relative integration of the H-4′ proton signal of **1** ($\delta_H = 4.79$) and poly(**1**) ($\delta_H = 5.75\text{-}5.68$), in the ^{1}H NMR spectrum; [d]Number-average molecular weight as calculated using $M_r(\mathrm{I})+(M_r(\mathrm{monomer}) \times [\mathrm{monomer}]_0/[\mathrm{I}]_0 \times \mathrm{conv}/100\%)$, units given in g mol^{-1}; [e]Number-average molecular weight and Dispersity ($M_{n,\mathrm{SEC}}$, $M_{w,\mathrm{SEC}}$, $Đ$), calculated by SEC relative to polystyrene standards in THF eluent, units given in g mol^{-1}.

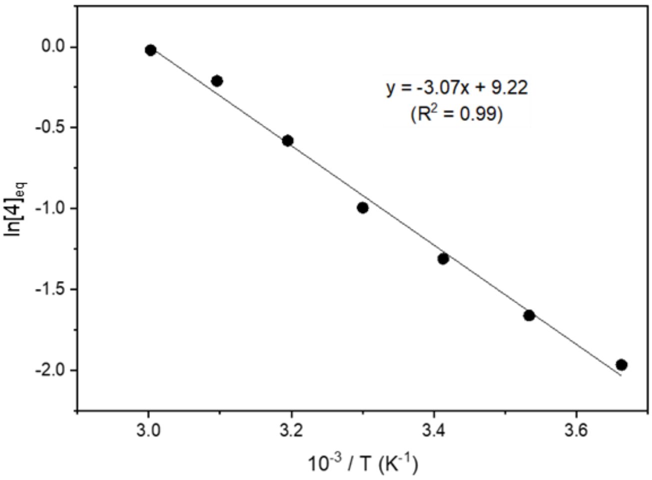

Fig. S46 ROP of **1** with 4-MeBnOH and TBD catalyst: calculation of the thermodynamic parameters from a plot of $\ln[\mathbf{1}]_{eq}$ as a function of 1/T, where T is the absolute temperature. Carried out in 1,2-dichloroethane, over a temperature range of 0–60 °C for $[\mathbf{1}]_0 = 1.0$ mol L^{-1} and $[\mathbf{1}]_0 : [\mathrm{TBD}]_0 : [\text{4-MeBnOH}]_0 = 100:1:1$.

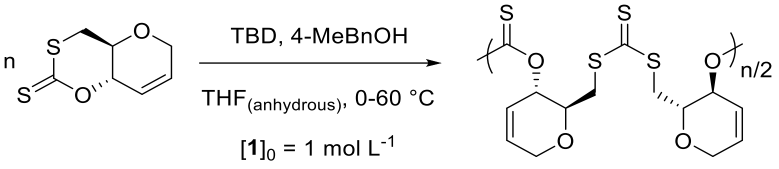

Table S3 Ring-opening polymerisation of **1** over a 0-60 °C temperature range.[a]

Run	Temp. (°C)	$[\mathbf{1}]_0$:[TBD]$_0$:[I]$_0$ [(b)]	Time (h)	Conv.[(c)] (%)	$M_{n,\mathrm{CALC}}$ [(d)]	$M_{n,\mathrm{SEC}}$ [(e)]	$M_{w,\mathrm{SEC}}$ [(e)]	$Đ$ [(e)]
1	10	100:1:1	20	74	14100	5200	9100	1.74
2	20	100:1:1	20	82	15600	4600	7800	1.68
3	30	100:1:1	20	78	14800	3900	5800	1.52
4	40	100:1:1	20	72	13700	4800	8200	1.70
5	50	100:1:1	20	58	-	5900	10200	1.72
6	60	100:1:1	20	23	-	7000	13000	1.84

[a] Polymerisations were carried out at different temperatures, under an argon atmosphere, in anhydrous THF solvent with initial $[\mathbf{1}]_0 = 1.0$ mol L^{-1} (**1** = monomer); [b] I = 4-methylbenzylalcohol; [c] Monomer conversion to polymer, calculated based on the relative integration of the H-4' proton signal of **1** ($\delta_H = 4.79$) and poly(**1**) ($\delta_H = 5.75$-5.68), in the ^{1}H NMR spectrum; [d] Number-average molecular weight as calculated using $M_r(I)+(M_r(\mathrm{monomer}) \times [\mathrm{monomer}]_0/[I]_0 \times \mathrm{conv}/100\%)$, units given in g mol^{-1}; [e] Number-average molecular weight and Dispersity ($M_{n,\mathrm{SEC}}$, $M_{w,\mathrm{SEC}}$, $Đ$), calculated by SEC relative to polystyrene standards in THF eluent, units given in g mol^{-1}.

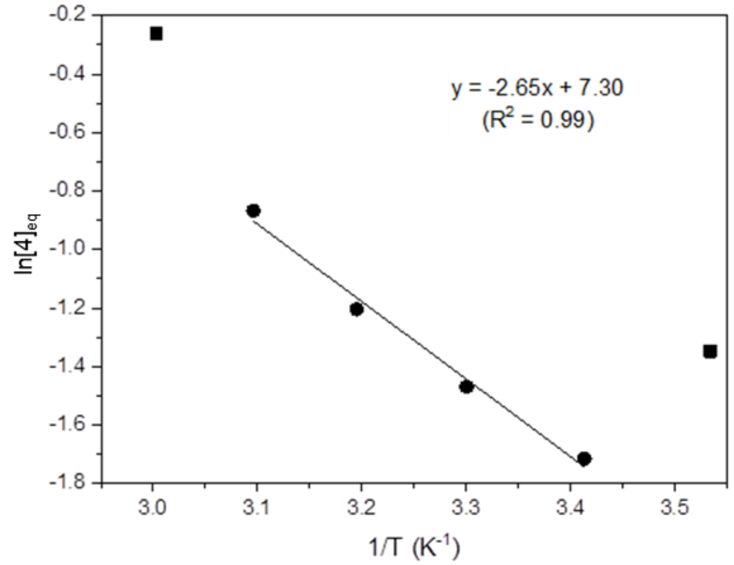

Fig. S47 ROP of **1** with 4-MeBnOH and TBD catalyst: calculation of the thermodynamic parameters from a plot of $\ln[\mathbf{1}]_{eq}$ as a function of 1/T, where T is the absolute temperature. Carried out in tetrahydrofuran, over a temperature range of 0–60 °C for $[\mathbf{1}]_0 = 1.0$ mol L^{-1} and $[\mathbf{1}]_0$: [TBD]$_0$: [4-MeBnOH]$_0$ = 100:1:1.

Temperature Experiments – Analytical data for high temperature experiments

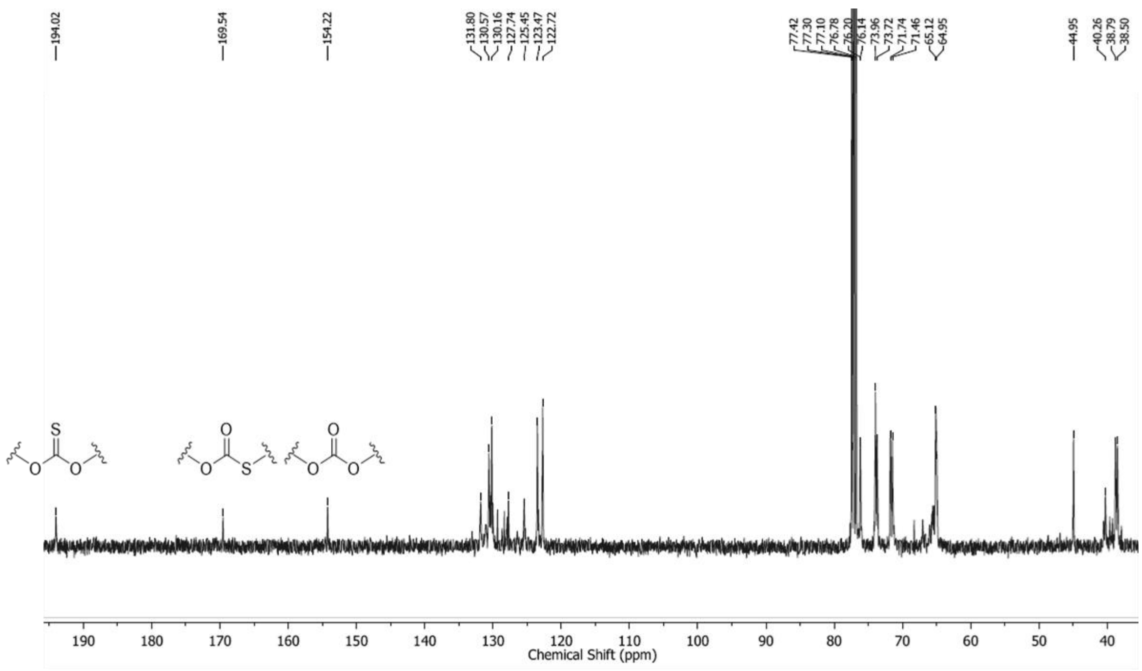

Fig. S48 Annotated $^{13}C\{^1H\}$ NMR of unidentifiable polymeric product in chloroform-d (Table S3, Run 5).

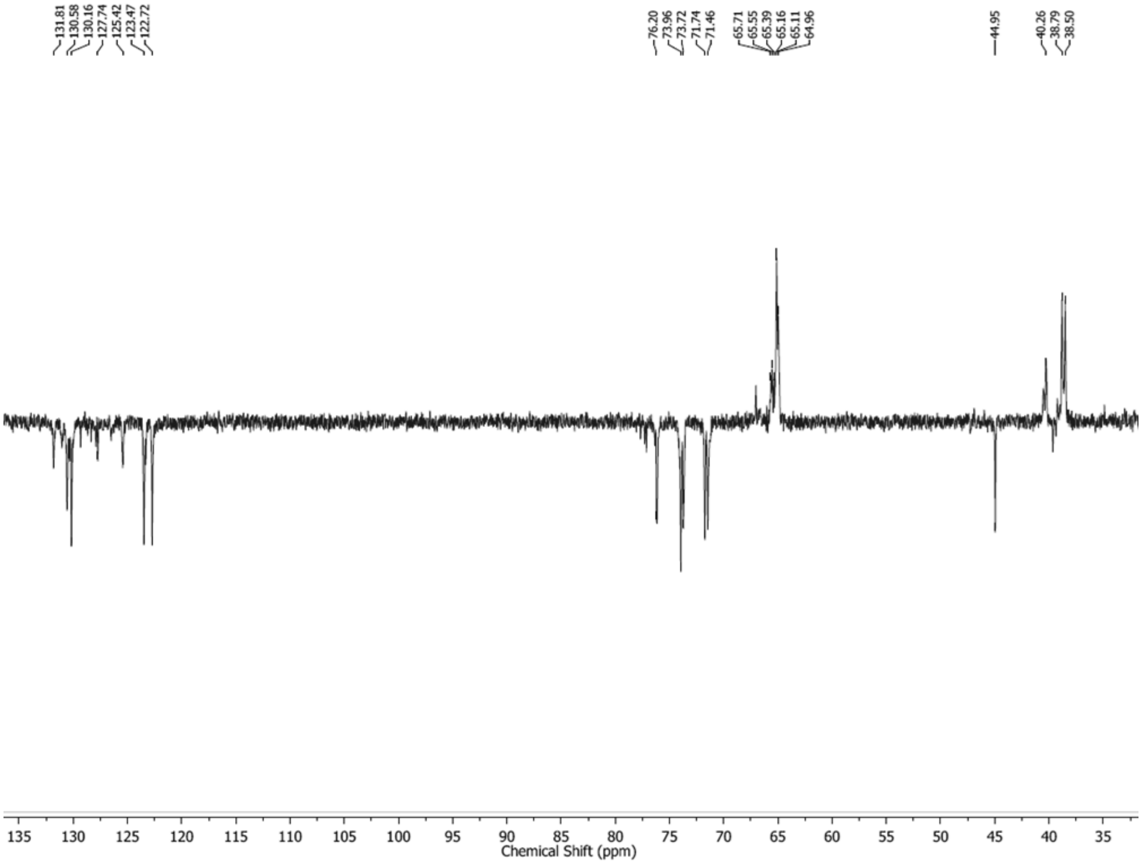

Fig. S49 $^{13}C\{^1H\}$ DEPT135 NMR spectrum of the unidentifiable polymeric product in chloroform-d (Table S3, Run 5).

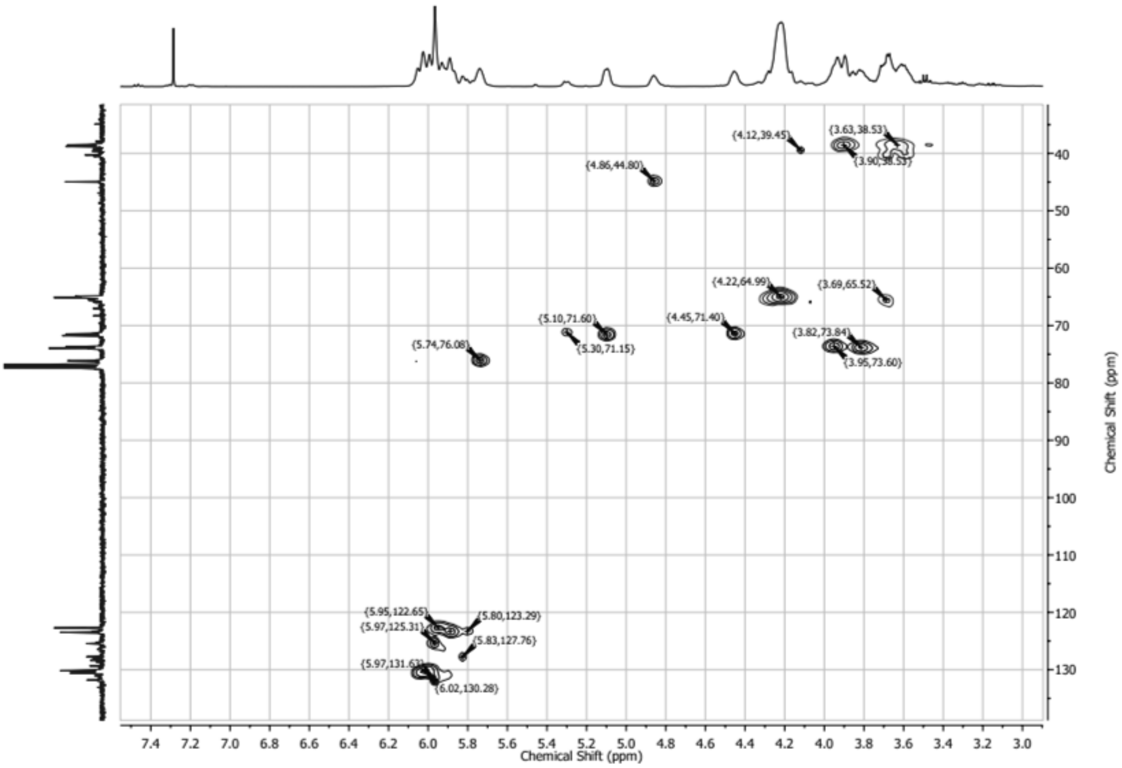

Fig. S50 HSQC (^1H–^{13}C) NMR spectrum of unidentifiable polymeric product in chloroform-d (Table S3, Run 5).

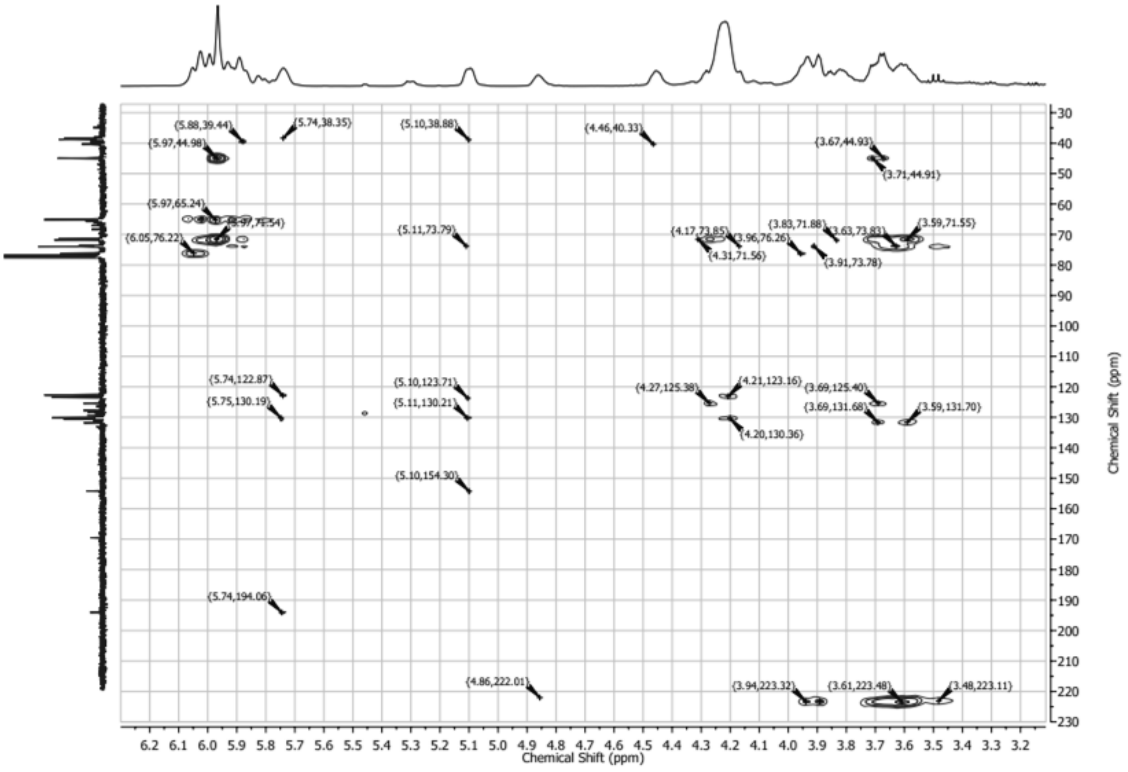

Fig. S51 HMBC (^1H–^{13}C) NMR spectrum of the unidentifiable polymeric product in chloroform-d (Table S3, Run 5).

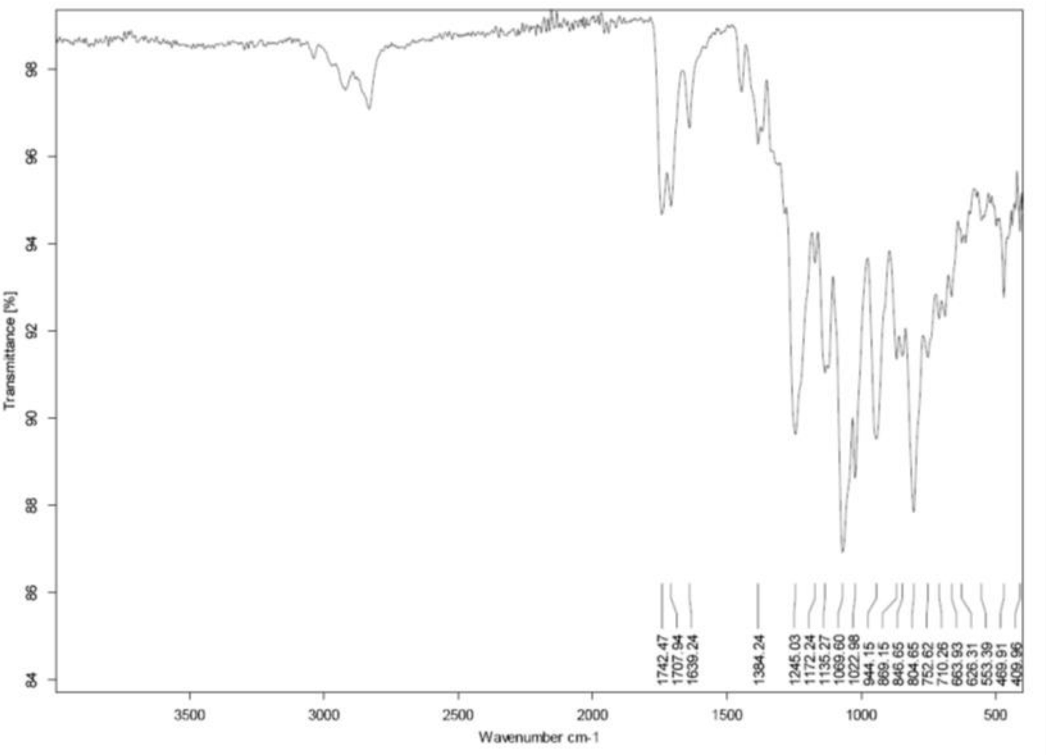

Fig. S52 Labelled FT-IR spectrum of unidentifiable polymeric product (Table S3, Run 5).

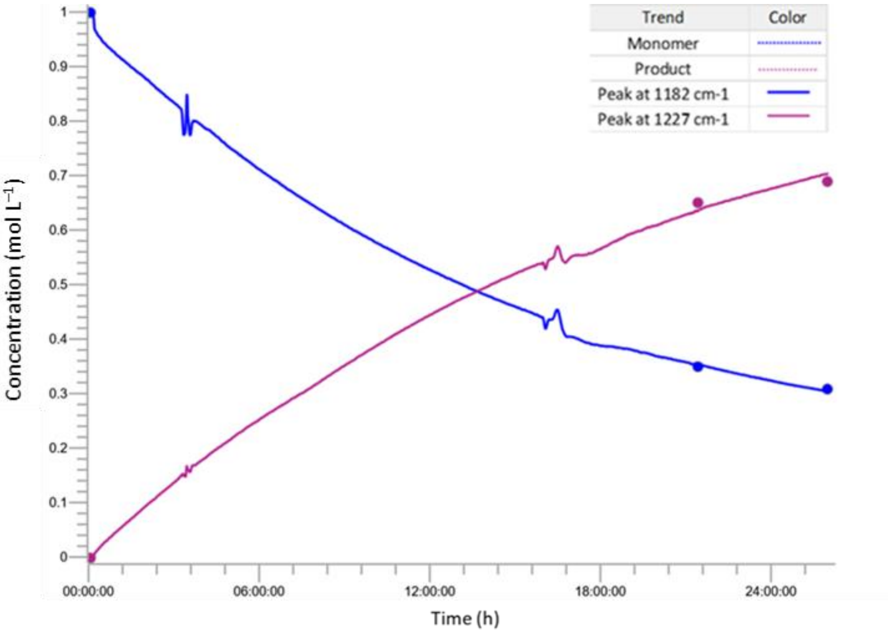

Fig. S53 In-situ IR reaction trends for the ROP of **1** with 4-MeBnOH and TBD catalyst. Carried out at 20 °C in THF for $[\mathbf{1}]_0$: $[\text{TBD}]_0$: $[\text{4-MeBnOH}]_0$ ratio of 100: 1: 1 and $[\mathbf{1}]_0$ = 1.0 mol L^{-1}. Monomer conversion was monitored by the vibrational modes at 1182 (C(S)SO) and 1227 ($C(S)O_2$) cm^{-1}, corresponding to the xanthate monomer **1** and its resultant polymer poly(**1**) respectively.

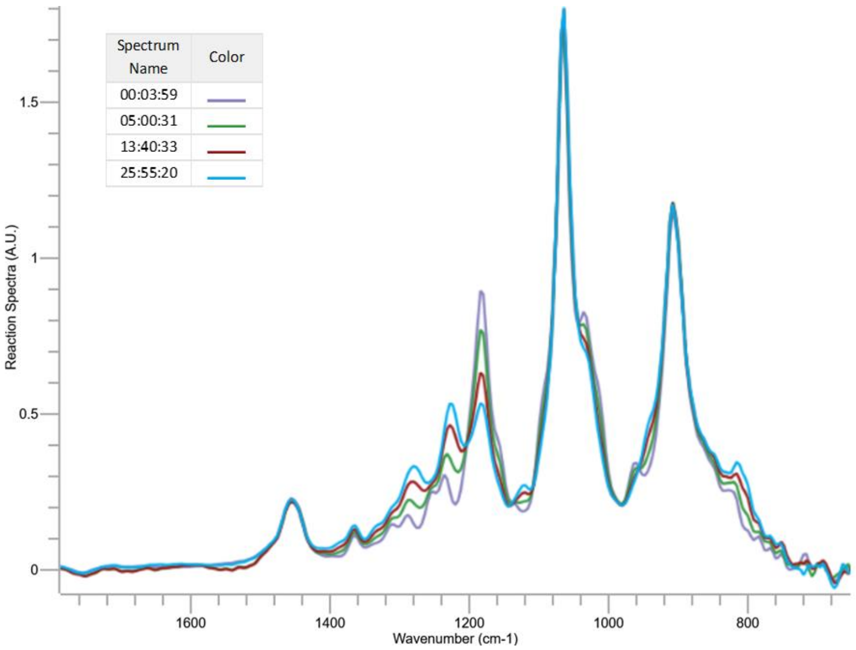

Fig. S54 In-situ IR reaction spectra for the ROP of **1** with 4-MeBnOH and TBD catalyst. Carried out at 20 °C in THF for [**1**]$_0$: [TBD]$_0$: [4-MeBnOH]$_0$ ratio of 100: 1: 1 and [**1**]$_0$ = 1.0 mol L^{-1}.

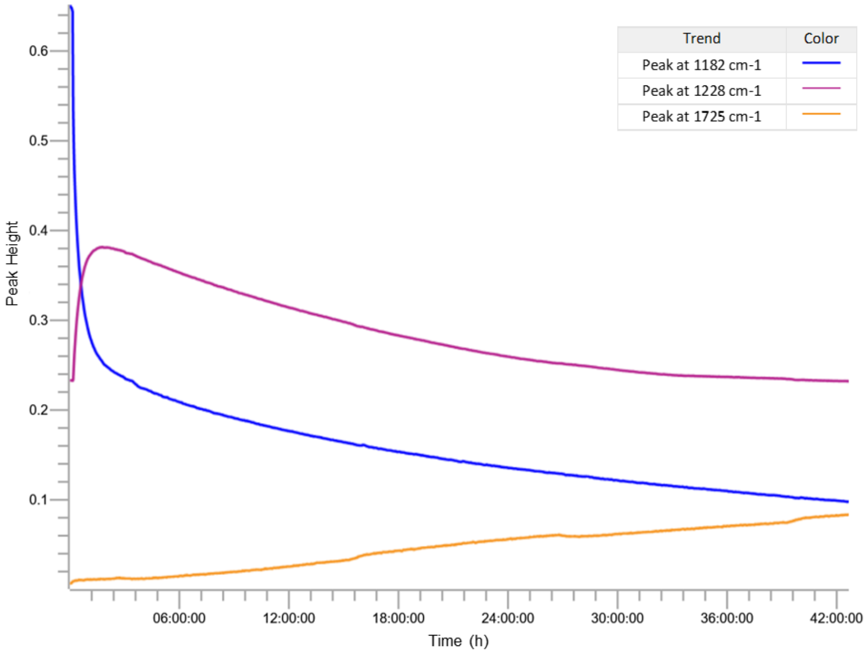

Fig. S55 In-situ IR reaction trends for the ROP of **1** with 4-MeBnOH and TBD catalyst. Carried out at 50 °C in THF for [**1**]$_0$: [TBD]$_0$: [4-MeBnOH]$_0$ ratio of 100: 1: 1 and [**1**]$_0$ = 1 mol L^{-1}. Monomer conversion was monitored by the vibrational modes at 1182 (C(S)SO) and 1227 (C(S)O$_2$) cm^{-1}, corresponding to the xanthate monomer **1** and its resultant polymer poly(**1**) respectively. A vibrational mode at 1725 (C(O)O$_2$) cm^{-1} was also monitored.

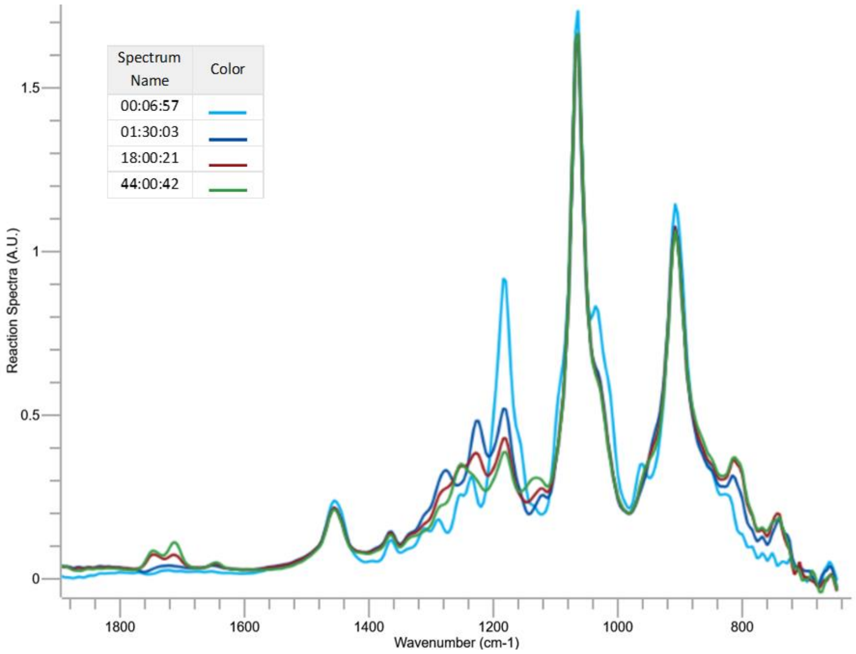

Fig. S56 In-situ IR reaction trends for the ROP of **1** with 4-MeBnOH and TBD catalyst. Carried out at 50 °C in THF for [**1**]$_0$: [TBD]$_0$: [4-MeBnOH]$_0$ ratio of 100: 1: 1 and [**1**]$_0$ = 1 mol L^{-1}.

4. General copolymerisation procedures

Sequential copolymerisation experiment

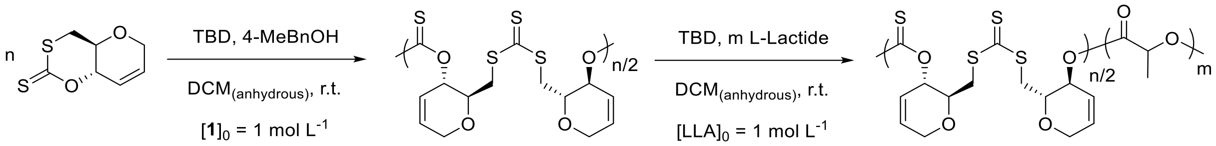

Under an argon atmosphere 4-MeBnOH (64 µL, 0.5 mol L^{-1} in anhydrous DCM, 0.199 mmol, 1.0 equiv.) and TBD (64 µL, 0.5 mol L^{-1} in anhydrous DCM, 0.199 mmol, 1.0 equiv.) were added to a solution of monomer **1** (0.150 g, 0.797 mmol, 25 equiv.) in anhydrous DCM (0.80 mL, 1.0 mol L^{-1}). The mixture was stirred at room temperature for 6 h and then treated with a solution of L-lactide (0.230 g, 1.59 mmol, 50 equiv.) in anhydrous DCM (1.59 mL, 1.0 mol L^{-1}) and TBD (64 µL, 0.5 mol L^{-1}in anhydrous DCM, 0.199 mmol, 1.0 equiv.). The mixture was stirred at room temperature for 2 h and quenched by the addition of a benzoic acid solution (≈30 equiv.). The solvent removed under reduced pressure and the crude solid was dissolved in $CHCl_3$ and precipitated from Et_2O. The product was isolated by centrifugation (3500 rpm, 2 x 5 minutes), washed twice with Et_2O and dried under vacuum. The polymer was isolated as a yellow solid.

δ_H (500 MHz; chloroform-d): 6.06-5.84 (C^2H, C^3H, 2H, m), 5.76-5.63 (C^4H, 1H, m), 5.15 (C^9H, 3H, q, J_{HH} = 7.0 Hz), 4.27-4.12 (C^1H, 2H, m), 4.01-3.79 (C^5H, C^6H, 2H, m), 3.71-3.53 (C^6H, 1H, m), 1.57 ($C^{10}H$, 9H, d, J_{HH} = 7.0 Hz) ppm; δ_C (126 MHz; chloroform-d): 223.4 (C^7), 194.0 (C^8), 169.6 (C^{11}), 130.6 (C^2), 122.7 (C^3), 76.1 (C^5), 73.8 (C^4), 69.3 (C^9), 65.0 (C^1), 38.5 (C^6), 16.6 (C^{10}) ppm.

NMR Spectroscopic Characterisation of poly(1-*b*-LLA) block copolymer

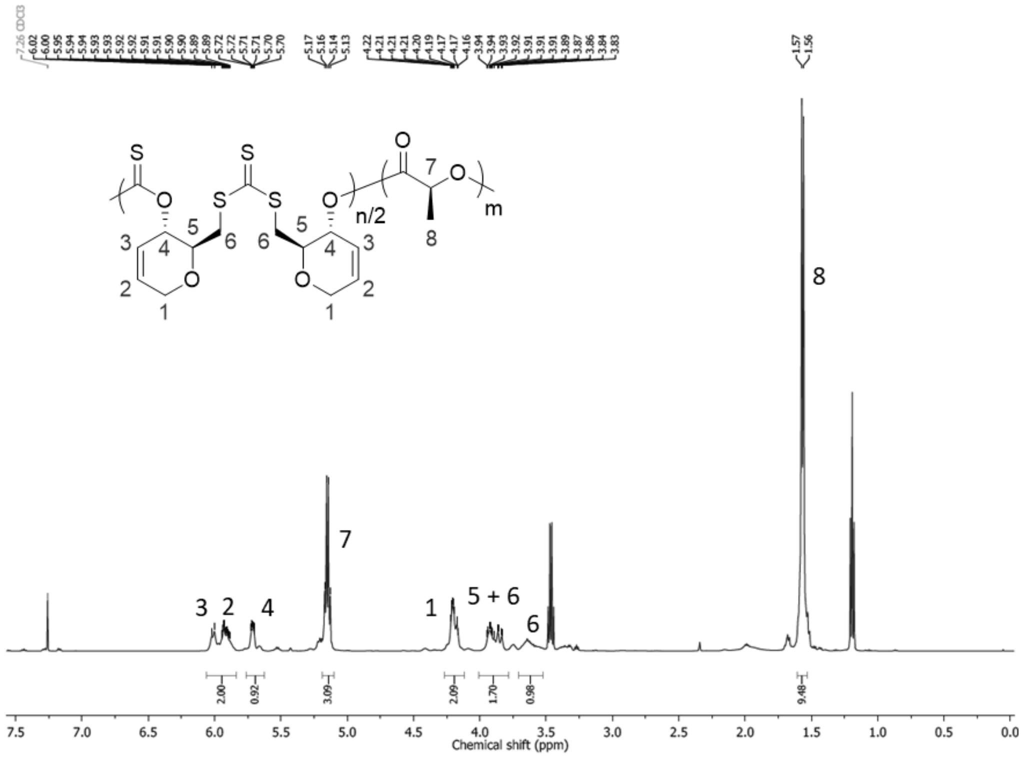

Fig. S57 Annotated ^{1}H NMR spectrum of poly(**1**-*b*-LLA) block copolymer (M_n 17300 g mol^{-1}, $Đ$ 1.84) in chloroform-d. Residual Et_2O signals at δ_H 1.12 (t) and 3.38 (q) ppm.

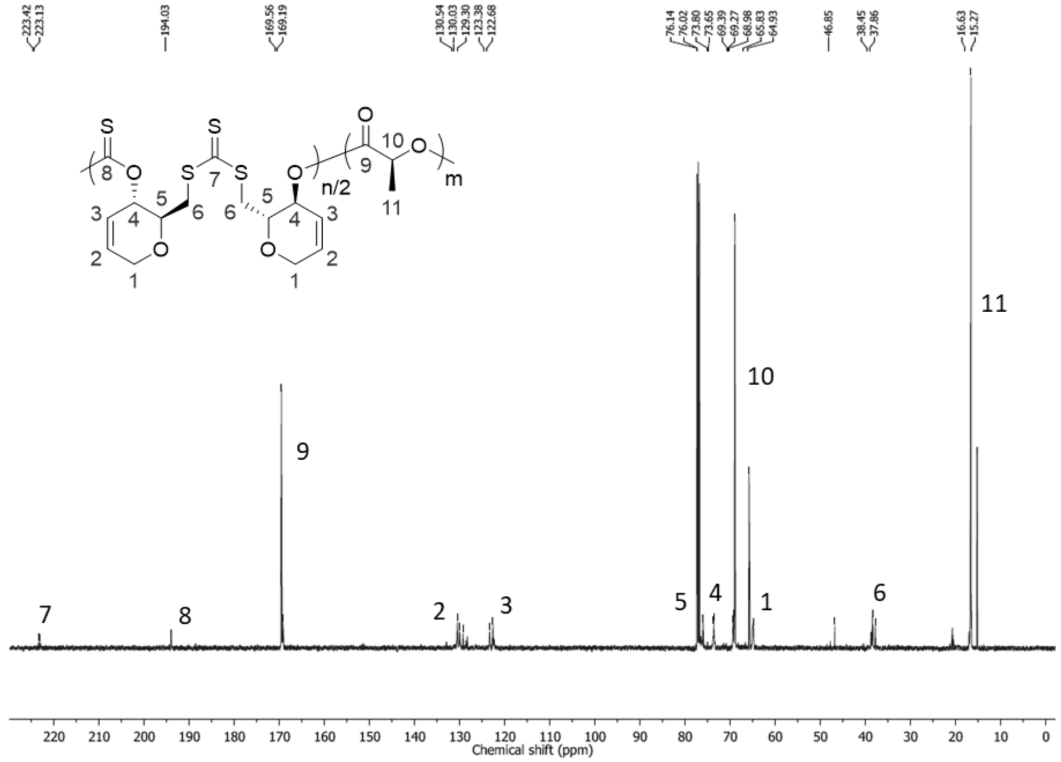

Fig. S58 Annotated $^{13}C\{^1H\}$ NMR spectrum of poly(**1**-*b*-LLA) block copolymer (M_n 17300 g mol^{-1}, $Đ$ 1.84) in chloroform-d. Residual Et_2O signals at δ_c 15.4 and 66.1 ppm.

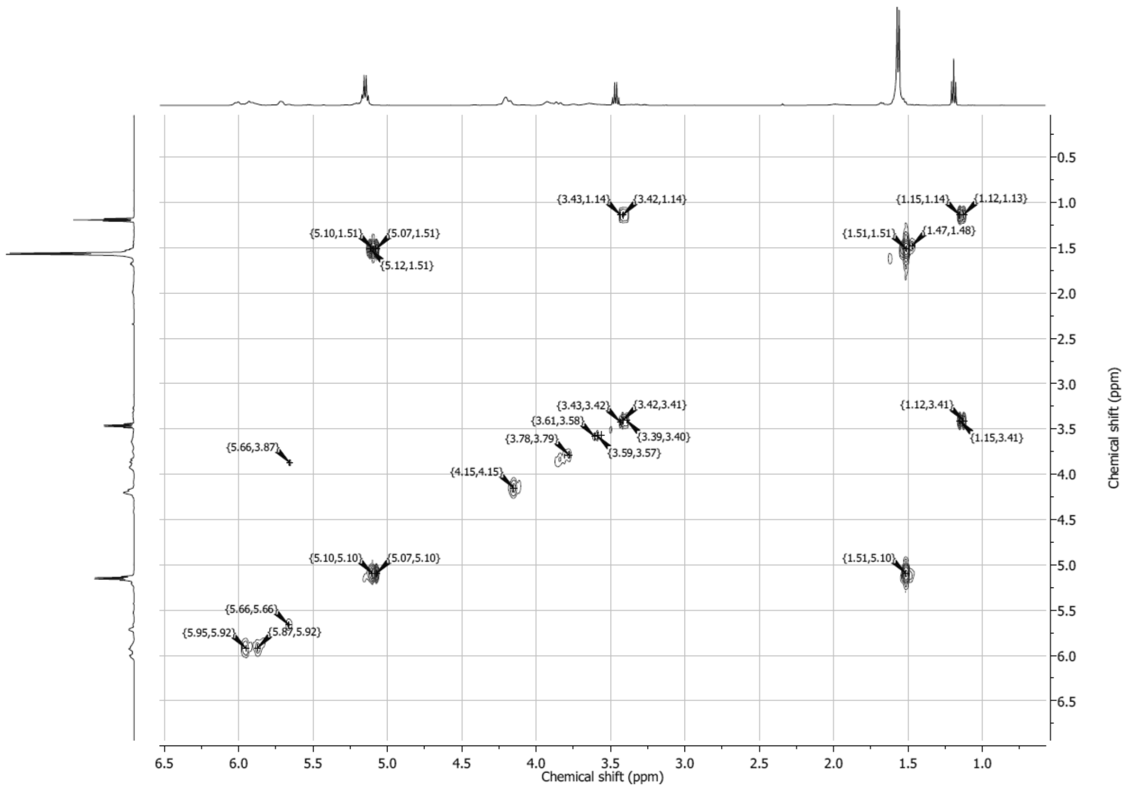

Fig. S59 COSY (^{1}H–^{1}H) NMR spectrum of poly(**1**-*b*-LLA) block copolymer (M_n 17300 g mol^{-1}, $Đ$ 1.84) in chloroform-d.

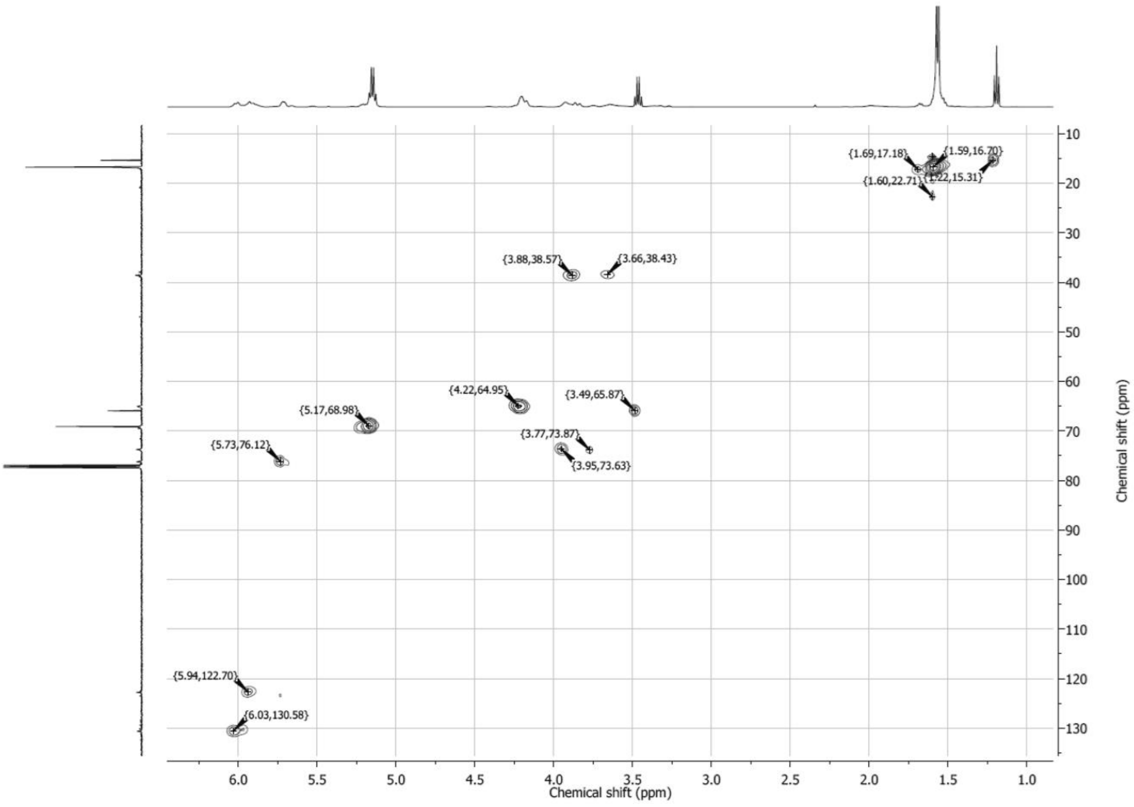

Fig. S60 HSQC (^{1}H–^{13}C) NMR spectrum of poly(**1**-*b*-LLA) block copolymer (M_n 17300 g mol^{-1}, $Đ$ 1.84) in chloroform-d.

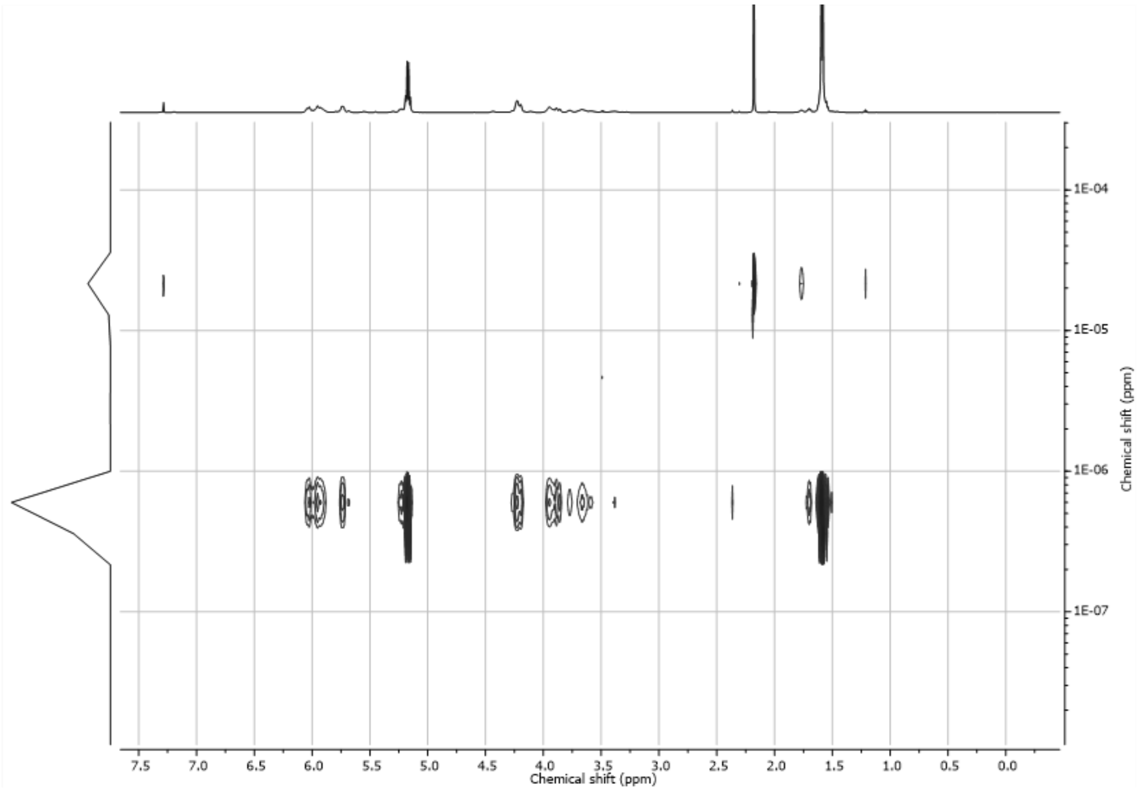

Fig. S61 DOSY NMR spectrum of poly(**1**-*b*-LLA) copolymer (M_n 17600 g mol^{-1}, $Đ$ 1.83) in chloroform-d. Residual solvent signals detected as independent peak.

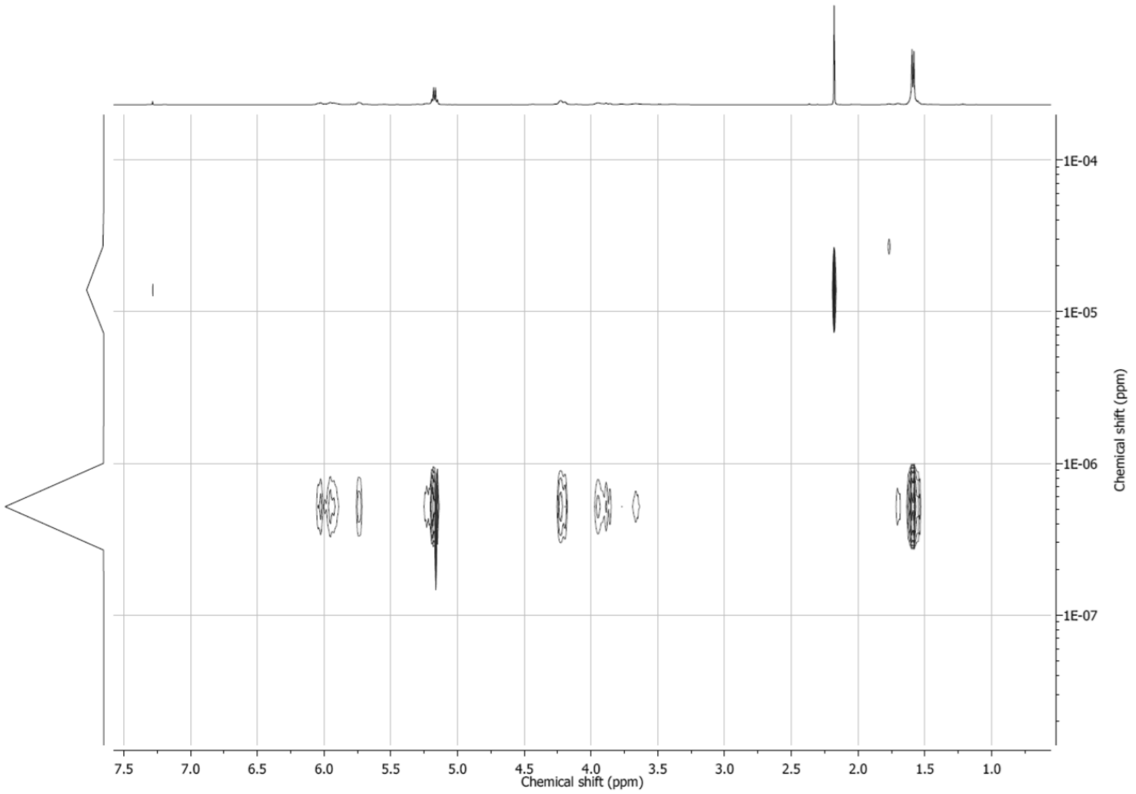

Fig. S62 DOSY NMR spectrum of acetone washed poly(**1**-*b*-LLA) block copolymer (M_n 17300 g mol^{-1}, $Đ$ 1.84) in chloroform-d. Residual solvent signals detected as independent peak.

Size-Exclusion Chromatography of poly(1-*b*-LLA) block copolymer

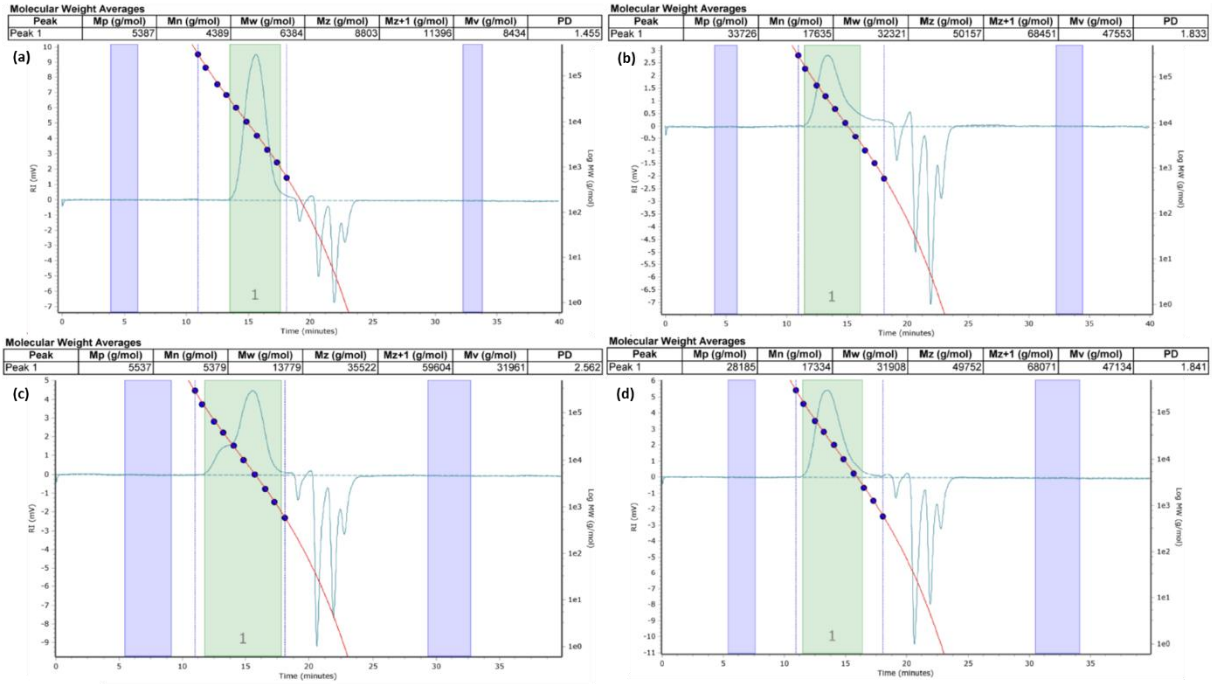

Molecular Weight Averages

Peak	Mp (g/mol)	Mn (g/mol)	Mw (g/mol)	Mz (g/mol)	Mz+1 (g/mol)	Mv (g/mol)	PD
Peak 1	5387	4389	6384	8803	11396	8434	1.455

Molecular Weight Averages

Peak	Mp (g/mol)	Mn (g/mol)	Mw (g/mol)	Mz (g/mol)	Mz+1 (g/mol)	Mv (g/mol)	PD
Peak 1	33726	17635	32321	50157	68451	47553	1.833

Molecular Weight Averages

Peak	Mp (g/mol)	Mn (g/mol)	Mw (g/mol)	Mz (g/mol)	Mz+1 (g/mol)	Mv (g/mol)	PD
Peak 1	5537	5379	13779	35522	59604	31961	2.562

Molecular Weight Averages

Peak	Mp (g/mol)	Mn (g/mol)	Mw (g/mol)	Mz (g/mol)	Mz+1 (g/mol)	Mv (g/mol)	PD
Peak 1	28185	17334	31908	49752	68071	47134	1.841

Fig. S63 SEC traces of the living polymerisation process: (a) After 6h, before the addition of L-lactide (M_n 4400 g mol^{-1}, *Đ* 1.46), (b) After 8h, the precipitated poly(**1**-*b*-LLA) copolymer (M_n 17600 g mol^{-1}, *Đ* 1.83), (c) A polymer mix of samples (a) and (b) (M_n 5400 g mol^{-1}, *Đ* 2.56), (d) Acetone washed poly(**1**-*b*-LLA) block copolymer (M_n 17300 g mol^{-1}, *Đ* 1.84).

One-pot copolymerisation experiments

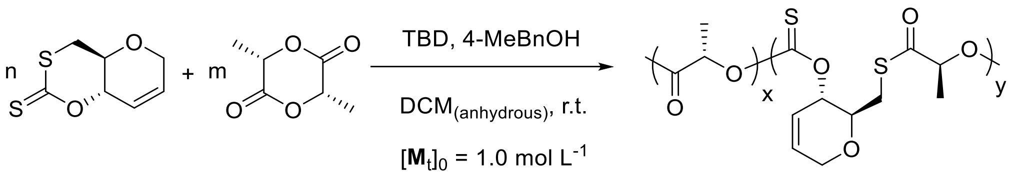

Under an argon atmosphere 4-MeBnOH (32 µL, 0.5 mol L^{-1} in anhydrous DCM, 0.016 mmol, 1.0 equiv.) and TBD (32 µL, 0.5 mol L^{-1} in anhydrous DCM, 0.016 mmol, 1.0 equiv.) were added to a solution of L-Lactide (0.115 g, 0.797 mmol, 50 equiv.) and monomer **1** (0.150 g, 0.797 mmol, 50 equiv.) in anhydrous DCM (1.6 mL, 1.0 mol L^{-1}). The mixture was stirred at room temperature for 20 h and quenched by the addition of a benzoic acid solution (≈30 equiv.). The solvent was removed under reduced pressure and the solid was dissolved in $CHCl_3$ and precipitated from Et_2O. The product was isolated by centrifugation (3500 rpm, 2 x 5 minutes), washed twice with Et_2O and dried under vacuum. The polymer was isolated as a yellow solid.

δ_H (500 MHz; chloroform-d): 6.08-5.80 (C^2H, C^3H, 2H, m), 5.74-5.63 (C^4H, 1H, m), 5.22-5.10 (C^8H, 7H, m), 4.22-4.13 (C^1H, 2H, m), 3.96-3.70 (C^5H, C^6H, 2H, m), 3.67-3.48 (C^6H, 1H, m), 1.60-1.49 (C^9H, 20H, m) ppm; δ_C (126 MHz; chloroform-d): 194.2 (C^7), 169.7 (C^{10}), 130.1 (C^2), 123.5 (C^3), 76.1 (C^5), 73.9 (C^4), 69.4 (C^9), 65.2 (C^1), 38.5 (C^6), 16.7 (C^9) ppm.

NMR Spectroscopic Characterisation of poly(1-*co*-LLA) random copolymer

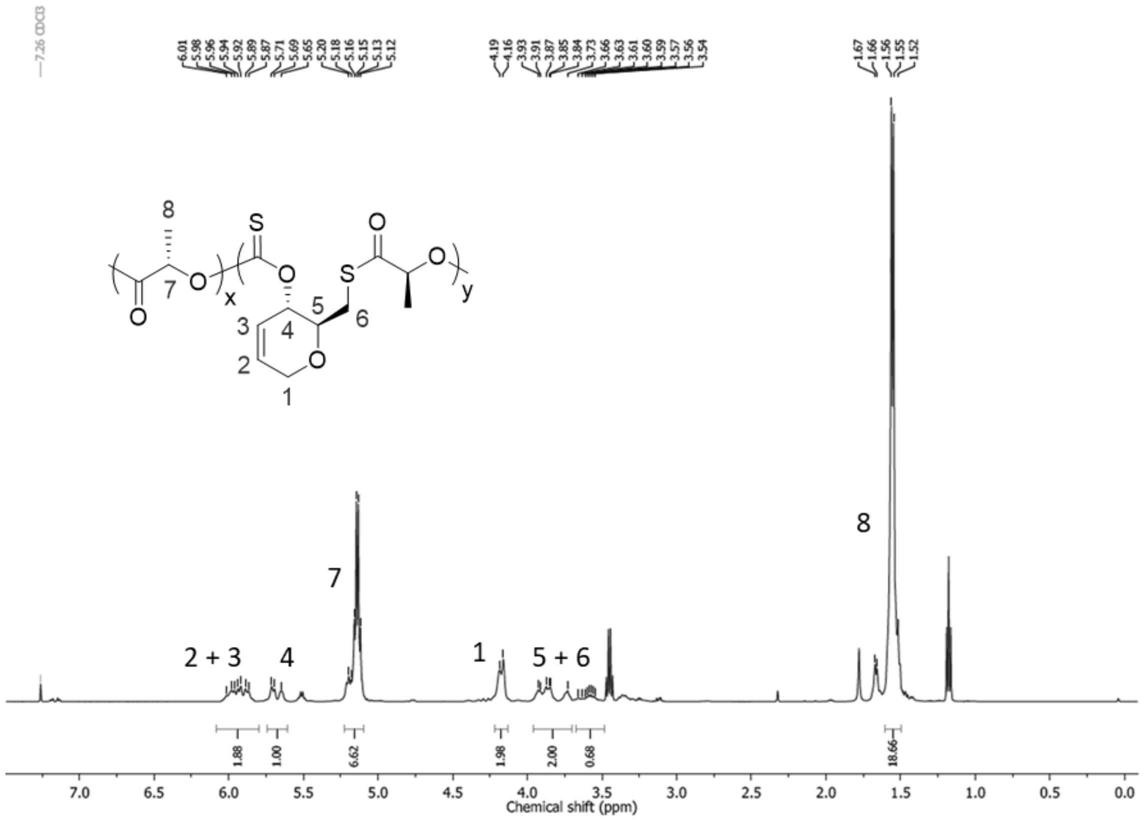

Fig. S64 Annotated ^1H NMR of poly(**1**-*co*-LLA) random copolymer (Table 2, Run 4) (M_n 25100 g mol^{-1} ($Đ$ 1.86)) in chloroform-d. Residual Et_2O signals at δ_H 1.12 (t) and 3.38 (q) ppm.

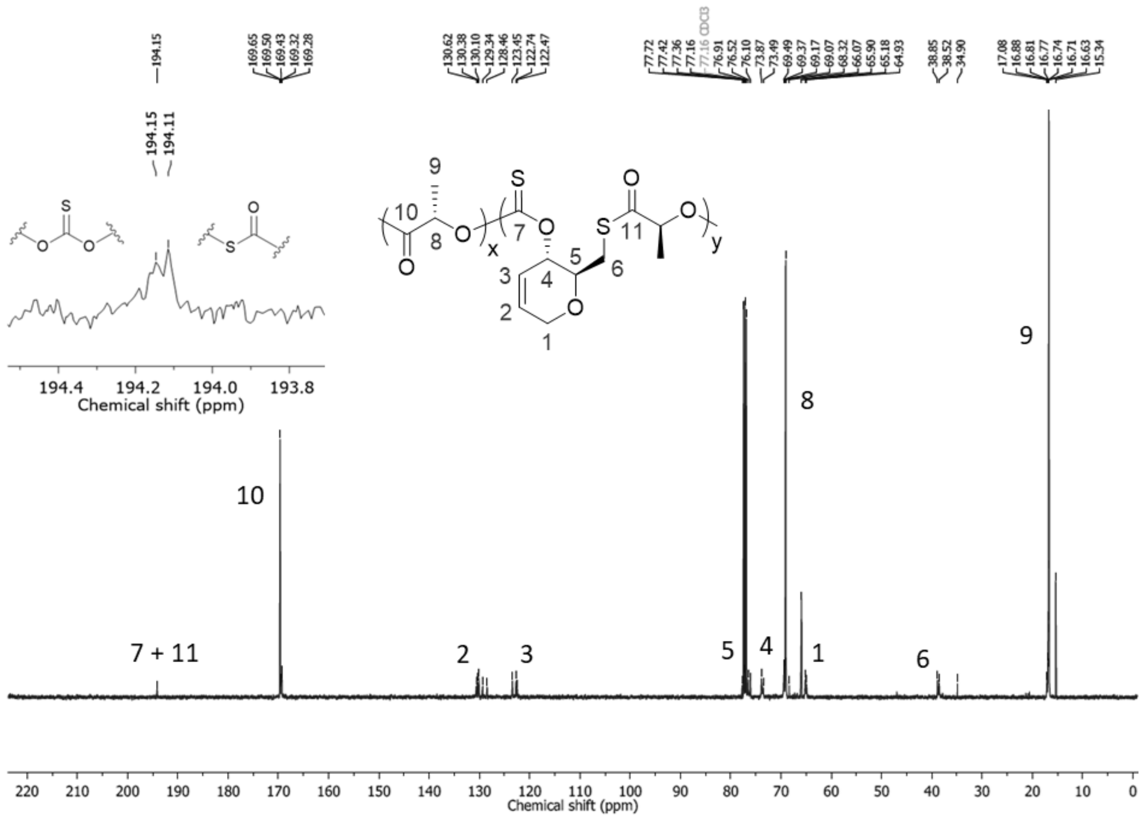

Fig. S65 Annotated ^{13}C{^{1}H} NMR of poly(**1**-*co*-LLA) random copolymer (Table 2, Run 4) (M_n 25100 g mol^{-1} ($Đ$ 1.86)) in chloroform-d. Residual Et$_2$O signals at δ$_c$ 15.4 and 66.1 ppm. (inset) Closely situated carbon environments corresponding to C(S)O$_2$ and C(O)S linkages of poly(**1**-*co*-LLA).

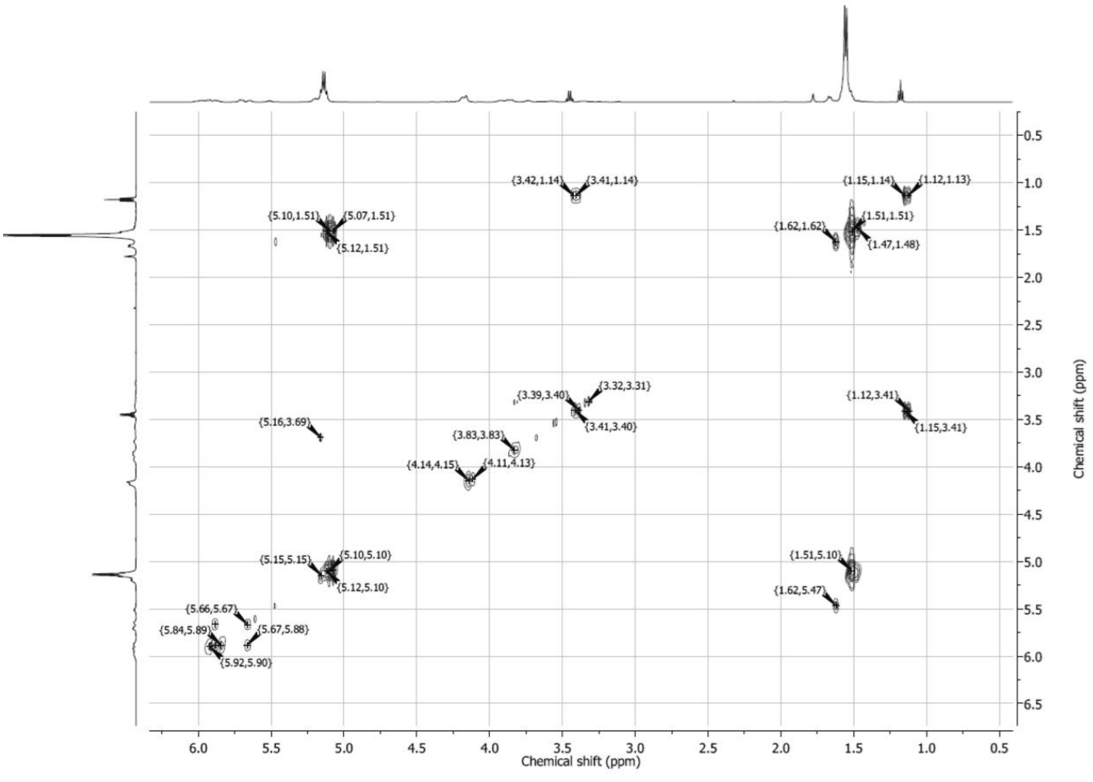

Fig. S66 COSY (^{1}H–^{1}H) NMR spectrum of poly(**1**-*co*-LLA) random copolymer (Table 2, Run 4) (M_n 25100 g mol^{-1} ($Đ$ 1.86)) in chloroform-d.

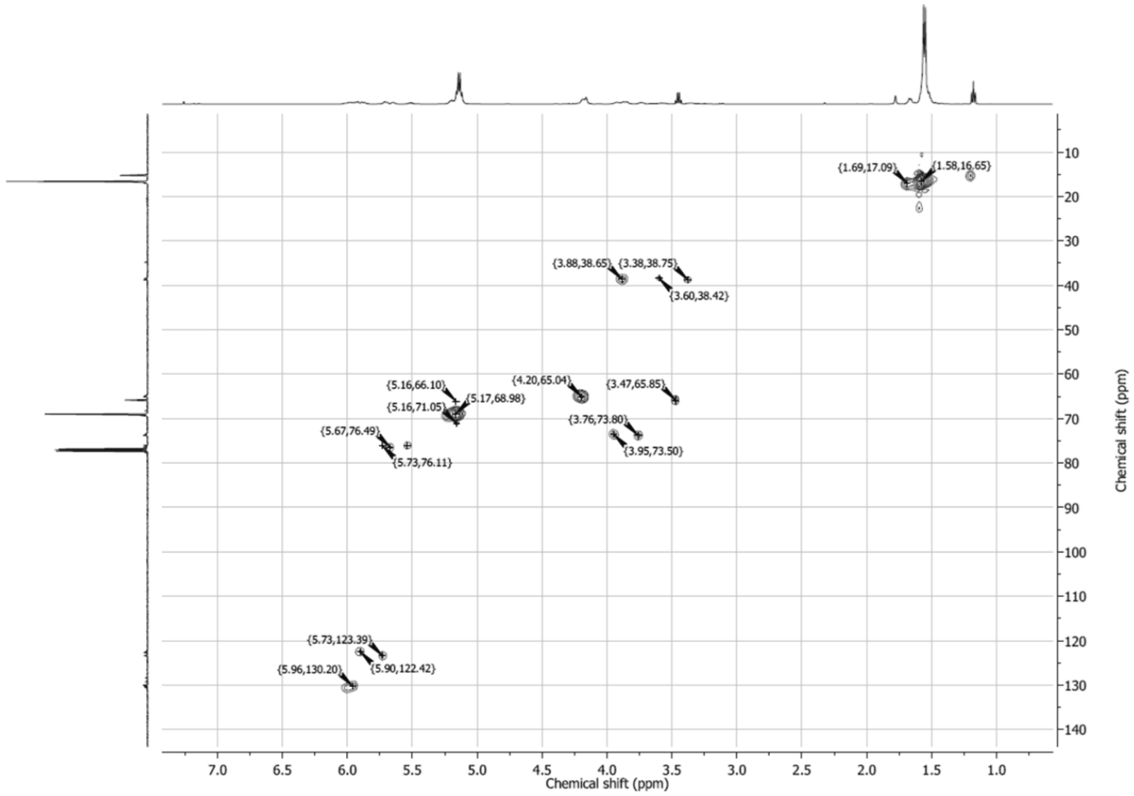

Fig. S67 HSQC (^{1}H–^{13}C) NMR spectrum of poly(**1**-*co*-LLA) random copolymer (Table 2, Run 4) (M_n 25100 g mol^{-1} ($Đ$ 1.86)) in chloroform-d.

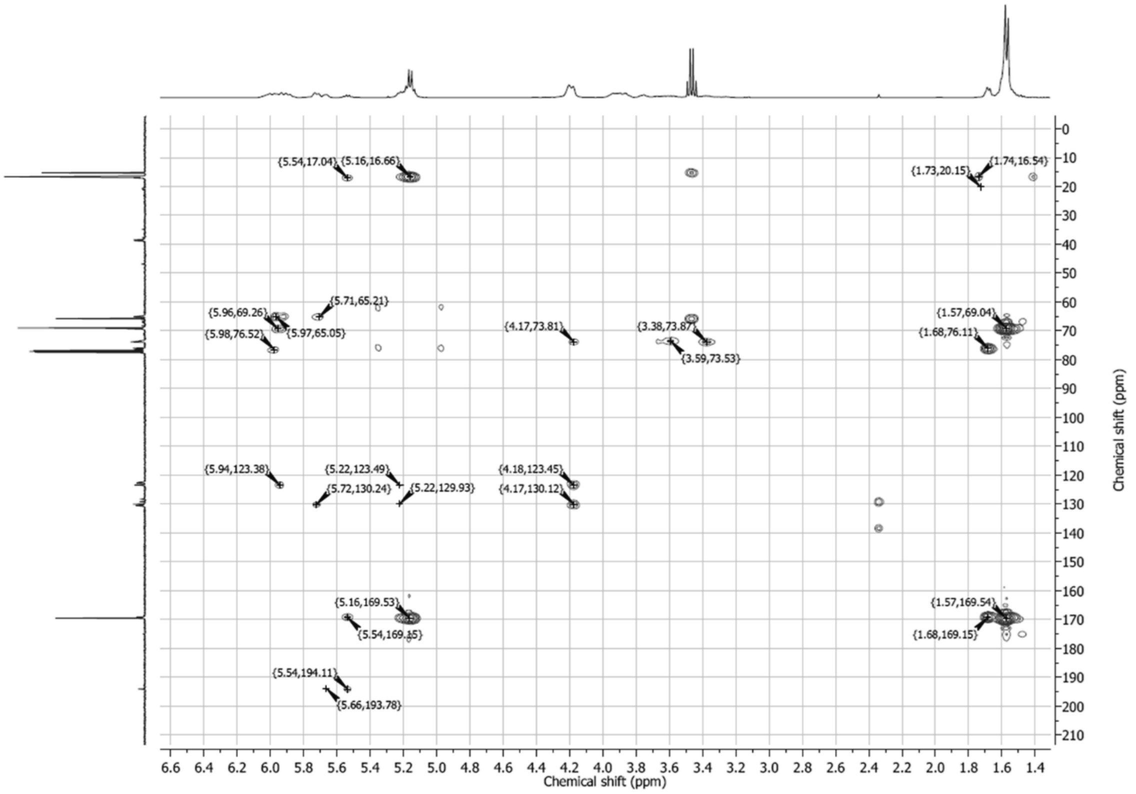

Fig. S68 HMBC (^{1}H–^{13}C) NMR spectrum of poly(**1**-*co*-LLA) random copolymer in chloroform-d.

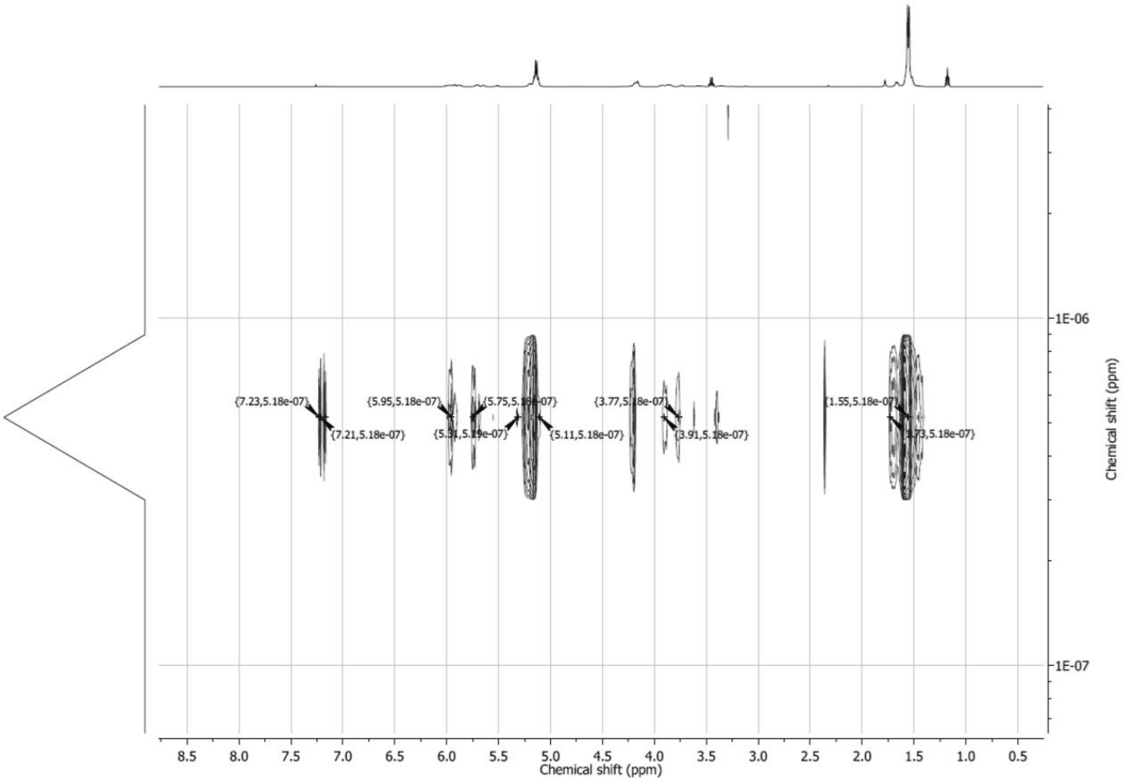

Fig. S69 DOSY NMR spectrum of poly(**1**-*co*-LLA) random copolymer (Table 2, Run 2) (M_n 13200 g mol^{-1} ($Đ$ 1.66)) in chloroform-d.

Size-Exclusion Chromatography of poly(1-*co*-LLA) random copolymer

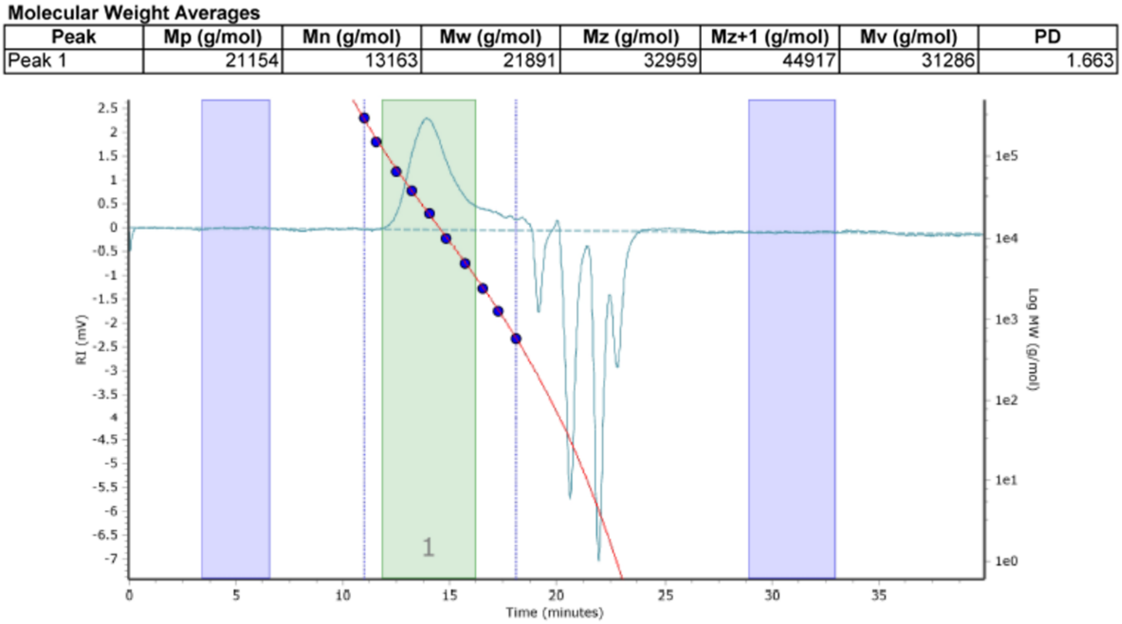

Molecular Weight Averages

Peak	Mp (g/mol)	Mn (g/mol)	Mw (g/mol)	Mz (g/mol)	Mz+1 (g/mol)	Mv (g/mol)	PD
Peak 1	21154	13163	21891	32959	44917	31286	1.663

Fig. S70 SEC trace of poly(**1**-*co*-LLA) random copolymer showing M_n 13200 g mol^{-1} ($Đ$ 1.66) (Table 2, run 2).

Molecular Weight Averages

Peak	Mp (g/mol)	Mn (g/mol)	Mw (g/mol)	Mz (g/mol)	Mz+1 (g/mol)	Mv (g/mol)	PD
Peak 1	27047	15797	28426	42731	56626	40701	1.799

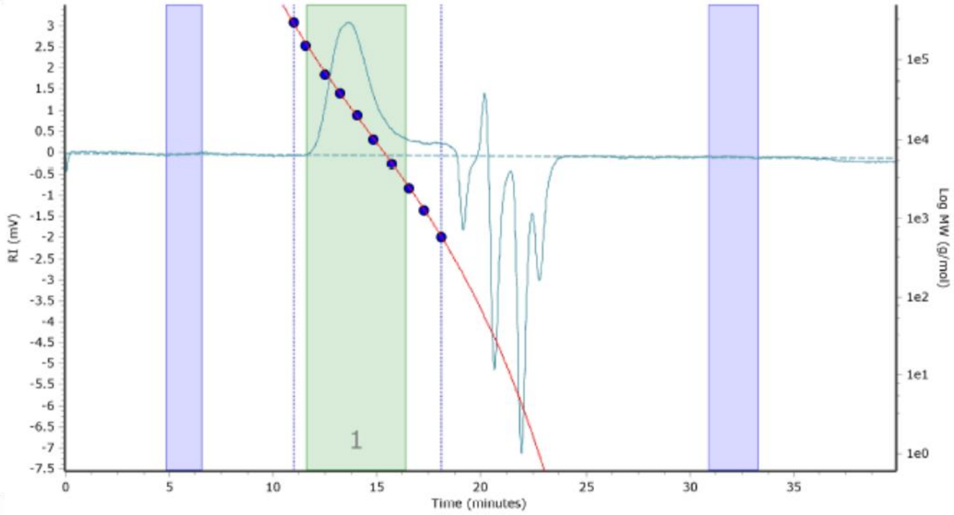

Fig. S71 SEC trace of poly(**1**-*co*-LLA) random copolymer showing M_n 15800 g mol^{-1} ($Đ$ 1.80) (Table 2, run 3).

DSC of poly(1-co-LLA) random copolymers

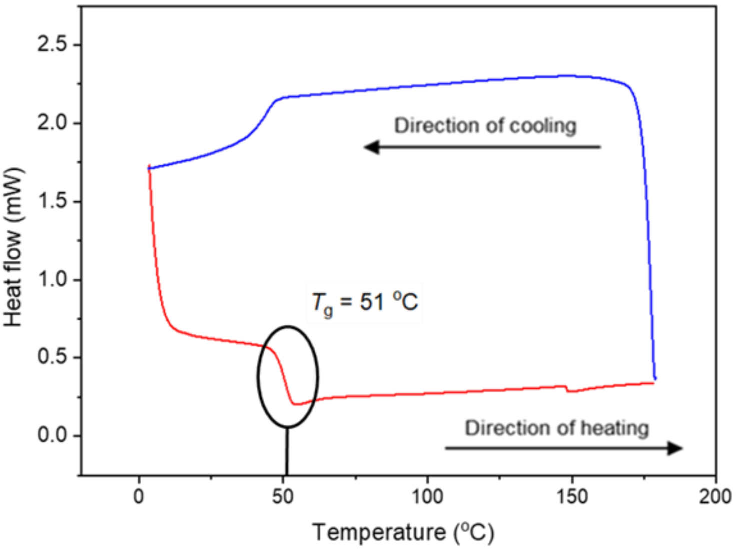

Fig. S72 DSC trace of poly(**1**-*co*-LLA) random copolymer (M_n 22500 g mol^{-1} ($Đ$ 1.59)) (Table 2, Run 1). Second heating and cooling cycle between 0 and 180 °C. Single exothermic peak, corresponding to the T_g = 51 °C of the polymer.

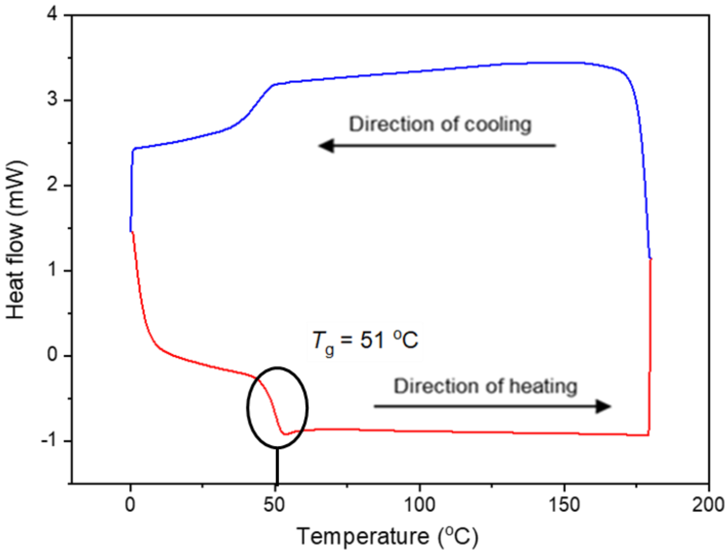

Fig. S73 DSC trace of poly(**1**-*co*-LLA) random copolymer (M_n 13200 g mol^{-1} (*Đ* 1.66)) (Table 2, Run 2). Second heating and cooling cycle between 0 and 180 °C. Single exothermic peak, corresponding to the T_g = 51 °C of the polymer.

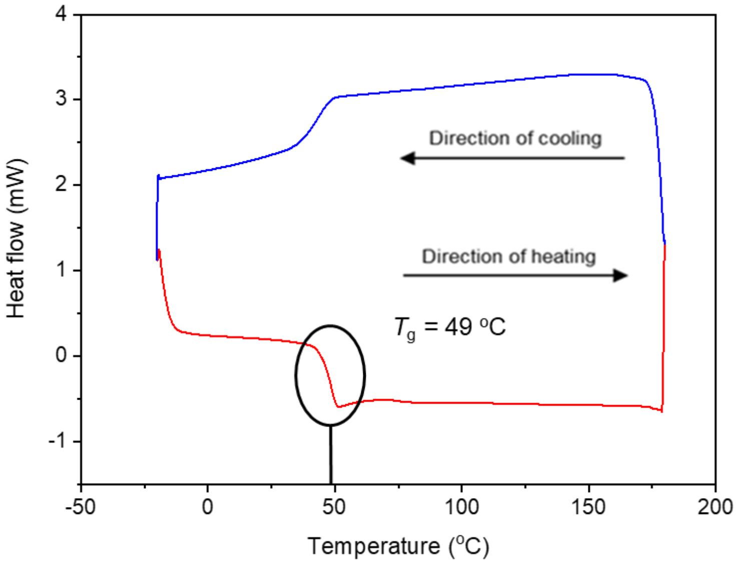

Fig. S74 DSC trace of poly(**1**-*co*-LLA) random copolymer (M_n 14800 g mol^{-1} (*Đ* 1.70)) (Table 2, Run 3). Second heating and cooling cycle between -20 and 180 °C. Single exothermic peak, corresponding to the T_g = 49 °C of the polymer.

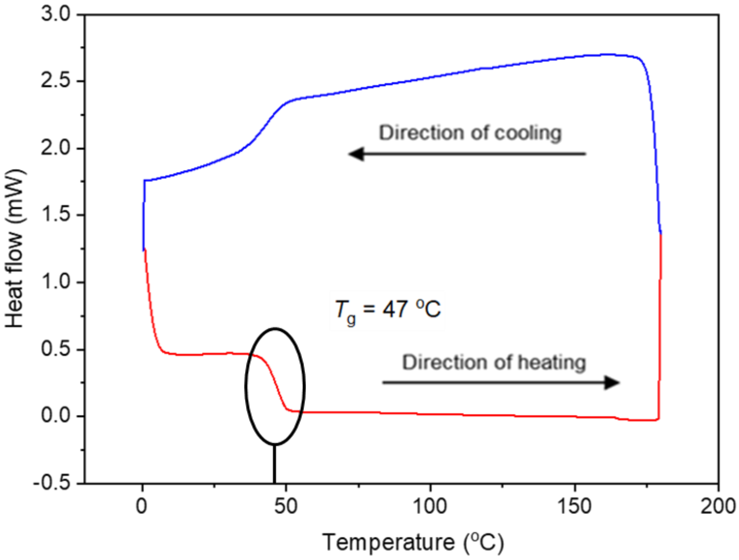

Fig. S75 DSC trace of poly(**1**-*co*-LLA) random copolymer (M_n 15800 g mol^{-1} (*Đ* 1.80)) (Table 2, Run 4). Second heating and cooling cycle between 0 and 180 °C. Single exothermic peak, corresponding to the T_g = 47 °C of the polymer.

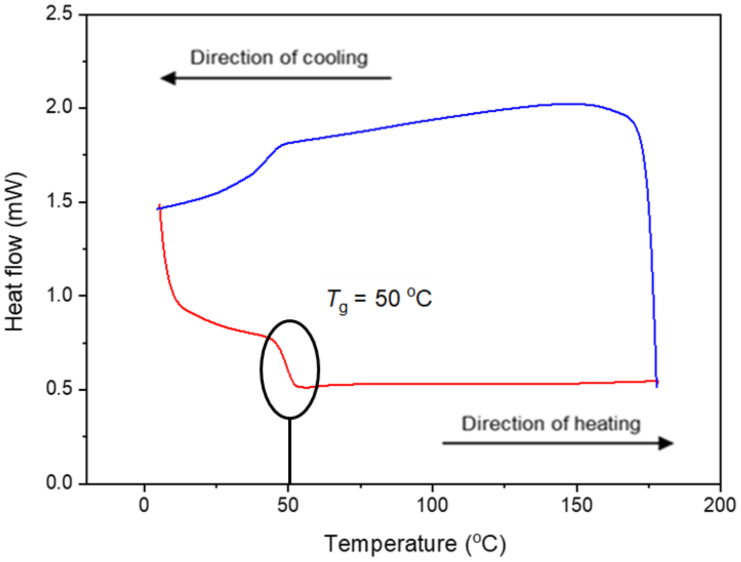

Fig. S76 DSC trace of poly(**1**-*co*-LLA) random copolymer (M_n 25100 g mol^{-1} (*Đ* 1.88)) (Table 2, Run 5). Second heating and cooling cycle between 0 and 180 °C. Single exothermic peak, corresponding to the T_g = 50 °C of the polymer.

TGA of poly(**1**-*co*-LLA) random copolymer

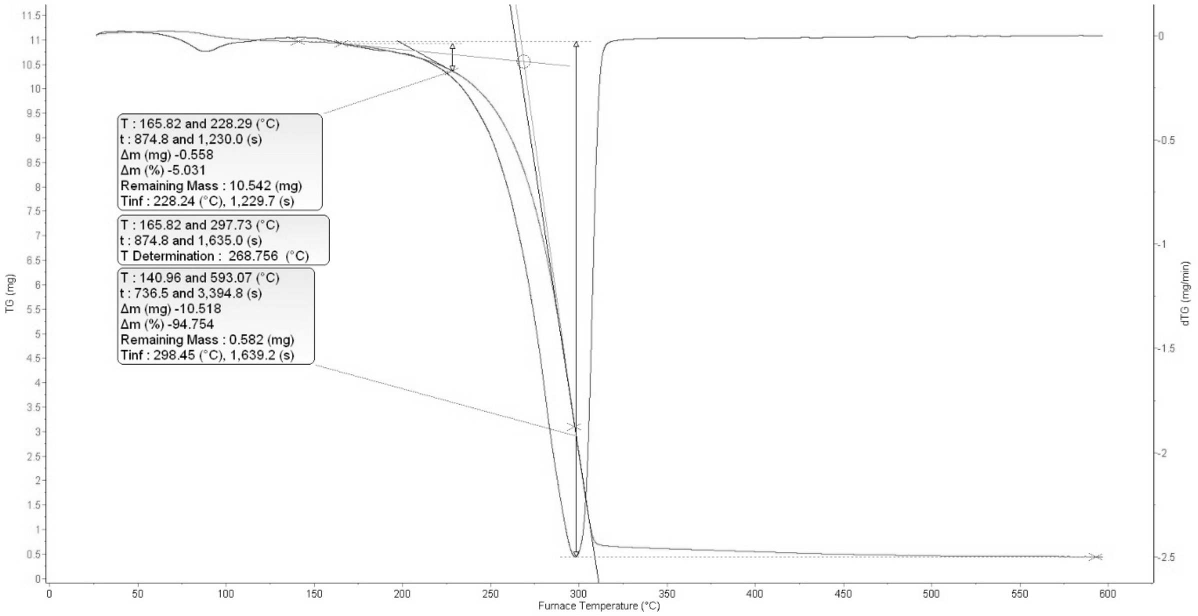

Fig. S77 TGA trace of poly(**1**-*co*-LLA) random copolymer (Table 2, Run 1) (M_n 22500 g mol^{-1} ($Đ$ 1.59)). The polymer was heated from 30 to 600 °C under argon at 10 °C min^{-1}. Obtained values: $T_{d5\%}$ = 228 °C and $T_{d,max}$ = 298 °C with 5 % char remaining at 600 °C.

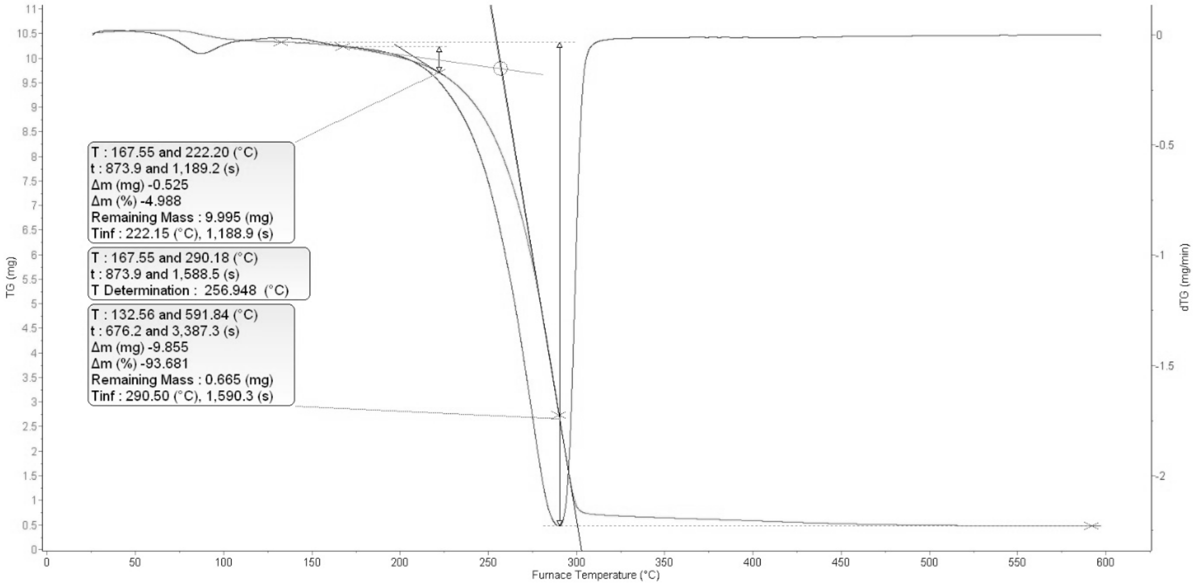

Fig. S78 TGA trace of poly(**1**-*co*-LLA) random copolymer (Table 2, Run 2) (M_n 13200 g mol^{-1} ($Đ$ 1.66)). The polymer was heated from 30 to 600 °C under argon at 10 °C min^{-1}. Obtained values: $T_{d5\%}$ = 222 °C and $T_{d,max}$ = 290 °C with 6 % char remaining at 600 °C.

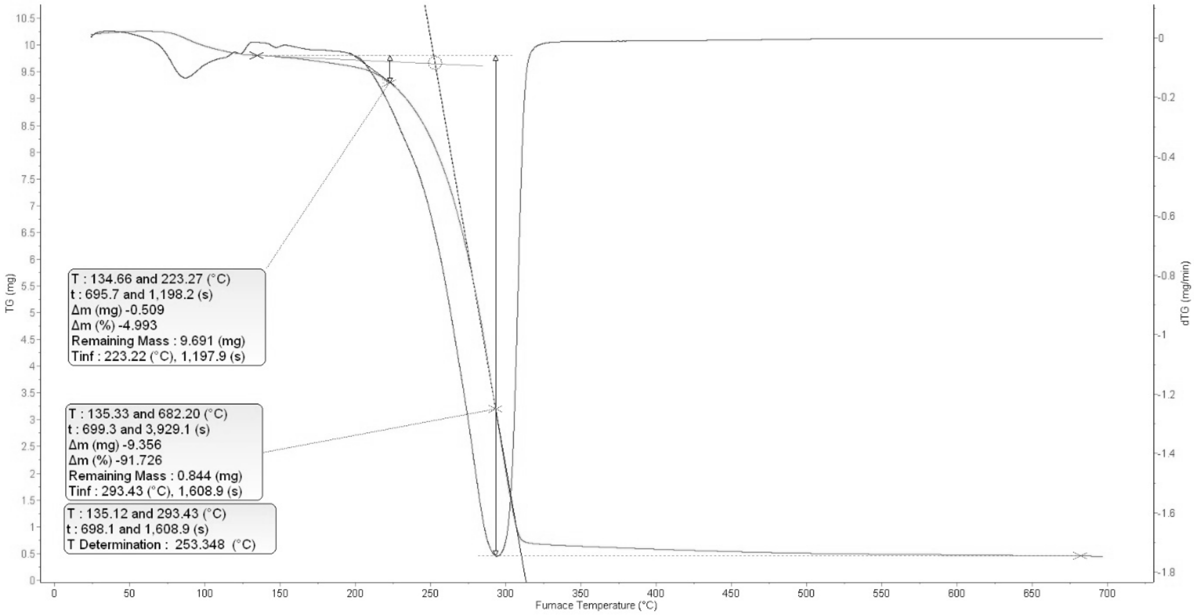

Fig. S79 TGA trace of poly(**1**-*co*-LLA) random copolymer (Table 2, Run 3) (M_n 14800 g mol^{-1} ($Đ$ 1.70)). The polymer was heated from 30 to 600 °C under argon at 10 °C min^{-1}. Obtained values: $T_{d5\%}$ = 223 °C and $T_{d,max}$ = 293 °C with 8 % char remaining at 700 °C.

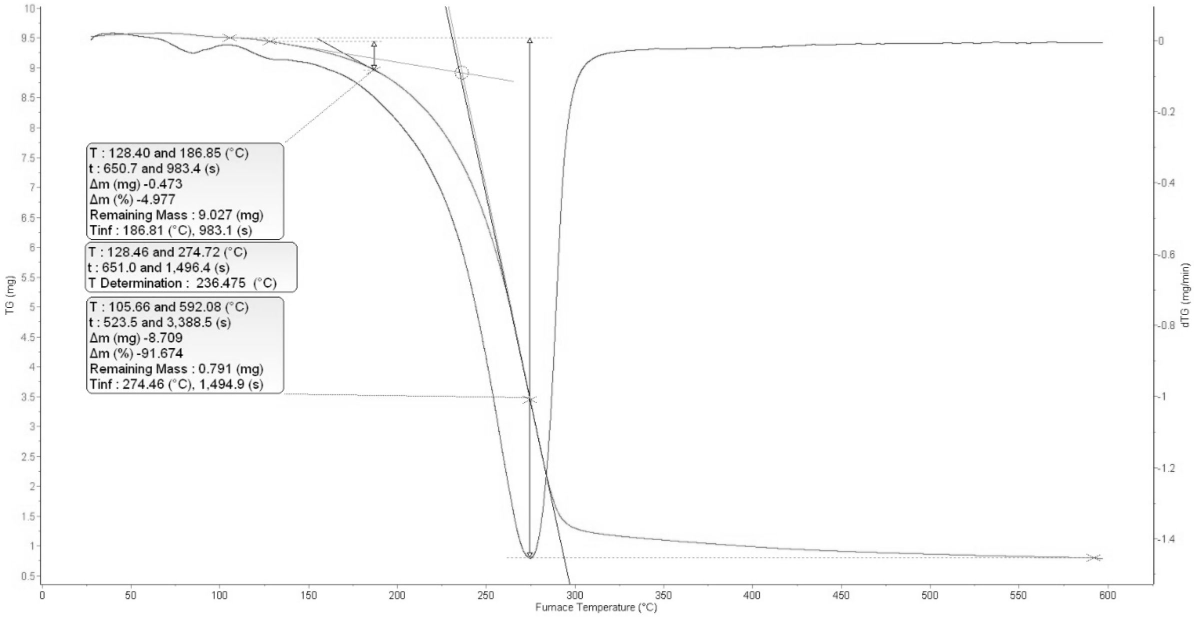

Fig. S80 TGA trace of poly(**1**-*co*-LLA) random copolymer (Table 2, Run 4) (M_n 15800 g mol^{-1} ($Đ$ 1.80)). The polymer was heated from 30 to 600 °C under argon at 10 °C min^{-1}. Obtained values: $T_{d5\%}$ = 187 °C and $T_{d,max}$ = 275 °C with 8 % char remaining at 600 °C.

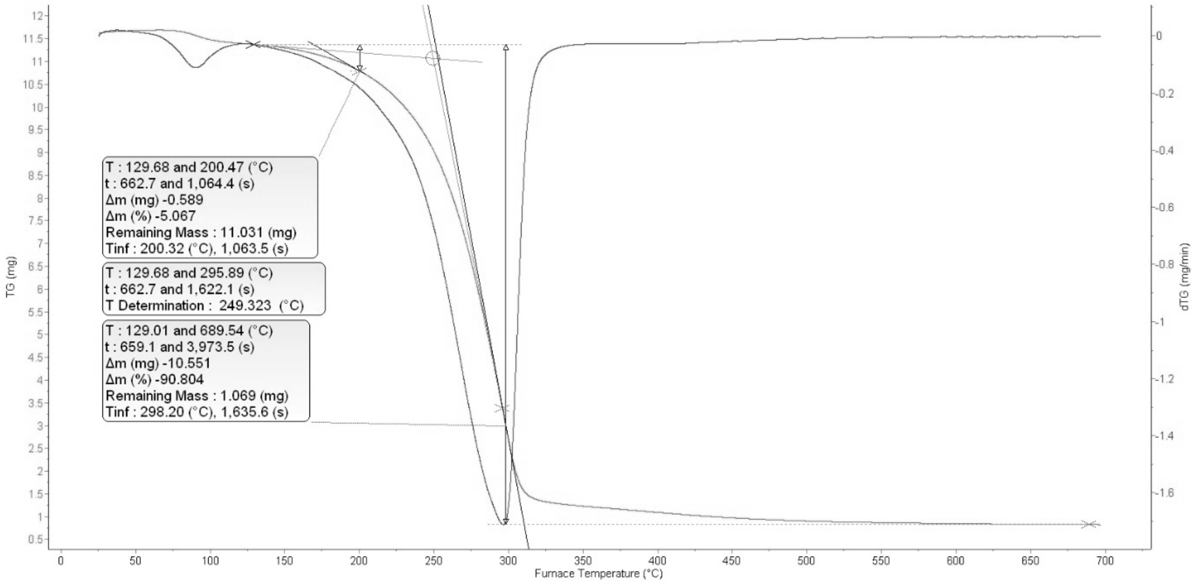

Fig. S81 TGA trace of poly(**1**-*co*-LLA) random copolymer (Table 2, Run 5) (M_n 25100 g mol^{-1} ($Đ$ 1.86)). The polymer was heated from 30 to 600 °C under argon at 10 °C min^{-1}. Obtained values: $T_{d5\%}$ = 200 °C and $T_{d,max}$ = 296 °C with 9 % char remaining at 700 °C.

UV-Vis analysis of poly(1-*co*-LLA) random copolymer

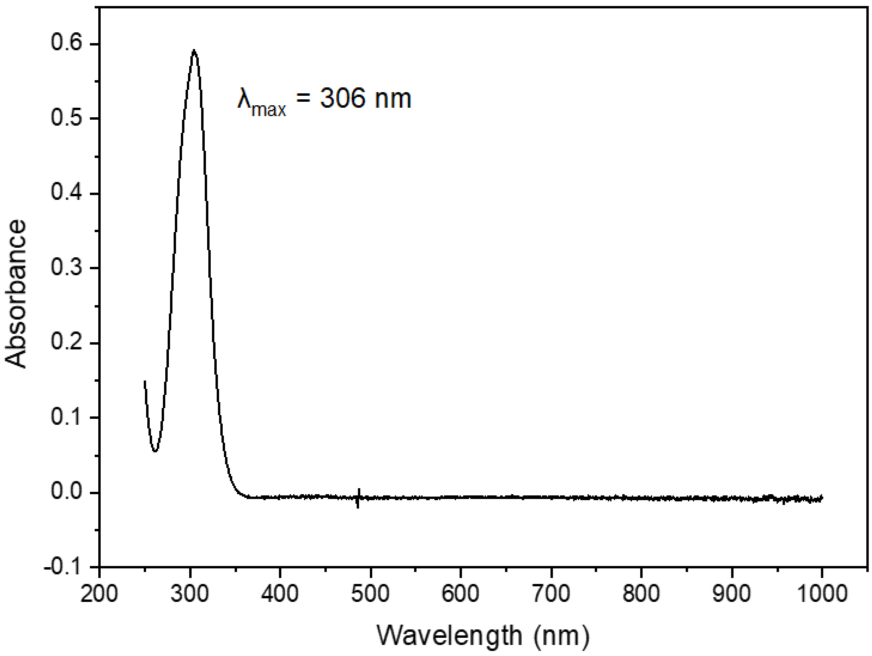

Fig. S82 UV-Vis absorption spectra of poly(**1**-*co*-LLA) (Table 2, Run 4) upon irradiation of sample solution in THF in a 10-mm glass cell ([poly(**1**-*co*-LLA)]$_0$ = 4.4 x 10^{-4} mol L^{-1} based on monomer repeat unit, at room temperature). Single absorption peak detected, λ_{max} = 306 nm.

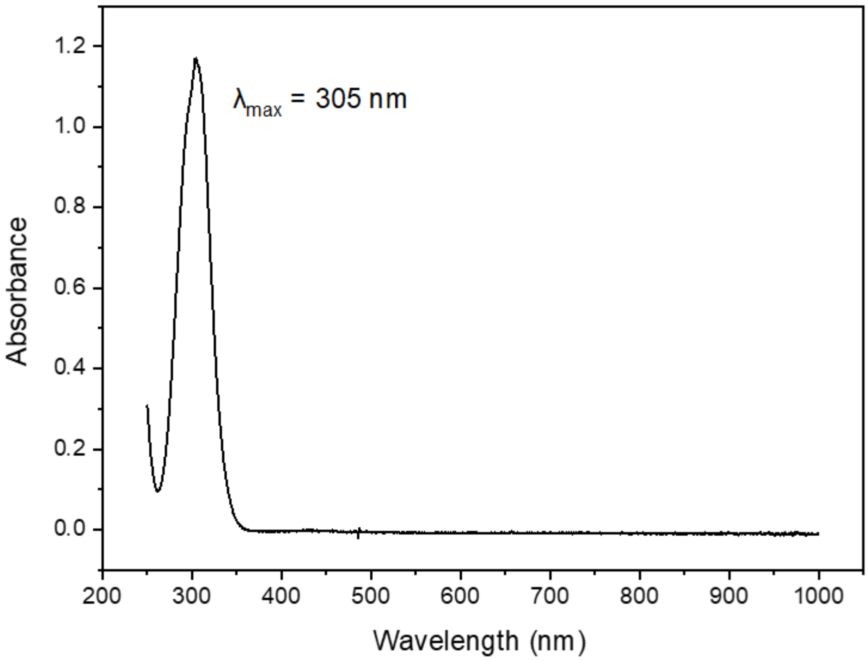

Fig. S83 UV-Vis absorption spectra of poly(**1**-*co*-LLA) (Table 2, Run 5) upon irradiation of sample solution in THF in a 10-mm glass cell ([poly(**1**-*co*-LLA)]$_0$ = 4.4 x 10^{-4} mol L^{-1} based on polymer repeat unit, at room temperature). Single absorption peak detected, λ_{max} = 305 nm.

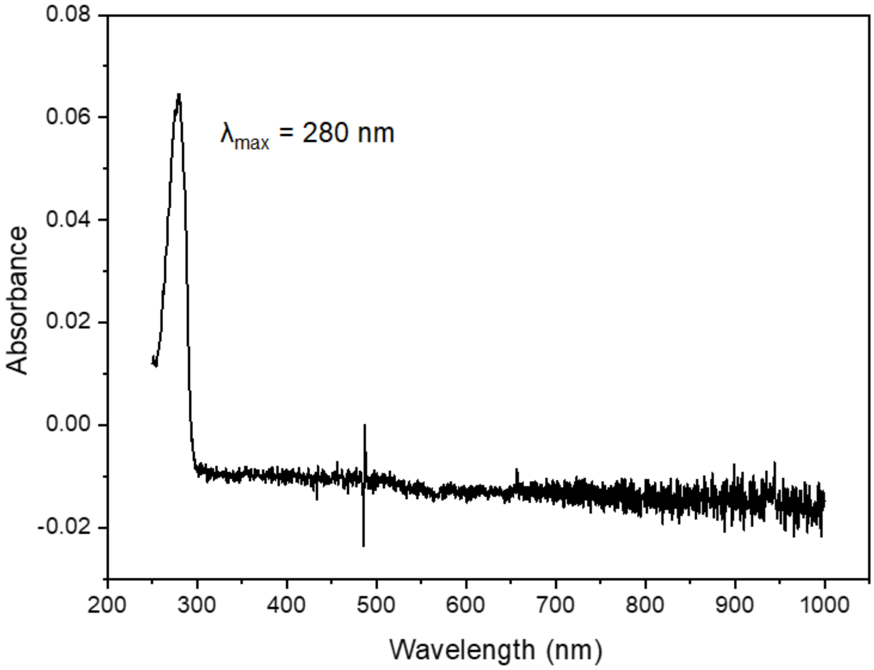

Fig. S84 UV-Vis absorption spectra of poly(LLA) upon irradiation of sample solution in THF in a 10-mm glass cell ([poly(LLA)]$_0$ = 1.7 x 10^{-3} mol L^{-1} based on polymer repeat unit, at room temperature). Single absorption peak detected, λ_{max} = 280 nm.

5. Polymer Degradation

UV degradation of poly(1)

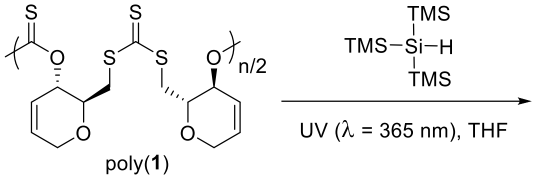

Under an argon atmosphere, tris(trimethylsilyl)silane (TTMSS) (0.43 mL, 1.39 mmol, 7.5 equiv.) was added to a THF solution (4.2 mL) of poly(**1**) (0.035 g, 0.019 mmol, 1.0 equiv.). The solution was divided equally between 6 vacuum-tight vials. The vials were placed under UV light (λ = 365 nm) and taken off at predetermined intervals. All crude reaction mixtures were then subjected to ^{1}H NMR spectroscopy and SEC analysis. *Degradation in the absence of TTMSS is identical to the procedure described above without addition of the silane reagent.*

Table S4 UV degradation of poly(**1**) with TTMSS.

Entry	Time (h)	$M_{n,SEC}$ $^{(a)}$	$M_{w,SEC}$ $^{(a)}$	% M_n $^{(b)}$	$Đ$ $^{(a)}$
1	0	10000	17800	100	1.77
2	0.17	2800	7200	28	2.55
3	0.5	1600	3400	16	2.13
4	1	1200	3000	12	2.50
5	2	880	2300	9	2.62
6	4	740	2100	7	2.84
7	6	600	1500	6	2.51

^{a}Number-average molecular weight and Dispersity ($M_{n,SEC}$, $M_{w,SEC}$, $Đ$), calculated by SEC relative to polystyrene standards in THF eluent, units given in g mol^{-1}; ^{b}Percentage of the original $\boldsymbol{M_{n,SEC}}$**.**

Table S5 UV degradation of poly(**1**) without TTMSS.

Entry	Time (h)	$M_{n,SEC}$ $^{(a)}$	$M_{w,SEC}$ $^{(a)}$	% M_n $^{(b)}$	$Đ$ $^{(a)}$
1	0	10000	17800	100	1.77
2	0.5	5100	11800	51	2.31
3	1	4100	10400	41	2.54
4	2	2300	7430	23	3.23
5	4	1300	4000	13	3.08
6	6	780	2150	8	2.75

^{a}Number-average molecular weight and Dispersity ($M_{n,SEC}$, $M_{w,SEC}$, $Đ$), calculated by SEC relative to polystyrene standards in THF eluent, units given in g mol^{-1}; ^{b}Percentage of the original $\boldsymbol{M_{n,SEC}}$**.**

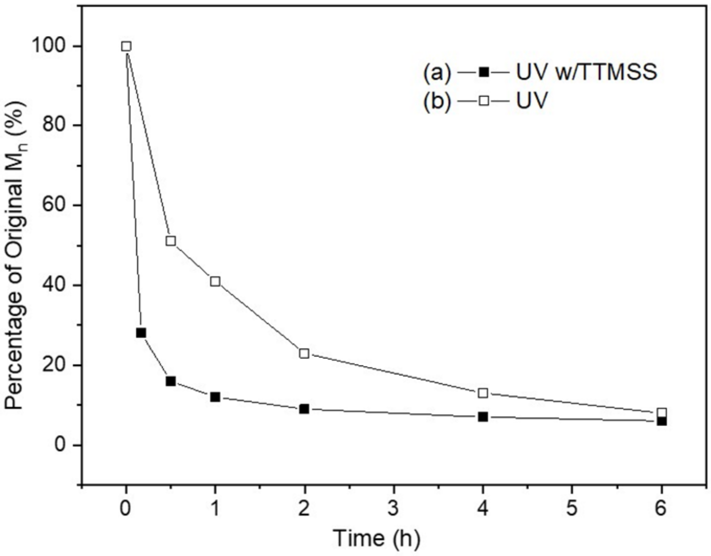

Fig. S85 Plot of original M$_n$ percentage versus time, following the degradation of poly(**1**) ($M_{n,SEC}$ = 10,000 g mol^{-1}, $Đ_M$ = 1.77) once exposed to UV irradiation (λ = 365 nm) in the presence of (a) TTMSS (7.5 equiv.) and (b) no TTMSS. The reactions were performed at room temperature with [poly(**1**)]$_0$ = 0.044 mol L^{-1}.

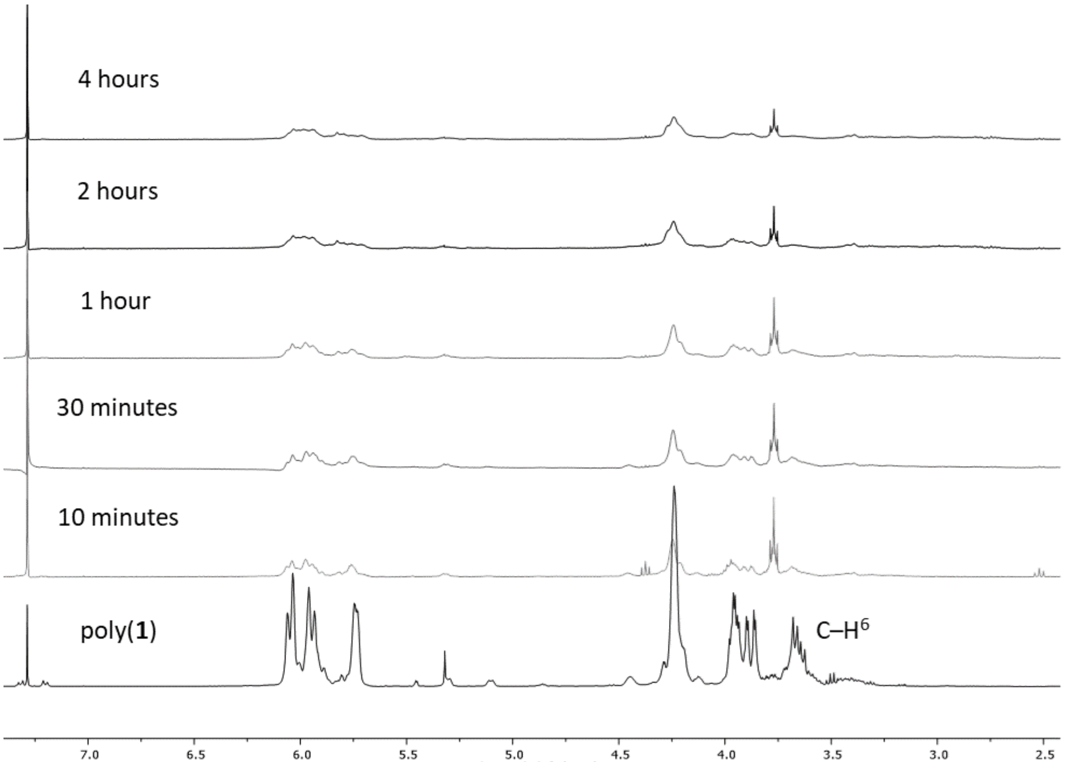

Fig. S86 Stacked ^{1}H NMR spectra following the degradation of poly(**1**) over 4 hours. Carried out at rt in THF, exposed to UV irradiation (λ = 365 nm) in the presence of TTMSS (7.5 equiv.). The H-6′ proton signal has been identified as an indication of the complete breakdown of the trithiocarbonate linkages.

UV degradation of poly(1-*co*-LLA) random copolymer

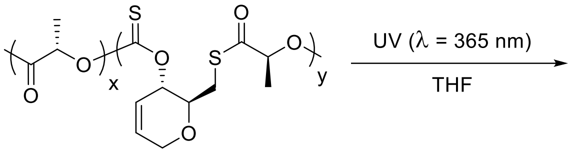

Under an argon atmosphere, a solution of copolymer (0.035 g, 0.019 mmol, 1.0 equiv.) in THF (4.2 mL) of was divided equally between 6 vacuum-tight vials. The vials were placed under UV light (λ = 365 nm) and taken off at predetermined intervals. All crude reaction mixtures were then subjected to ^{1}H NMR spectroscopy and SEC analysis.

Table S6 UV degradation of poly(**1**-*co*-LLA) random copolymer (Table 2, Run 2, 3/97).

Entry	Time (h)	$M_{n,SEC}$$^{(a)}$	$M_{w,SEC}$$^{(a)}$	% $M_n$$^{(b)}$	$Đ$$^{(a)}$
1	0	13200	21900	100	1.66
2	0.5	11200	26800	85	2.39
3	1	10400	23900	79	2.30
4	2	9500	22500	72	2.36
5	3	8900	21900	67	2.45
6	4	8400	19700	63	2.35
7	6	7500	19600	57	1.61

[a]Number-average molecular weight and Dispersity ($M_{n,SEC}$, $M_{w,SEC}$, $Đ$), calculated by SEC relative to polystyrene standards in THF eluent, units given in g mol^{-1}; [b]Percentage of the original $M_{n,SEC}$.

Table S7 Degradation of poly(**1**-*co*-LLA) random copolymer (Table 2, Run 4, 16/84).

Entry	Time (h)	$M_{n,SEC}$$^{(a)}$	$M_{w,SEC}$$^{(a)}$	% $M_n$$^{(b)}$	$Đ$$^{(a)}$
1	0	15800	28400	100	1.80
2	0.5	14600	32300	92	2.22
3	1	13400	36300	85	2.71
4	2	11800	36100	75	3.06
5	3	10500	34100	66	3.25
6	4	9800	32700	62	3.35
7	6	8500	30700	54	3.61

[a]Number-average molecular weight and Dispersity ($M_{n,SEC}$, $M_{w,SEC}$, $Đ$), calculated by SEC relative to polystyrene standards in THF eluent, units given in g mol^{-1}; [b]Percentage of the original $M_{n,SEC}$.

Table S8 Degradation of pure poly(lactide).

Entry	Time (h)	$M_{n,SEC}$[(a)]	$M_{w,SEC}$[(a)]	% M_n[(b)]	$Đ$[(a)]
1	0	12800	14300	100	1.12
2	0.5	12700	14600	99	1.15
3	1	12900	14500	101	1.13
4	2	12600	13900	98	1.10
5	3	12800	14500	100	1.14
6	4	12700	14300	99	1.12
7	6	12700	14200	99	1.13

[a]Number-average molecular weight and Dispersity ($M_{n,SEC}$, $M_{w,SEC}$, $Đ$), calculated by SEC relative to polystyrene standards in THF eluent, units given in g mol^{-1}; [b]Percentage of the original $M_{n,SEC}$.

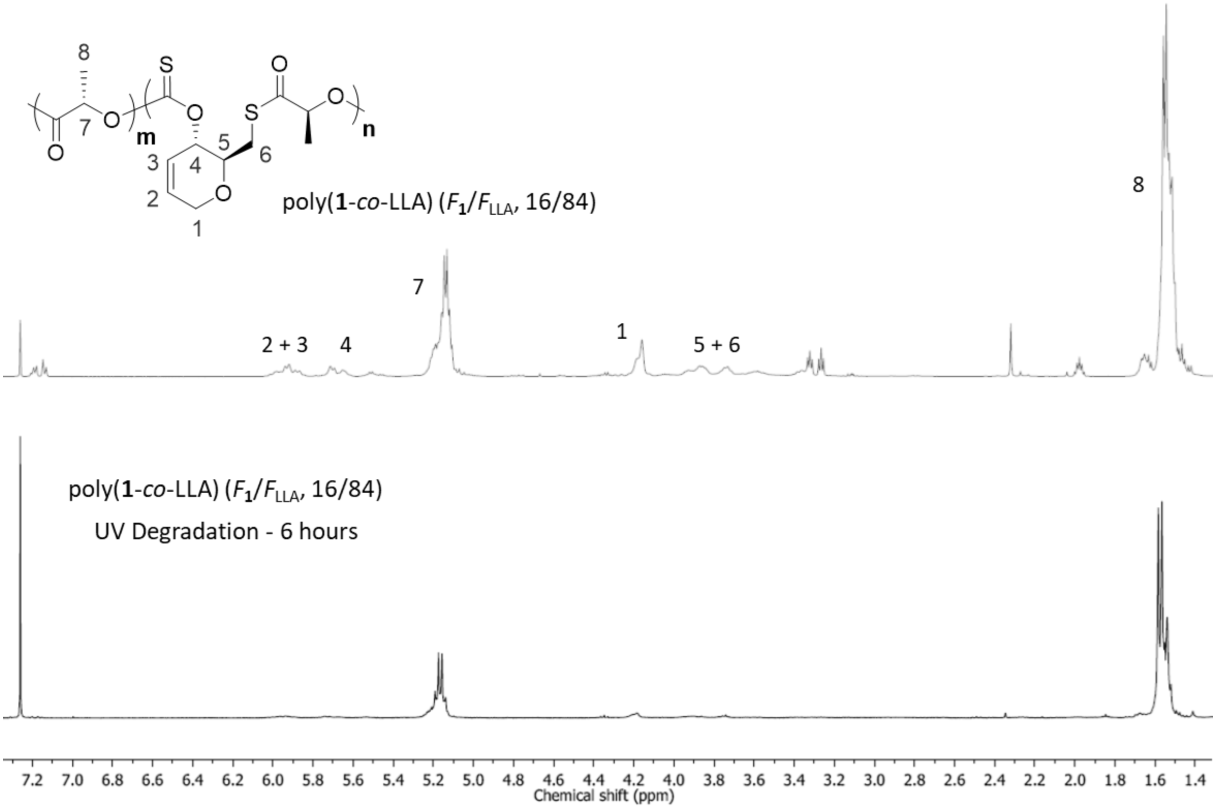

Fig. S87 Stacked ^{1}H NMR spectra of poly(**1**-*co*-LLA) over the degradation products after 6 hours. Carried out at rt in THF, exposed to UV irradiation (λ = 365 nm). The proton signal of poly(**1**-*co*-LLA) have been annotated as an indication of the structural breakdown of the copolymer.

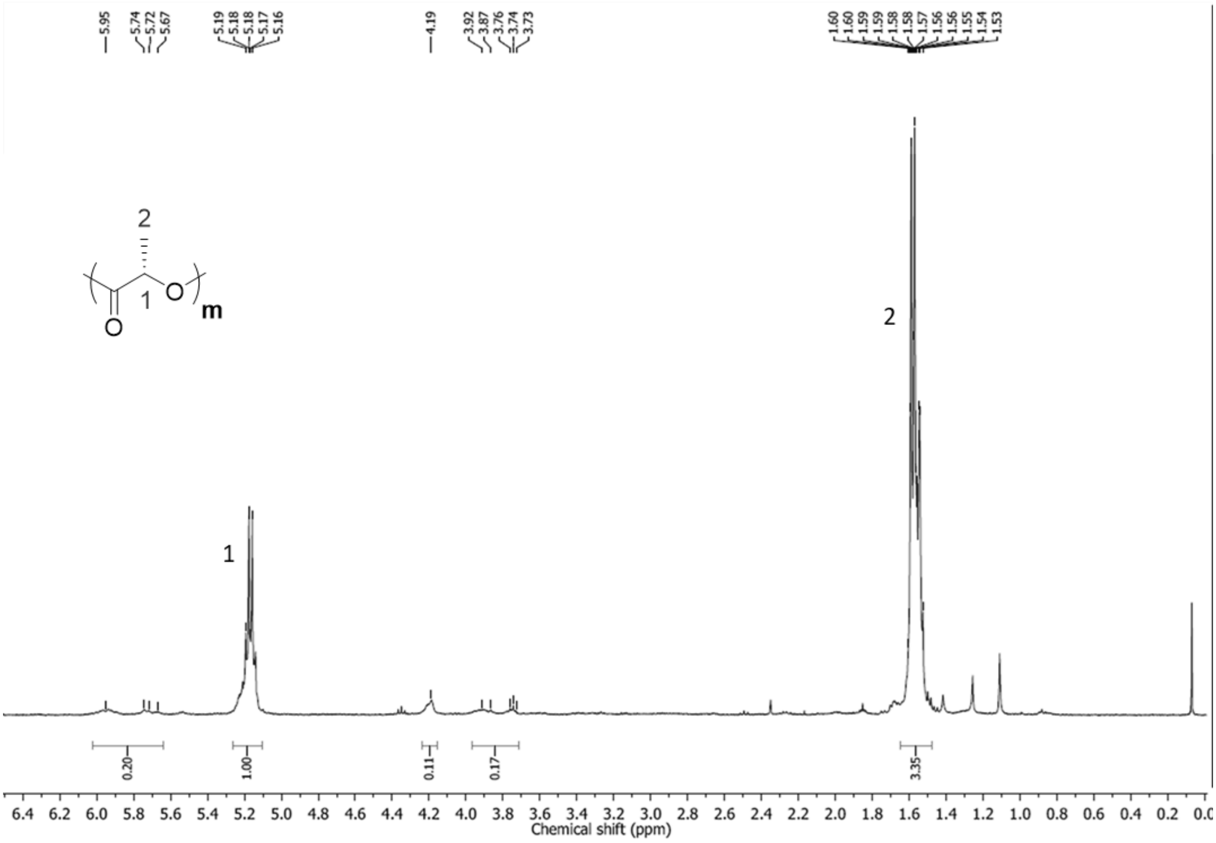

Fig. S88 Annotated ^{1}H NMR spectra of the degradation products of poly(**1**-*co*-LLA) (F_1/F_{LLA}, 16/84) after 6 hours in chloroform-d.

References

1. R. Sakai, T. Koike, M. Sasaki, K. Shimamoto, C. Oiwa, A. Yano, K. Suzuki, K. Tachibana and H. Kamiya, *Org. Lett.*, 2001, **3**, 1479–1482.
2. K. C. Nicolaou, C. K. Hwang, B. E. Marron, S. A. DeFrees, E. A. Couladouros, Y. Abe, P. J. Carroll and J. P. Snyder, *J. Am. Chem. Soc*., 1990, **112**, 3040–3054.
3. M. E. Evans and M. E. Parrish, *Carbohydr. Res.*, 1977, **54**, 105–114.
4. M. J. Frisch, G. W. Frucks, H. B. Schlegel, G. E. Scuseria, M. A. Robb, J. R. Cheeseman, G. Scalmani, V. Barone, B. Mennucci, G. A. Petersson, H. Nakatsuji, M. Caricato, X. Li, H. P. Hratchian, A. F. Izmaylov, J. Bloino, G. Zheng, J. L. Sonnenberg, M. Hada, M. Ehara, K. Toyota, R. Fukuda, J. Hasegawa, M. Ishida, T. Nakajima, Y. Honda, O. Kitao, H. Nakai, T. Vreven, J. Montgomery, J. A.;, J. E. Peralta, F.Ogliaro, M. Bearpark, J. J. Heyd, E. Brothers, K. N. Kudin, V. N. Staroverov, R. Kobayashi, J. Normand, K. Raghavachari, A. Rendell, J. C. Burant, S. S. Iyengar, J. Tomasi, M. Cossi, N. Rega, J. M. Millam, M. Klene, J. E. Knox, J. B. Cross, V. Bakken, C. Adamo, J. Jaramillo, R. Gomperts, R. E. Stratmann, O. Yazyev, A. J. Austin, R. Cammi, C. Pomelli, J. W. Ochterski, R. L. Martin, K. Morokuma, V. G. Zakrzewski, G. A. Voth, P. Salvador, J. J. Dannenberg, S. Dapprich, A. D. Daniels, Ö. Farkas, J. B. Foresman, J. V. Ortiz, J. Cioslowski and D. J. Fox, Gaussian 09 (Revision D.01), Gaussian, Inc., Wallingford CT, 2009.
5. a) J. -D. Chai and M. J. Head-Gordon, *Phys. Chem. Chem. Phys.*, 2008, **10**, 6615–6620; b) J. -D. Chai and M. J. Head-Gordon, *Chem. Phys.*, 2008, **128**, 084106; c) A. Buchard, F. Jutz, M. R. Kember, A. J. P. White, H. S. Rzepa and C. K. Williams, *Macromolecules*, 2012, **45**, 6781–6795.